Discovery and characterization of the ligands of NK-cell receptors implicated in human diseases

Discovery and characterization of the ligands of NK-cell receptors implicated in human diseases

A dissertation presented

by

Wilfredo F. Garcia Beltran

to

The Division of Medical Sciences

in partial fulfillment of the requirements

for the degree of

Doctor of Philosophy

in the subject of

Immunology

Harvard University

Cambridge, Massachusetts

May 2016

Discovery and characterization of the ligands of NK-cell receptors implicated in human diseases

ABSTRACT

Natural killer (NK) cells are cytotoxic lymphocytes of the innate immune system that act as first-line defenders against intracellular pathogens. Their functions are dictated by germline-encoded activating and inhibitory receptors, of which the most diverse family is the killer-cell immunoglobulin-like receptors (KIRs). Whereas many KIRs bind well-described HLA class I (HLA-I) ligands, many remain "orphaned" despite robust disease associations. KIR3DS1, in particular, is an activating receptor that has been associated to delayed HIV-1 disease progression, as well as the outcome of several other human diseases. However, despite knowing the ligands of its highly homologous inhibitory counterpart KIR3DL1, a ligand that accounts for the biological effects of KIR3DS1 remained unknown.

To identify HLA-I ligands of KIR3DS1, we screened 100 HLA-I proteins and found that KIR3DS1 binds HLA-F, which was validated biochemically and functionally. Primary human KIR3DS1$^+$ NK cells exhibited a polyfunctional response upon encountering HLA-F, and suppressed HIV-1 replication *in vitro*. Next, we probed the cellular contexts for HLA-F expression, and found that CD4$^+$ T-cell activation induced HLA-F expression and binding of soluble KIR3DS1-Fc. Although HLA-F was expressed intracellularly in transduced cell lines, HLA-F mobilization to the cell surface could be

achieved by cellular activation and inflammatory cytokines, suggesting that HLA-F is expressed in the context of inflammation.

To ascertain non–HLA-I ligands of KIR3DS1, we found that cell lines of various tissue origins bound KIR3DS1-Fc irrespective of HLA-F expression. Using a genome-wide CRISPR/Cas9 knock-out screen, we discovered that KIR3DS1 bound to heparan sulfate proteoglycans (HSPGs), which was validated biochemically and using cell lines and primary cells. In addition, given the previously assumed binding of KIR3DS1 to HLA-B*57:01, as well as the well-document binding of KIR3DL1 to HLA-B*57:01, we investigated these interactions and found that binding of KIR3DL1 to HLA-B*57:01 is *N*-glycan dependent, which has not been previously described and may play a modulatory role in KIR:HLA-I interactions.

Thus, we established HLA-F and HSPGs as ligands of KIR3DS1, demonstrated cell-context–dependent expression of HLA-F and HSPGs, and revealed dependency of the HLA-I *N*-glycan in KIR:HLA-I interactions that may explain the widespread influence of KIR3DS1 and other NK-cell receptors in human diseases.

TABLE OF CONTENTS

ACKNOWLEDGEMENTS

When I first began my PhD in August 2012, I believed that the harder and longer I worked, the more results I would get. Three months in, I realized that this was not the case (at some point it even became the opposite), and I learned that a healthy balance between lab work and personal recreation was essential to maintain mental stamina and creativity. Fortunately, I was privileged to have my dissertation advisor Dr. Marcus Altfeld frequently advising me to “take a day off” to recoup my mind and begin fresh when he saw me hitting my head against a wall. This was of particular importance in my PhD work, which under wise advice from Dr. Altfeld, was divided into two endeavors: (*i*) my main, very risky thesis project, namely, finding a ligand no one had found in over a decade; and (*ii*) a safer back-up project using humanized mice to model HIV-1 infection. Although I fortuitously succeeded in my “ligand hunt,” as we often referred to it, this was not without significant obstacles and moments of almost completely giving up. It was not without the continuous encouragement and practical advice from Dr. Altfeld—as well as the help from many members of the lab and within and outside the Ragon Institute of MGH, MIT, and Harvard—that I was able to identify the ligand(s), which along the way taught me one of the most important skills in science: collaboration.

Although I still have much to learn to become a fully independent scientist, I feel I am miles closer to this career goal because of the invaluable advice and mentoring that I received from Dr. Altfeld. In addition to his massive amount of field knowledge, his ability to forming long-lasting networks of collaborations, write clearly and persuasively, engage an audience in scientific presentations, and manage people are skills that I will hold onto for the rest of my career and will try to emulate in my own way. I also truly

admire his work-life balance and commitment to maintain integrity and fairness amongst a great amount of pressures. Very importantly, I cannot be grateful enough for his commitment to meet with me regularly and adapt his mentoring style to my personality and flaws; in particular, focusing me when I became derailed, teaching me time-management skills, uplifting my spirits when experiments were failing, and unwaveringly sharing my enthusiasm for my work. I also appreciate his generosity, allowing me to attend and present at two scientific conferences every year, putting me in contact with renowned scientists, and encouraging me to form new collaborations. I could not have hoped for a better PhD experience—something that I hear is uncommon to say—and I owe this to Dr. Altfeld.

Another wonderful mentor that I was extremely fortunate to meet early in my PhD and became very close to is Dr. Mary Carrington, the scientific pioneer of KIR3DS1 involvement in human disease. I deeply thank her for many enjoyable and rigorous scientific discussions, meetings, and critical analyses of my data, as well as exciting collaborative projects she invited me into. I also owe great gratitude to Dr. Stephanie Jost, who mentored me extensively and taught me essential lab immunology techniques, particularly for NK cells, and was always available for scientific, technical, practical, and experiential advice. In addition, I would like to thank Dr. Galit Alter, who co-sponsored me on my NIH F31 grant, and Dr. Todd Allen, who provided funding and guidance, particularly helping me on presentation style and skills.

Two individuals that I will forever be indebted to are Dr. Angelique Hoelzemer and Dr. Yovana Pacheco Nieva. The years we spent together in lab have been of the happiest and productive times in our lives, where we were intertwined in all aspects of

our personal, social, and research lives. We supported and learned from each other, and together experienced moments of intense tears and joy when experiments would fail and succeed. From the moment Dr. Hoelzemer began working as a post-MD PhD student in the lab, she became my “other half”, with our favorite “acquired” talent being working efficiently as a single operator at the bench (me pipetting with my left hand and her with her right), a skill that is a testament to what her sister would call “one mind in two bodies.” Dr. Hoelzemer and I developed and optimized basic molecular biology, cloning, and lentiviral transduction techniques in the lab with the help from an esteemed collaborator, Dr. Thomas Pertel, which opened the door to many of our subsequent research endeavors. Dr. Pacheco Nieva was and continues being an overabounding source of scientific and personal support and advice, and her friendship is invaluable. There was not a single experiment I performed that I did not discuss with her and modify in accordance to her recommendations, deeming her as my “lab mother,” as she often referred to herself as. These two individuals will forever be my scientific collaborators and lifelong friends, and have left a special handprint on my heart.

I would also like to specially acknowledge collaborators and researchers without whose help my work would not be possible. Dr. Pedro A. Lamothe-Molina has provided a wealth of ideas and resources for my project, and I am always fond of our intense and fruitful brainstorming sessions. Dr. Gloria Martrus taught me many new experimental techniques that she optimized, including flow cytometry-based fluorescent *in situ* hybridization, and has provided significant advice and support. I would also like to thank Dr. Marijana Rucevic, my “go to” mass spectrometry expert, who carried out laborious experiments involving an immunoprecipitation and mass-spectrometry–based

approach to ligand discovery, and was also a great source of encouragement. Dr. Eileen Scully is an post-doctoral clinical/research fellow in the laboratory from whom I got a great wealth of research ideas and physician-scientist career advice, for which I am very grateful. I have also been very fortunate to collaborate with Dr. Jodie Goodridge, an HLA-F expert who provided vital scientific and experimental advice and suggestions for my work. In addition, I am very grateful for the genome-wide CRISPR/Cas9 knock-out screening studies performed by Tim Wang and Klara Klein. I would also like to acknowledge Dr. Christian Korner and Angela Crespo for many scientific discussions. Special thanks to Tae-Eun Kim, an undergraduate student that worked for me for an entire year as a volunteer and catalyzed a faster pace in my research. Additional special thanks to many technicians and master's students that worked in the lab and provided crucial technical help, particularly Camille R. Simoneau, Haley Dugan, Suppreetha Gubbala, and Simon Gressens.

I would also like to thank Dr. Shiv Pillai, who has mentored and advised me since I arrived to Boston in 2010 under many "hats" (i.e. as HST (MD) mentor, MD/PhD mentor, and dissertation advisory committee chair), particularly in moments of struggle and uncertainty. He was the key person that directed me to rotate in and ultimately join the Altfeld lab, for which I am forever grateful. I would also like to thank the rest of my dissertation advisory committee, Dr. Kai Wucherpfennig and Dr. Ulrich von Andrian, for very constructive and valuable advice and recommendations throughout my PhD.

I also want to appreciate and acknowledge the support and assistance from the Ragon Institute Flow Cytometry Core and Virology Core, as well as members of the Altfeld lab and the Ragon Institute of MGH, MIT, and Harvard, many of which have

become great colleagues and friends. I would also like to thank the human blood donors, which through their donations have allowed this human-based research to be possible.

I would also like to give immense thanks to my classmates, professors, and administrative staff in the Harvard Immunology Program and Harvard/MIT MD/PhD and HST programs, and my close friends and family—in particular my mother E. Ivonne Beltrán Silvagnoli, my sister Lyan García Beltrán, and my father Carlos Roldán Cortés—for always being there for me.

This work would not be possible without funding sources. I and/or the projects described were supported by the National Institute of General Medical Sciences (T32GM007753), the National Institute of Health (R01-AI067031-08, P01-AI104715, F31AI116366), and the Ragon Institute of MGH, MIT and Harvard. The content in this body of work is solely the responsibility of the authors and does not necessarily represent the official views of the National Institute of General Medical Sciences or the National Institutes of Health.

And last but by no means least, I would like to thank God for blessing me with wonderful mentors, friends, and family, and giving me the privilege to work in what I love.

DEDICATION

I would like to dedicate this to my mother, E. Ivonne Beltrán Silvagnoli, who has given me truly unconditional love my whole existence and has dedicated her life to see me grow as a person and succeed. Without her care, advice, and guidance, I would not be where I am today.

LIST OF ILLUSTRATIONS, FIGURES, AND TABLES

GLOSSARY OF TERMS

KIR: killer-cell immunoglobulin-like receptor

HLA-I: human leukocyte antigen (HLA) class I

MHC-I: major histocompatibility complex (MHC) class I

HIV-1: human immunodeficiency virus type 1

NK cell: natural killer cell

KIR-Fc: soluble chimeric construct composed the extracellular domain of the indicated KIR and the Fc region of human IgG1 (dimerized)

KIRζ: KIR-CD3ζ chimeric receptor composed the extracellular and transmembrane domain of the indicated KIR and the cytoplasmic tail of CD3ζ

NKCL: natural killer-cell clone

IFN-γ: interferon γ

MIP-1β: macrophage inflammatory protein 1β

TNF-α: tumor necrosis factor α

PMA: phorbol 12-myristate 13-acetate

iono: ionomycin

GAG: glycosaminoglycan

HA: hyaluronic acid

HS: heparan sulfate

PG: proteoglycan

HSPG: heparan sulfate proteoglycan

NCR: natural cytotoxicity receptor

CRISPR: clustered regularly interspaced short palindromic repeats

EPIGRAPH

During my 8th grade graduation, my science teacher, Dr. Sara Spurlock (now Dr. Sara Gamby) said awkwardly but zealously to the audience,

I know that in the future, Wilfredo will be working in a lab for two weeks straight, and one day suddenly realize, "Oh wait! I have a wife and kids at home I have to go to!"

I don't know how, but in me she saw passion and potential that I did not see, and she unlocked it in the two years I took class with her. Her comical statement stuck with me strongly, and has become not far from the truth at all.

CHAPTER 1: Introduction

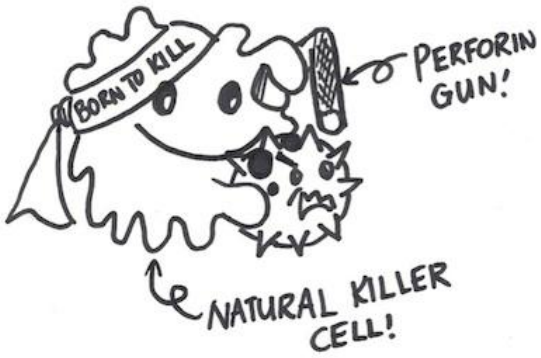

1.1 *Natural killer cells and their receptor families*

In spite of their undeserving origins as 'unspecific assassins,' natural killer (NK) cells are proving to bear increasingly recognized roles in innate and adaptive immune responses, adopting characteristics of both arms of the immune system. These innate cytotoxic lymphocytes are most notoriously known for killing HLA class I-deficient cells and exerting antibody-dependent cell-mediated cytotoxicity (ADCC). However, their variegated expression of highly diverse germline-encoded activating and inhibitory receptors bestows upon them the ability to act as a multi-specific, poly-functional army of first-line defenders against intracellular pathogens as part of their many crucial functions.

The major classes of NK-cell receptors are depicted in **Illustration 1.1**[1], all of which allow NK cells to discriminate between healthy "self" and a variety of pathological cell states, including "missing self," "altered/stress-induced self," and "infectious non-self."[2] Of these, the most diverse family is the killer-cell immunoglobulin (Ig)-like receptors (KIRs), exhibiting the most polymorphisms in the entire human genome secondary only to the major histocompatibility complex (MHC)[3]. The *KIR* locus encodes for a plethora of activating and inhibitory receptors that bind to HLA class Ia and Ib molecules with variable specificity.

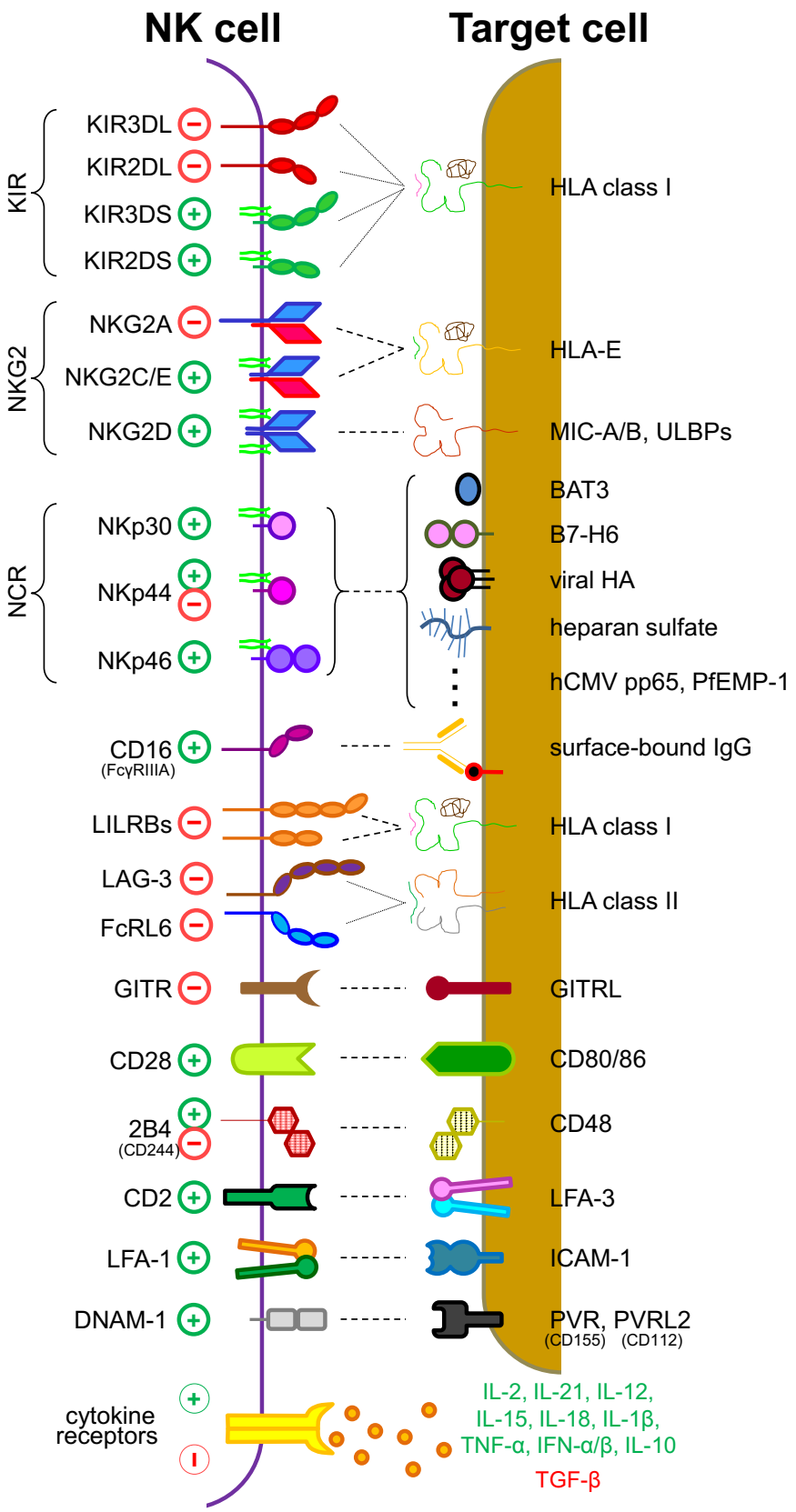

Illustration 1.1: NK-cell receptors and ligands

1.2 *Overview of the KIR family*

KIR family receptors are categorized by the number of Ig-like extracellular domains (2D or 3D) they contain and by whether they have a long (L) or short (S) cytoplasmic tail. Overall, KIR2D molecules bind HLA-C ligands, whereas KIR3D molecules bind HLA-A and -B ligands[4], although there are many exceptions. KIR-L molecules are inhibitory, as they have long immune tyrosine inhibitory motif (ITIM)-bearing cytoplasmic tails. KIR-S molecules, on the other hand, have a truncated cytoplasmic tail and possess a positively-charged residue in their transmembrane domain that allows association to immune tyrosine activating motif (ITAM)-bearing adaptor molecules such as DAP12[5] (for detailed information about KIRs used in this body of work, see **Illustration 1.2**). Although KIR binding to HLA ligands was previously deemed non–peptide-specific, an increasing amount of studies have discovered exquisite peptide sensitivity in this interaction[6,7], a finding that has only begun to be appreciated.

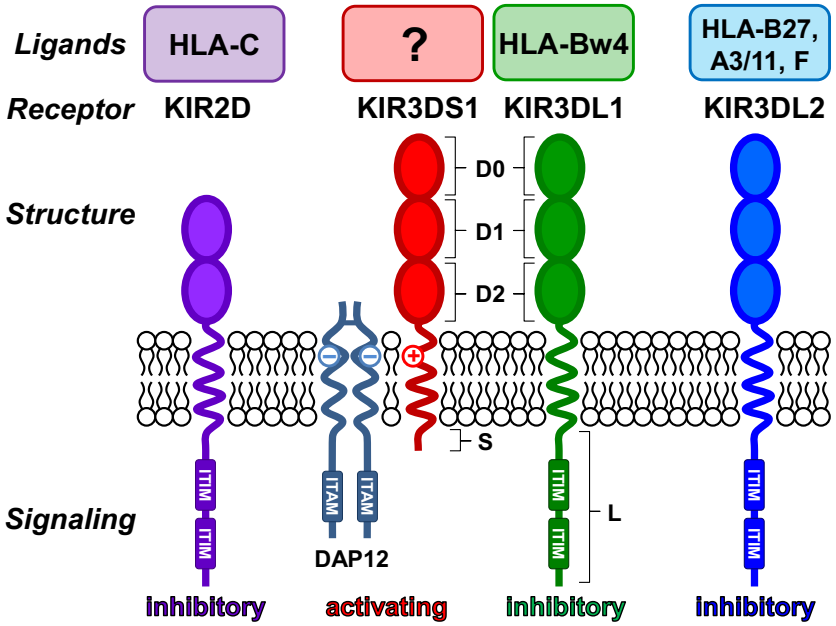

Illustration 1.2: Schematic of the structure, signaling, and ligands of KIRs studied.

The high polymorphicity of both *KIR* and *HLA* genes highlights a deep-seated evolutionary interplay of receptor:ligand pairs driven by forces of reproduction and infectious disease survival[3]. However, the role KIR:HLA interactions play in dictating NK-cell function has been continually shown to be crucial in five major areas of human health and disease: cancer, transplantation, autoimmunity, reproduction, and infectious diseases. In the realm of infectious diseases, control of viral pathogen and intracellular bacteria is an essential NK-cell function necessary for host survival, as exemplified by the rare of cases of human NK-cell deficiency that result in death in early life[8], but of particular interest to us was the well-documented role of NK cells and their receptors in HIV-1 infection.

1.3 *Previously unrecognized role of NK cells in immune responses to HIV-1*

HIV-1 first arose in Africa as a cross-species transmission event from simian immunodefiency virus (SIV) in the 1930s[9]. As such, there has been no time for human evolution to take place and establish a 'truce' between host and pathogen, as occurred for other viral infections (e.g. herpes viruses). Today it affects 36.9 million adults and children worldwide and in 2014 alone led to 2 million new infections and 1.2 million deaths[10]. Amidst our efforts to combat HIV/AIDS, however, a great deal has been learned about the immune system and how this virus has been able to cripple it. HIV immunology and virology research has largely focused on understanding the HIV life cycle, elucidating virion structure, aiding anti-retroviral drug and vaccine development, and characterizing cellular and humoral immune responses throughout infection.

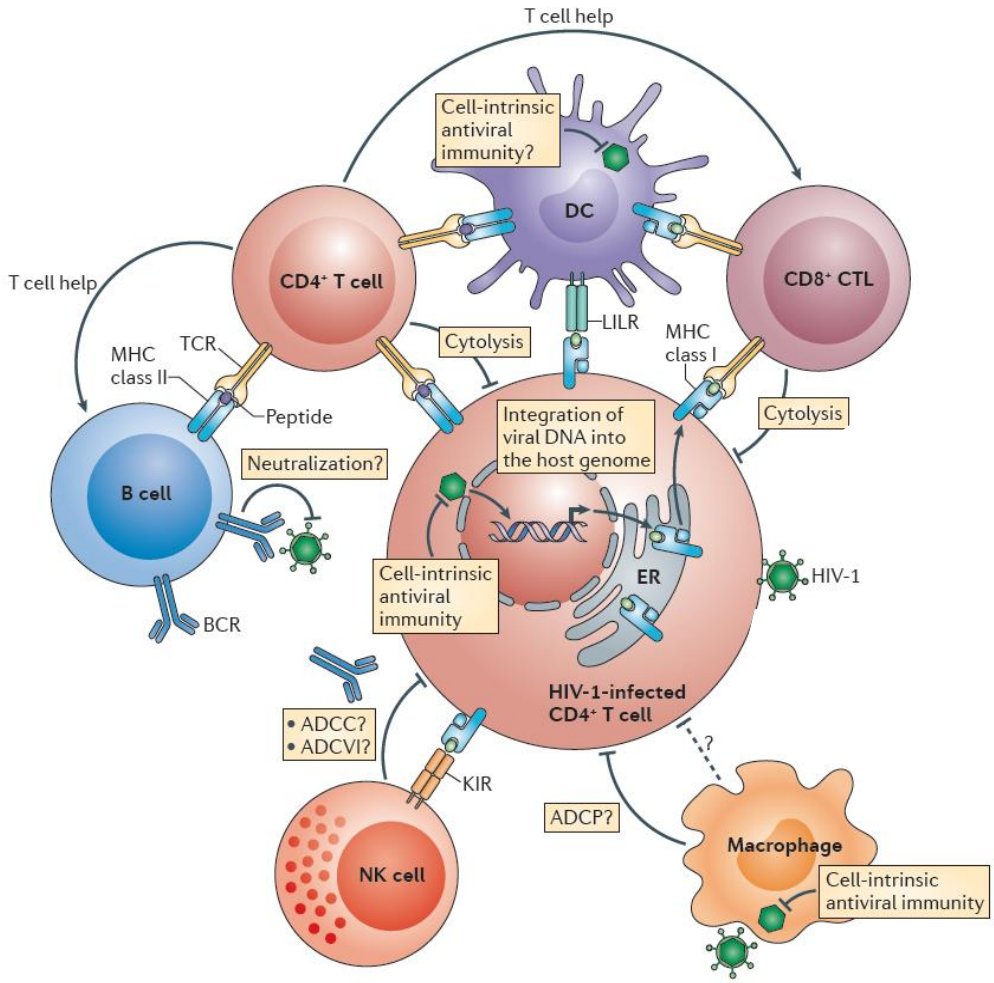

Illustration 1.3: Immune response to HIV-1 (published in [11])

The interplay between HIV-1 and the human immune response is one of rapid micro-evolution[12]. The virus employs an armamentarium of immune evasion strategies, the most significant being its extraordinary ability to rapidly mutate and escape recognition by the immune system. Immune pressure driving escape arises from exhuberant anti-viral $CD8^+$ T cell responses targeting HLA-presented viral epitopes as well as B-cell antibody responses that attempt to neutralize HIV envelope protein (see **Illustration 1.3**, diagram published in [11]). However, one previously unexpected source of immune control and immune pressure is NK cells. Studies from our laboratory have

shown that NK cells alone mediate viral inhibition in co-cultures with HIV-1–infected $CD4^+$ T-cells via *in-vitro*/*ex-vivo* assays[13]. Additionally, we have described the existence of 'KIR footprints'—that is, HIV-1 peptide variants found more commonly in individuals bearing a specific KIR—that lead to increased NK cell inhibition and, potentially, reduced elimination of HIV-1–infected cells[14,15]. As a consequence, these innate cytotoxic effectors highlight a previously ignored but increasingly important role that NK cells and their KIRs play in killing HIV-1–infected cells and influencing HIV-1 acquisition and disease progression.

1.4 *Association between KIRs and HIV-1 acquisition and disease progression*

The first association between KIRs and HIV-1 was made in an epidemiologic study in 2002 by Martin *et al*.[16], where patients possessing both the activating NK-cell receptor *KIR3DS1* gene and one of various *HLA-A* or *HLA-B* alleles with a Bw4 motif and an isoleucine at position 80 ($HLA\text{-}Bw4^{I80}$) were found to progress more slowly to AIDS, when compared to patients having either or neither alleles. *KIR3DS1* is a functionally divergent allele of the *KIR3DL1/S1* gene, a unique *KIR* gene locus in that it contains both inhibitory *KIR3DL1* alleles and activating *KIR3DS1* alleles[3]. KIR3DL1 had previously been shown to bind HLA-Bw4 allotypes with sensitivity to polymorphisms in position 80[17], but this epistatic association between *KIR3DS1* and *HLA-B* in HIV-1 disease progression seemed to have uncovered a new KIR:HLA interaction. More importantly, this was the first time an association had ever been made between a KIR and a viral infection. This opened the path for a multitude of investigators to seek out and dissect further associations between KIR3DL1/S1 and HIV-1 infection.

Additional findings showed that individuals possessing particular *KIR3DL1* alleles and HLA-Bw4 progressed more slowly to AIDS when compared to individuals without HLA-Bw4[18].Furthermore, it appeared that the protective effect with HLA-Bw4 was most prominent in a *KIR3DL1/S1* heterozygous state[19]. Additionally, two studies[20,21] found a significant overrepresentation of *KIR3DS1* in HIV-1-exposed seronegative individuals that possessed HLA-Bw4 allotypes. This supported the notion that although both KIR3DL1 and KIR3DS1 protected from HIV-1 disease progression in patients bearing HLA-Bw4 allotypes, KIR3DS1 also protected against HIV-1 acquisition. This finding paralleled a study which observed a protective effect against HIV-1 acquisition in HIV-1–discordant couples that were KIR:HLA mismatched for KIR2DL1/L3 and HLA-C2/C1 ligands[22]. These findings are in agreement with the known functions of KIRs in NK cells, one of which is to mediate licensing. Licensing is a tolerance-ensuring phenomenon in which NK cells acquire the ability to kill target cells deficient in a specific HLA ligand only after having that HLA ligand engage an inhibitory KIR during development[23]. For example, Martin *et al*.'s study[18] supports the idea that KIR3DL1$^+$ NK cells licensed by HLA-Bw4 killed HIV-1–infected CD4$^+$ T cells undergoing Nef-induced downregulation of HLA-A and -B, whereas Jennes *et al*.[22] proposed that KIR2DL1$^+$ NK cells licensed by HLA-C2 killed transmitted HIV-1–infected CD4$^+$ T cells lacking the appropriate HLA-C ligands. However, research attempting to characterize and dissect the protective effect of KIR3DS1 in HIV-1 has yielded mixed results, despite it being the first described KIR–virus association.

1.5 *A definite but mechanistically controversial role for KIR3DS1 in HIV-1 infection*

The major reason for controversy over the mechanism by which KIR3DS1 confers protection in HIV-1 infection is because there was no proven ligand. Epidemiologic and functional studies have provided circumstantial evidence implicating HLA-Bw4^{I80} as a likely ligand, but efforts to establish this interaction using techniques used to identify KIR3DL1 ligands failed to do so. Even in light of the published crystal structure of self-peptide:HLA-B*57:01 bound to KIR3DL1*001[24], a prototypical allotype of *KIR3DL1* that has 97.5% protein sequence homology to the most common allotype of *KIR3DS1* (*013) in its extracellular domain, no significant advances were made. The only exception is a single recent study that demonstrated KIR3DS1 binding to HLA-B*57:01 refolded around two HIV-1 peptides that arose from an exhaustive screen of various self and viral peptide databases[25]. However, it is not clear whether this interaction has real functional consequences, or represents an exceptional case where a peptide can overcome KIR3DS1 mutations that normally abrogate HLA-Bw4 binding.

Thus far, investigations attempting to elucidate the ligand have done so through cellular immunology, functional studies, and cohort analyses, the results of which are not always in agreement. Increased frequencies of KIR3DS1$^+$ NK cells have been reported in HLA-Bw4^{I80}–positive individuals when compared to HLA-Bw4–negative individuals[26]. Also, KIR3DS1$^+$ NK cells specifically expanded in acute HIV-1 infection and persisted throughout chronic infection in HLA-Bw4^{I80}–positive versus HLA-Bw4–negative individuals[27]. Indeed, many studies have cogently demonstrated the ability of KIR3DS1$^+$ NK cells, but not KIR3DL1$^+$ NK cells, to effectively inhibit HIV-1 viral replication in co-culture with autologous HIV-1–infected CD4$^+$ T cells from HLA-Bw4^{I80}–

positive individuals[13,28]. However, a study by Long *et al*.[29] revealed that while KIR3DS1 positivity correlated with increased CD107a and IFN-γ expression by bulk NK cells in acute HIV-1 infection, there was no association to the co-presence of HLA-Bw4^{I80}. Morvan *et al*.[26] also described a preferential expansion of KIR3DS1^{+} NK cells in response to various non-specific stimuli such as HLA-deficient targets, interleukin treatment, and *Toll*-like receptor agonists, but found that these cells responded indiscriminately to HLA-Bw4 and HLA-Bw6–transduced cells. One controversial study by Barbour *et al*.[30] analyzed a cohort of 255 HIV-1–infected individuals and showed that KIR3DS1 and HLA-Bw4^{I80} were independently associated with higher CD4^{+} T cells counts and lower viral loads, respectively, when compared to subjects without these allotypes, thus contesting the argument of synergy and favoring a phenomenon of additive independence between KIR3DS1 and HLA-Bw4^{I80}. Overall, investigators have been limited in proving a direct interaction between KIR3DS1 and any ligand, leaving a gap in our understanding of KIR3DS1 biology.

1.6 *The need to discover the ligand for KIR3DS1*

It has been over a decade since the first association between KIR and a viral infection was made between KIR3DS1 and HIV-1 disease progression, and yet there has been no ligand discovered to understand the underlying mechanism of this phenomenon. Since then, numerous associations between KIR3DS1 and various clinical outcomes have arisen—highlighted in **Table 1.1**[31–42]—but with no known mechanism for further study. As there is compelling evidence that NK cells and their

receptors play a major role in anti-viral and anti-tumor immunity not only in their innate immune functions but also in their ability to act as 'rheostats' to adaptive immune

Viral Infections	↓ HIV-1 disease progression (HLA-Bw4^{I80+}) ↑ spontaneous recovery from hepatitis B infection ↑ severe pandemic H1N1 influenza A infections ↑ HCV clearance after treatment in HIV/HCV co-infection (HLA-Bw4^{+}) ↓ BK virus infection/nephropathy after kidney transplant
Malignancies	↓ HCV-related hepatocellular carcinoma (HLA-Bw4^{I80+}) ↓ Hodgkin's lymphoma ↓ respiratory papillomatosis ↑ risk of cervical neoplasia
BMT/HSCT	↓ progression-free survival in multiple myeloma (autologous) ↓ acute GvHD (donor allogeneic) ↓ overall survival (HLA-Bw4^{-})
Autoimmunity	↑ susceptibility to ankylosing spondylitis (HLA-B27^{+})

Table 1.1 Disease associations when KIR3DS1 is present

responses[43,44] and adopt characteristics such as antigen specificity and possibly memory[45], it is imperative that the elusive KIR3DS1 ligand be found. The implications of finding such ligand and unraveling KIR3DS1 biology would offer potential new targets to manipulate in future preventative and therapeutic HIV-1 vaccine strategies and bolster the use of NK-cell-receptor–directed immunotherapeutics, as has already been done in a phase I clinical trial targeting KIR2DLs in multiple myeloma patients[46]. Consequently, **the goal of this work was to discover the ligand of KIR3DS1 by designing and employing unbiased biochemical, molecular biological, and cellular immunological strategies, in the hopes of elucidating the mechanism by which KIR3DS1 confers protection in HIV-1 infection and alters the course of other human diseases.**

Undertaking this endeavor, multiple lines of investigation arose concerning other NK-cell receptors, particularly KIRs, and their ligands. In **Chapter 2** and **Chapter 3**, the discovery and biological implications of HLA-F binding to KIR3DS1 are explored, with a summary of background information between presented in the section **2.1 Background**. In **Chapter 4**, heparan sulfate proteoglycans are described as ligands for KIR3DS1 and other NK-cell receptors; information concerning NK-cell receptor:carbohydrate interactions and heparan sulfate biology can be found in the section **4.1 Background**. In **Chapter 5**, where HLA-I *N*-glycosylation is studied and manipulated in the context of KIR:HLA-I binding, information regarding HLA-I *N*-glycans can be found in the section **5.1 Background** section. Conclusions and discussion of the implications of all each of these findings are discussed in **Chapter 6** (**Discussion**).

CHAPTER 2: Open conformers of HLA-F are high-affinity ligands of the activating NK-cell receptor KIR3DS1

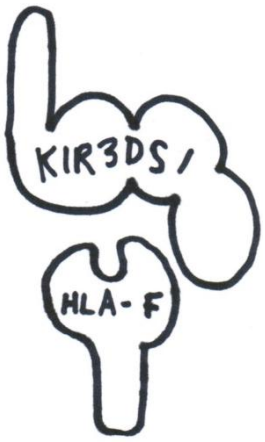

2.1 SUMMARY

The activating NK-cell receptor KIR3DS1 has been implicated in the outcome of various human diseases, including delayed HIV-1 disease progression, yet for over a decade, a ligand that accounts for its biological effects remained unknown. We screened 100 classical and non-classical HLA-I proteins as complexes and open conformers (OCs) and found that KIR3DS1—along with its functionally divergent allotype KIR3DL1 and the phylogenetically related KIR3DL2—bound to HLA-F OCs. KIR-Fc binding to HLA-F OCs was validated by surface plasmon resonance, which showed the highest affinity binding between KIR3DS1 and HLA-F OCs, followed by KIR3DL2 and KIR3DL1. These interactions were assessed at the cellular level using Jurkat cells stably expressing KIR-CD3ζ chimeric receptors. These confirmed that KIR3DS1 strongly signaled upon engagement of HLA-F OCs on target cells, while KIR3DL2 and KIR3DL1 also signaled although to a lesser extent. These findings establish that HLA-F OCs are functionally relevant, high-affinity ligands of KIR3DS1 and open the door to future studies seeking to understand the wide-spread biological roles of KIR3DS1 in human disease.

2.2 BACKGROUND

Killer-cell immunoglobulin (Ig)-like receptors (KIRs) are a family of HLA class I-binding receptors expressed on natural killer (NK) cells that are implicated in various areas of human health and disease. The *KIR* locus contains some of the most highly polymorphic human genes, a diversity comparable to *HLA* genes in the major histocompatibility complex (MHC) locus[3]. This highlights a deep-seated evolutionary interplay of receptor:ligand pairs driven mainly by forces of reproduction and infectious disease survival[3]. Through variegated expression of KIRs and other highly diverse germline-encoded receptors, NK cells are able to discriminate between healthy "self" and a variety of pathological cell states[2]. As such, it is unsurprising that NK cells and KIRs have a broad involvement in human disease[47], especially in light of their increasingly recognized roles in innate and adaptive immune responses[43,48].

KIR family receptors are categorized by the number of Ig-like extracellular domains they contain (2D or 3D) and by whether they have a long (L) or short (S) cytoplasmic tail. KIR-L receptors are inhibitory, as they have immune tyrosine inhibitory motif (ITIM)-bearing cytoplasmic tails, whereas KIR-S receptors have truncated cytoplasmic tails and possess a transmembrane positive charge that allows association to immune tyrosine activating motif (ITAM)-bearing adaptor molecules such as DAP12. In general, KIR2D receptors bind HLA-C, whereas KIR3D receptors bind HLA-A and -B. Nevertheless, while many HLA class I (HLA-I) ligands have been identified for multiple KIRs, several have remained more elusive, particularly for activating KIRs.

KIR3DS1 was the first KIR to be associated with the outcome of a viral infection, namely, delayed human immunodeficiency virus (HIV)-1 disease progression in patients

with certain *HLA-B* alleles[16]. Since then, it has been linked to other viral infections[16,19,31,42,49], autoimmune disorders[41], cancer development/clearance[33,34,36,37], and transplantation outcomes[38–40], and therefore has become one of the most studied KIRs. KIR3DS1 is an activating receptor that stimulates cytotoxicity and IFN-γ production in NK cells[5]. It is encoded in the *KIR3DL1/S1* gene locus, a unique KIR locus because it encodes for functionally divergent alleles[3]. Remarkably, while sharing >95% homology in their extracellular domain, KIR3DS1 and its inhibitory counterpart KIR3DL1 have different ligand binding profiles. KIR3DL1 has conclusively been shown to bind HLA-A and -B allotypes with a Bw4 motif, with variable sensitivity to C-terminal residues of HLA-Bw4-bound peptides and to residues at position 80 of HLA-I[17]. However, attempts to identify a KIR3DS1 ligand by various groups have repeatedly failed[50,51], save for a single recent study demonstrating peptide-dependent binding of KIR3DS1 to HLA-B*57:01 *in vitro*[25]. Both KIR3DL1 and KIR3DS1 have been strongly linked to HLA-Bw4 allotypes in disease association studies, including HIV-1 pathogenesis[16,18], but direct KIR3DS1:HLA-Bw4 interactions are a major point of controversy. Indeed, some studies report an independence between KIR3DS1 and HLA-Bw4[29,30]. Furthermore, even in studies linking KIR3DS1 and HLA-Bw4, the vast majority of *KIR3DS1*$^{+}$ subjects also possessed *KIR3DL1*, imposing a confounding variable since KIR3DL1 binds HLA-Bw4 proteins. Of note, while *KIR3DL1* exhibits significant sequence polymorphisms that have been shown to alter KIR3DL1 protein surface expression[52] and ligand binding[53,54], *KIR3DS1* is remarkably conserved and virtually monomorphic. This is despite *KIR3DS1* having arisen in the human genome >3 million years ago along with various alleles of *KIR3DL1*, and being present in almost all human populations worldwide[3].

2.3 RESULTS

2.3.1 *Comprehensive HLA-I screening shows that KIR3DS1 binds to HLA-F OCs*

We aimed to systematically assess KIR3DS1 binding to a panel of HLA-I proteins in two biologically relevant conformation states: as HLA-I complexes, which are folded heavy chains bound to β_2-microglobulin (β_2m) and peptide, and as HLA-I open conformers (OCs), which are HLA-I heavy chains without bound β_2m or peptide (reviewed in [55]). To accomplish this, we tested binding of soluble KIR3DS1-Fc and other KIR-Fc fusion constructs to HLA-I-coated beads individually bearing 97 allotypes of classical HLA-I (i.e. HLA-A, -B, and -C) that were either untreated or acid pulsed. Acid pulsing is a well-established method of stripping away β_2m and HLA-I-bound peptides to rapidly generate HLA-I OCs. KIR3DS1-Fc did not bind appreciably to any classical HLA-I alleles tested either as complexes (untreated) or OCs (acid pulsed) (**Fig. 2.1a**). However, KIR3DL1-Fc bound preferentially to HLA-Bw4 complexes, and KIR2DL3-Fc and KIR2DS4-Fc bound to HLA-C complexes (**Fig. 2.1a**), as expected. KIR3DL2-Fc did not have any preferential binding to specific HLA-I proteins. Of note, HLA-I complexes on these beads presented a diverse repertoire of peptides derived from the human cell line the HLA-I proteins were produced in, which precludes any peptide specificity analysis. Thus, KIR3DS1 does not bind to classical HLA-I complexes (presenting a diverse immunopeptidome) or HLA-I OCs.

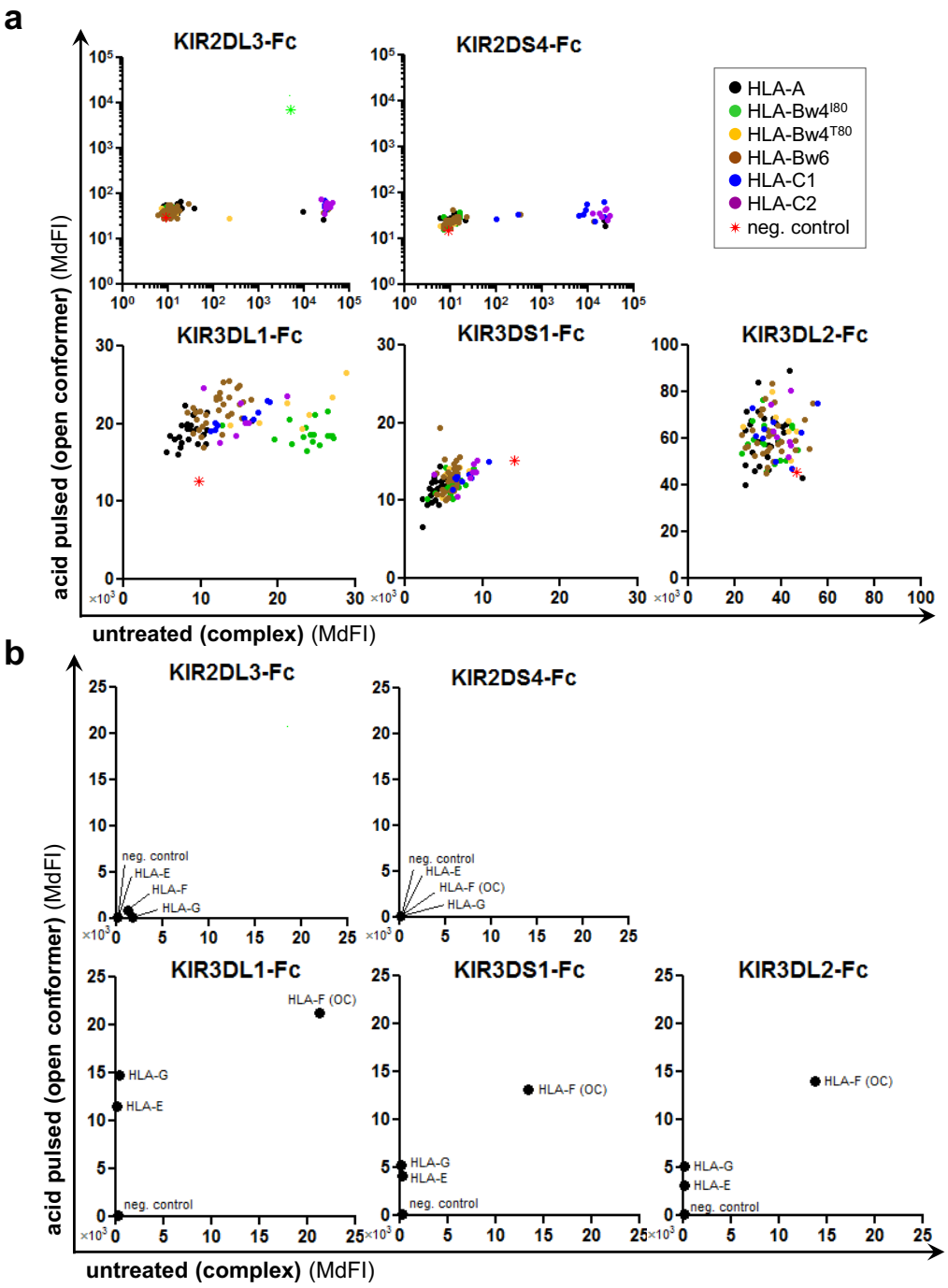

Figure 2.1: KIR-Fc binding to beads coated with classical and non-classical HLA-I proteins. (***a***) HLA-I-coated beads (from One Lambda) were untreated or acid pulsed and stained with the indicated KIR-Fc constructs (200 µg/mL each) to assess binding to complexes (untreated) versus open conformers (acid treated) of each classical HLA-I gene allotype; negative control beads (red star) were used to assess background staining. For KIR3DL1-Fc and KIR3DS1-Fc, similar results were achieved with two other KIR-Fc concentrations (100 µg/mL and 20 µg/mL) done in parallel and also when repeated independently with a flow cytometry-based HLA-I-coated bead kit (data not shown). (***b***) HLA-E, -F, and -G-coated beads (generated in this study) were untreated or acid pulsed and stained with the indicated KIR-Fc constructs (25 µg/mL each). Negative control beads (neg. control) were used to assess background staining; 'HLA-F (OC)' denotes HLA-F in open conformation on both untreated and acid-pulsed beads.

Because non-classical HLA-I proteins (i.e. HLA-E, -F, and -G) were not included in the original HLA-I-coated bead panel, we separately produced these. We coated streptavidin-beads with biotinylated HLA-E, -F, or -G monomers refolded around β_2m and peptide (no peptide in the case of HLA-F given that it does not present peptide[56]; details in **Materials and Methods**). In order to confirm that HLA-I proteins were in complex conformation after loading them onto beads, we assessed anti-pan-HLA-I complex (clone: W6/32) antibody binding to HLA-I-coated beads before and after acid pulsing by flow cytometry; this antibody can recognize all HLA-A, -B, -C, -E, -F, and -G proteins but only when they are bound to β_2m. As expected, all acid-pulsed beads did not bind anti-pan-HLA-I complex antibody due to stripping of β_2m (**Supplementary Fig. S2.1a**). However, we found that for untreated beads, while HLA-E and -G readily bound anti-pan-HLA-I complex antibody, HLA-F did not (**Supplementary Fig. S2.1a**). We assessed β_2m content on the untreated HLA-I-coated beads by anti-β_2m antibody staining, and found that HLA-F-coated beads had ~60% less β_2m content than HLA-E- and HLA-G-coated beads (**Supplementary Fig. S2.1b**). This indicated that unlike other HLA-I proteins, HLA-F readily dissociates from β_2m and spontaneously forms HLA-F OCs on artificial surfaces, which is in line with its unique property of being stable as an open conformer[57].

Upon testing KIR-Fc binding to non-classical HLA-I-coated beads, we found that KIR3DS1-Fc strongly bound to HLA-F-coated beads; this was independent of acid treatment, consistent with the fact that both untreated and acid-pulsed beads contained HLA-F OCs (**Fig. 2.1b** and **Fig. 2.2**). KIR3DL1-Fc and KIR3DL2-Fc were similarly able to bind HLA-F-coated beads (both acid pulsed and untreated); however, KIR2DL3-Fc

and KIR2DS4-Fc did not bind to any non-classical HLA-I-coated beads (**Fig. 2.1b**). Consequently, we determined from this assay that KIR3DS1, along with its functionally divergent allotype KIR3DL1 and the phylogenetically related KIR3DL2[3], bind HLA-F OCs.

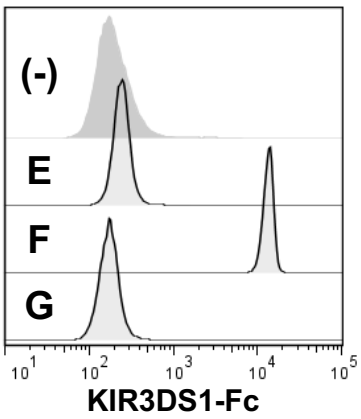

Figure 2.2: KIR3DS1-Fc binding to beads coated with non-classical HLA-I proteins. Flow cytometry histograms showing results for binding of KIR3DS1-Fc (25 µg/mL) to untreated non-classical HLA-I-coated beads; '(-)' denotes negative control beads, and 'E', 'F', and 'G' denote HLA-E-, -F-, and -G-coated beads, respectively.

2.3.2 *Surface plasmon resonance confirms KIR3DS1 binding to HLA-F OCs*

To confirm our findings, we performed surface plasmon resonance to quantitatively assess the affinities between HLA-F OCs and various KIRs. KIR3DS1 had the highest affinity to HLA-F OCs of the tested KIRs (K_D = (25 ± 1) nM), followed by KIR3DL2 (K_D = (118 ± 1) nM) and KIR3DL1 (K_D = (157 ± 2) nM), while KIR2DS4 and KIR2DL3-Fc did not exhibit any binding even at the highest tested concentrations (**Fig. 2.3** and **Table 2.1**). The kinetic data showed that the affinity of KIR3DS1 to HLA-F OCs is mainly driven by a relatively small dissociation rate (k_d = (7.0 ± 0.3) × 10^{-4} s^{-1}) as compared to KIR3DL1 (k_d = (6.91 ± 0.09) × 10^{-3} s^{-1}) and KIR3DL2 (k_d = (5.08 ± 0.04) × 10^{-3} s^{-1}), reflecting a higher stability of the interaction once formed. Together, these data demonstrated that all 'lineage II KIRs' (i.e. KIR3DL1, KIR3DS1, and KIR3DL2) can bind HLA-F OCs, although with varying affinities and in a manner that is opposite to that

involving binding to classical HLA-I molecules, where inhibitory KIRs normally bind with significantly higher affinity.

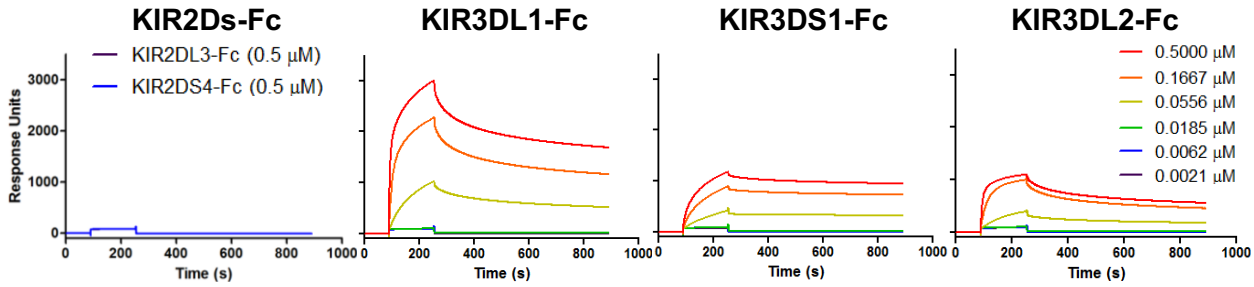

Figure 2.3: Surface plasmon resonance of KIR-Fc binding to HLA-F OCs. Each panel represents flow sensograms of the indicated KIR-Fc constructs at the indicated concentrations flowed over a flow cell with approximately 1000 response units of immobilized HLA-F OCs. Colored lines legends apply for all graphs. Similar results were achieved in two independent experiments (data not shown).

Constant	k_a ($M^{-1}s^{-1}$) ($\times 10^4$)	k_d (s^{-1}) ($\times 10^{-4}$)	K_D (nM)
KIR3DL1	4.40 ± 0.04	69.1 ± 0.9	157 ± 2
KIR3DS1	2.84 ± 0.02	7.0 ± 0.3	25 ± 1
KIR3DL2	4.30 ± 0.02	50.8 ± 0.4	118 ± 1
KIR2DL3	–*	–*	–*
KIR2DS4	–*	–*	–*

Table 2.1: Kinetic values of KIR binding to HLA-F OCs as determined by surface plasmon resonance. All values represent monomeric interaction kinetic values calculated from the 'bivalent analyte' fitting model on BIAevaluation software and are presented as mean ± standard error of the mean. Asterisk (*) indicates there was no binding detected at highest tested concentration (0.5 μM) of KIR-Fc. ***Kinetic constants:*** k_a, association rate constant (a.k.a. on-rate); k_d, dissociation rate constant (a.k.a. off-rate); K_D, equilibrium dissociation constant.

2.3.3 *Functional activation of KIR3DS1ζ Jurkat reporter cells is triggered by target cells expressing HLA-F OCs*

To determine whether cell-expressed KIR3DS1 can bind to and be activated by HLA-F OC-expressing target cells, we developed a reporter cell assay using Jurkat cells. Jurkat cells are a human $CD4^+$ T-cell leukemia line that is HLA-F- and -G-deficient and does not have HLA-Bw4. We furthermore performed CRISPR/Cas9-mediated

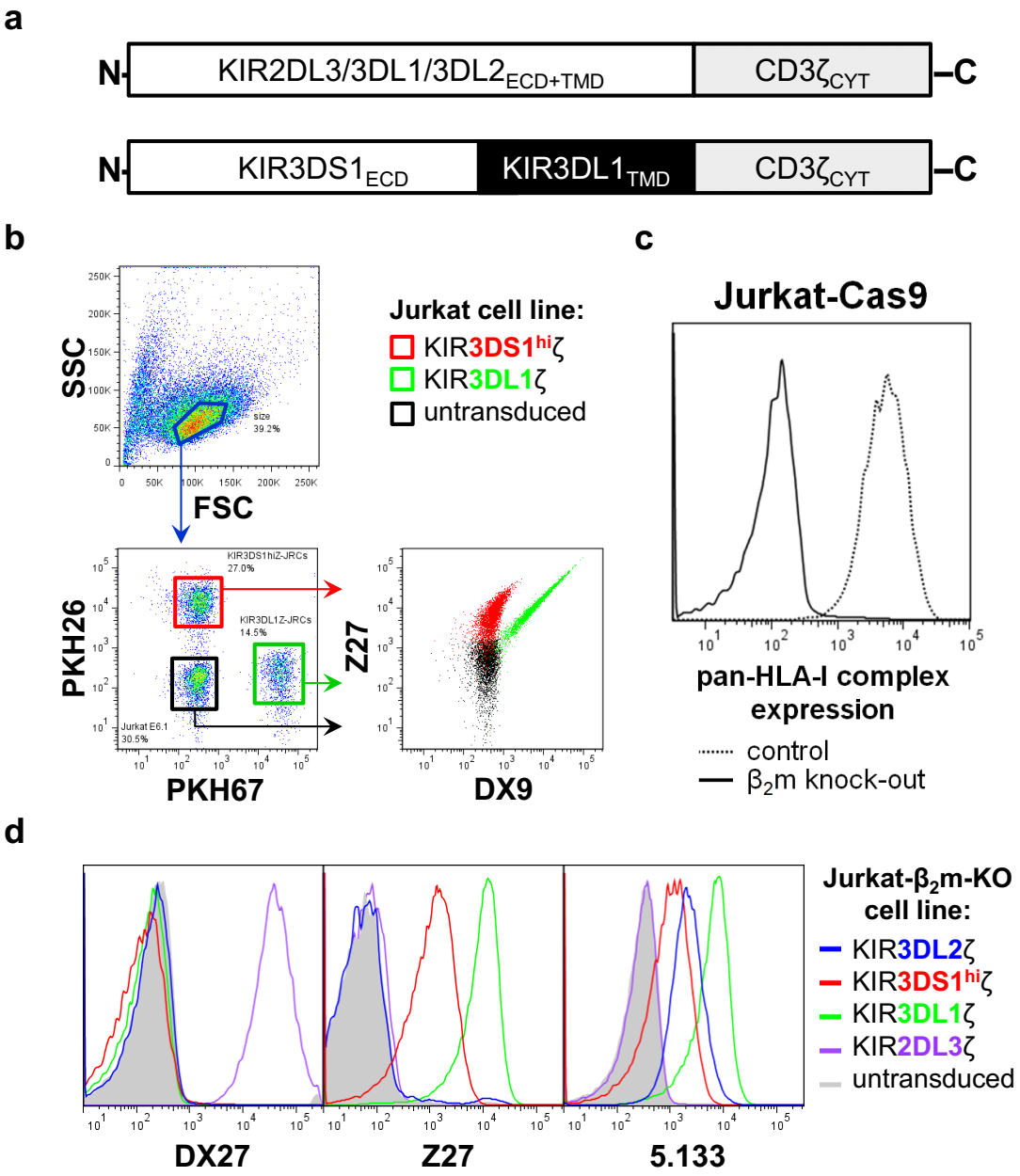

Figure 2.4: Generation of KIRζ Jurkat reporter cell lines. (***a***) KIRζ chimeric receptors for inhibitory and activating KIRs were designed by fusing the extracellular domain (ECD) and transmembrane domain (TMD) of the indicated KIRs with the triple immune tyrosine activating motif (ITAM)-containing cytoplasmic tail (CYT) of CD3ζ. (***b***) KIRζ-Jurkat reporter cell lines were labelled with fluorescent membrane dyes to allow for distinction and anti-KIR antibody staining was done for confirmation of KIR expression. PKH26 and PKH67 are red and green fluorescence membrane dyes, respectively; Z27 and DX9 are anti-KIR3DS1/L1 and anti-KIR3DL1 antibodies, respectively (***c***) CRISPR/Cas9-mediated β_2m knockout in Jurkat cells was confirmed by absent expression of HLA-I as measured by staining with anti-pan-HLA-I antibody (clone: W6/32). (***d***) Jurkat-β_2m-KO cells were stably transduced with indicated KIRζ chimeric receptors and staining with anti-KIR antibodies was performed to assess KIR expression; DX27, Z27, and 5.133 are anti-KIR2DL2/L3, anti-KIR3DS1/L1, and anti-KIR3DL2/S1/L1 antibodies, respectively.

knock-out of β_2m in Jurkat cells to eliminate surface HLA-I expression (**Fig. 2.4c**) and prevent potential self-activation. Jurkat cells were then stably transduced with chimeric receptors containing the extracellular and transmembrane domain of the KIR of interest and the cytoplasmic domain of CD3ζ, from herein called 'KIRζ' (**Fig. 2.4a**). For KIR3DS1, the transmembrane domain of KIR3DL1 was used instead to ensure cell surface expression in the absence of its adaptor DAP12, as has been previously shown[58]; we denoted this construct 'KIR3DS1^{hi}ζ'. Surface expression of KIRζ on Jurkat cells was confirmed by staining with the relevant anti-KIR antibodies (**Fig. 2.4b** and **Fig. 2.4d**), and CD69 expression was used as a reporter cell output, which was validated by anti-KIR antibody-mediated crosslinking (**Fig. 2.5**).

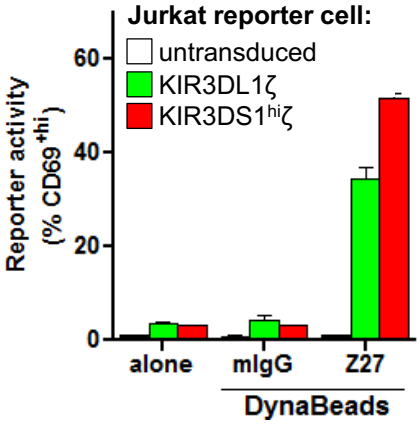

Figure 2.5: Functionality of KIRζ Jurkat reporter cell lines. Cell-sized Dynabeads covalently conjugated to anti-KIR3DL1/S1 (Z27) antibody or irrelevant mouse IgG (mIgG) were used for antibody-mediated crosslinking and activation of KIRζ Jurkat reporter cells as a functional positive control.

Initially, the ability of KIRζ-Jurkat reporter cells to bind to and be triggered by HLA-I-coated cell-sized beads was tested, and this assay showed that KIR3DS1ζ-Jurkat reporter cells avidly bound to and were potently triggered by HLA-F-coated beads, as were KIR3DL2ζ-Jurkat cells and KIR3DL1ζ-Jurkat cells to a much lesser extent (**Fig. 2.6a** and **Fig. 2.6b**). As expected, no binding or triggering by HLA-F-coated beads was observed for KIR2DL3ζ-expressing or untransduced Jurkat reporter cells. Next, KIRζ-Jurkat reporter cell activity was tested against cell lines that were untreated or acid

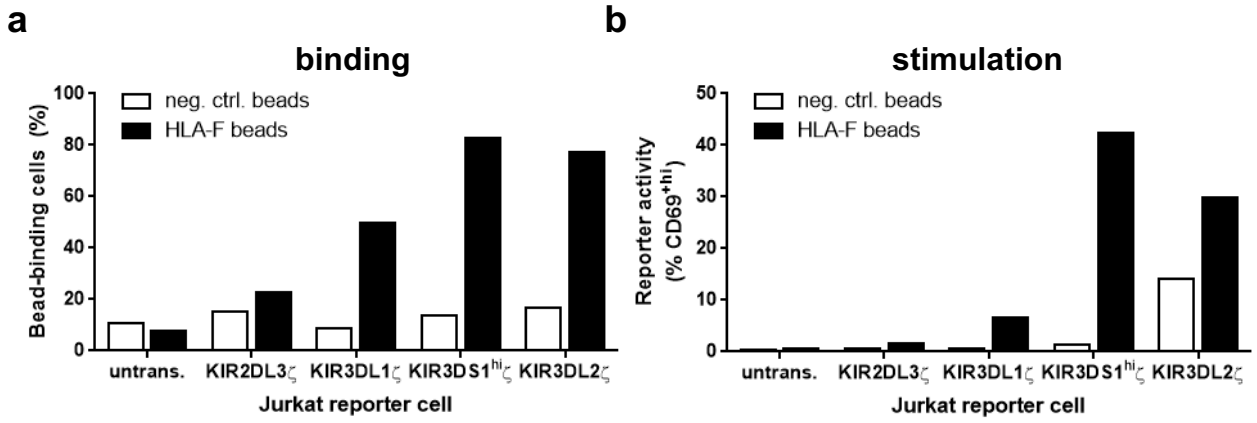

Figure 2.6: HLA-F-coated bead binding to and stimulation of KIRζ Jurkat reporter cell lines. Streptavidin beads were coated with free biotin (neg. ctrl. beads) or biotinylated HLA-F monomers (HLA-F beads), and these were co-incubated with the indicated KIRζ Jurkat reporter cells at a reporter:bead ratio of 1:50 for 8 h. The percentage of cells that bound beads (measured as a positive shift in side-scatter) (in ***a***) and the reporter cell activity (percentage of cells that highly expressed CD69) (in ***b***) was determined by flow cytometry.

pulsed to generate HLA-I OCs at the cell-surface, which was confirmed by anti-HLA-I OC antibody staining (**Supplemental Fig. S2.2**). 721.221 cells are a highly-mutated EBV-transformed B-cell line commonly used as NK-cell targets that are deficient in classical HLA-I genes and only express HLA-E and -F (i.e. *HLA-A*$^{-}$*B*$^{-}$*C*$^{-}$*E*$^{+}$*F*$^{+}$*G*$^{-}$). KIRζ-Jurkat reporter activity against 721.221 cells revealed that acid-pulsed 721.221 cells potently stimulated KIR3DS1^{hi}ζ-Jurkat cells (**Fig. 2.7a**), a finding that occurred independent of other expressed HLA-I allotypes (**Supplemental Fig. S2.3**). KIR3DL2ζ- and KIR3DL1ζ-Jurkat cells, but not KIR2DL3ζ-Jurkat cells, were also triggered by acid-pulsed 721.221 cells, but less potently, especially in the case of KIR3DL1ζ-Jurkat cells, in line with binding data (**Fig. 2.7a**). These data indicated that KIR3DS1 (as well as KIR3DL2 and to a lesser extent KIR3DL1) binds HLA-F OCs independent of classical HLA-I.

In assessing KIRζ-Jurkat reporter activity to other cell lines, we found that acid-pulsed EBV-transformed B cell lines (BCLs) derived from HLA-typed patients also

stimulated KIR3DS1^{hi}ζ-Jurkat cells, while other cell lines not encoding for HLA-F did not (i.e. Jurkat, EL-4, K562, and THP-1 cells) (**Fig. 2.7a** and **Supplementary Fig. S2.4**). In a separate experiment where KIRζ surface expression was accounted for, triggering of KIRζ Jurkat reporter cells by acid-pulsed BCLs revealed the highest level of reporter activity by KIR3DS1^{hi}ζ, followed by KIR3DL2ζ and then KIR3DL1ζ (**Fig. 2.8**), which

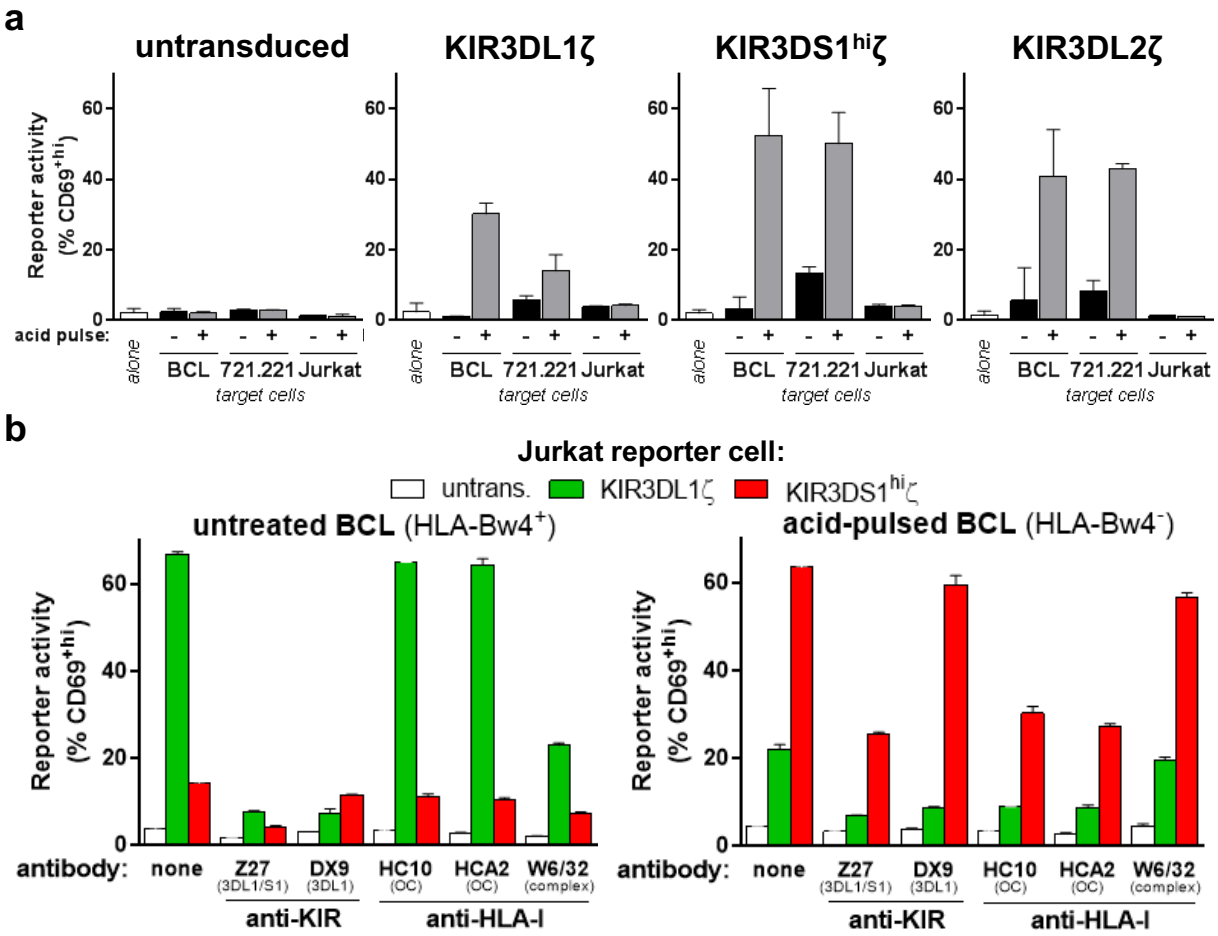

Figure 2.7: Functional triggering of KIR3DS1 on reporter cell lines by HLA-F OCs. (***a***) KIR3DL1ζ (*second panel*), KIR3DS1^{hi}ζ (*third panel*), KIR3DL2ζ (*fourth panel*), and untransduced (*first panel*) Jurkat reporter cells were co-incubated with untreated (–; *black bars*) or acid-pulsed (+; *gray bars*) cell lines (2.5-h incubation and reporter:target cell ratio of 1:10); reporter activity was measured as the percentage of CD69^{+hi} Jurkat reporter cells. Target cell lines used were an HLA-Bw4$^{–}$ donor-derived EBV-transformed B-cell line (BCL), 721.221 cells, and Jurkat cells. Data represent pooled data from n = 2 – 4 independent experiments. (***b***) KIR3DL1ζ (*green bars*), KIR3DS1^{hi}ζ (*red bars*), KIR3DL2ζ (*blue bars*), and untransduced (*white bars*) Jurkat reporter cells were co-incubated with an untreated HLA-Bw4^{+} BCL or an acid-pulsed HLA-Bw4$^{–}$ BCLs in the presence of anti-KIR or anti-HLA-I antibodies (each at 25 µg/mL) and reporter activity was measured. Antibodies used on graph are labeled with antibody clone and target antigen in parenthesis, and are the following: Z27, anti-KIR3DL1/S1 antibody; DX9, anti-KIR3DL1 antibody; HC10, anti-HLA-B,C OC (indirectly downregulates HLA-F); HC10, anti-HLA-A,G antibody (exhibits reactivity to HLA-F); W6/32, anti-pan-HLA-I complex antibody. Data represent n = 3 technical replicates.

correlated to SPR-determined affinities. These data showed that compared to other lineage II KIRs, KIR3DS1 exhibits the most potent functional signaling capacity upon engagement of HLA-F OCs on target cells.

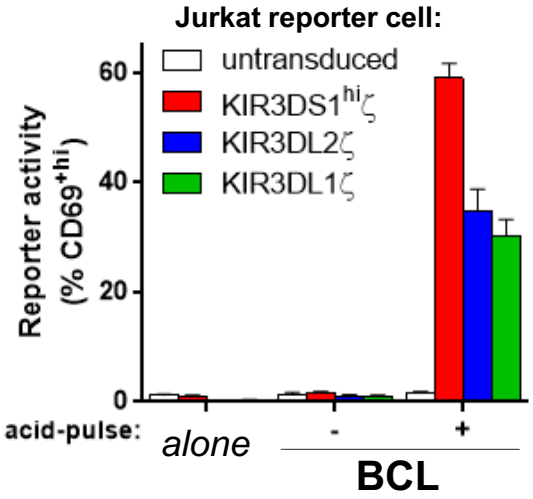

Figure 2.8: Comparison of KIRζ Jurkat reporter cell functional triggering by HLA-F OC-expressing target cells. KIR3DL1ζ (*green bars*), KIR3DS1^{hi}ζ (*red bars*), KIR3DL2ζ (*blue bars*), and untransduced (*white bars*) Jurkat reporter cells were co-incubated with untreated (-) or acid-pulsed (+) HLA-Bw4^{-} BCLs and reporter activity was measured. KIRζ expression was tightly controlled for when assessing percentage of CD69^{+hi} cells. Data represent *n* = 3 technical replicates.

To further confirm the interaction between KIR3DS1 and HLA-F OCs, antibody blockade experiments were performed. Of note, we did not have a specific anti-HLA-F OC blocking antibody at our disposal. Instead, two anti-HLA-I OC antibodies were used: HC10, which binds HLA-B, -C, and -E OCs but has been shown to indirectly down-regulate HLA-F OCs from the cell surface of target cells via endocytosis[57], and HCA2, which binds HLA-A and -G OCs but we determined exhibits reactivity to HLA-F OCs (data not shown). Accordingly, KIR3DS1^{hi}ζ Jurkat reporter cell activity induced by acid-pulsed BCLs could be blocked by anti-KIR3DS1/L1 and both anti-HLA-I OC antibodies, but not by anti-KIR3DL1 or anti-pan-HLA-I complex antibodies (**Fig. 2.7b**). In addition, adding soluble KIR3DS1-Fc to block ligands on target cells also abrogated KIR3DS1^{hi}ζ Jurkat reporter cell activity induced by acid-pulsed BCLs (**Fig. 2.9**). The results of these antibody blockade experiments are consistent with the finding that KIR3DS1 interacts with HLA-F OCs. On the other hand, KIR3DL1ζ Jurkat reporter cell activity triggered by

HLA-Bw4^{I80} expressing BCLs could be blocked by both anti-KIR3DL1 and anti-pan-HLA-I complex antibodies, but not by either anti-HLA-I open conformer antibody (**Fig. 2.7b**). This confirms the well-documented interaction between KIR3DL1 and HLA-Bw4^{I80} complexes. Of note, the weak reporter cell activity of KIR3DL1ζ-Jurkat cells stimulated by acid-pulsed HLA-Bw4-negative BCLs could be blocked by both anti-KIR3DL1 and anti-HLA-I open conformer antibodies, but not the anti-pan-HLA-I complex antibody (**Fig. 2.7b**). This further indicated a low-level interaction between KIR3DL1 and HLA-F OCs that is functionally much weaker as compared to KIR3DS1, which is remarkable in light of their high homology.

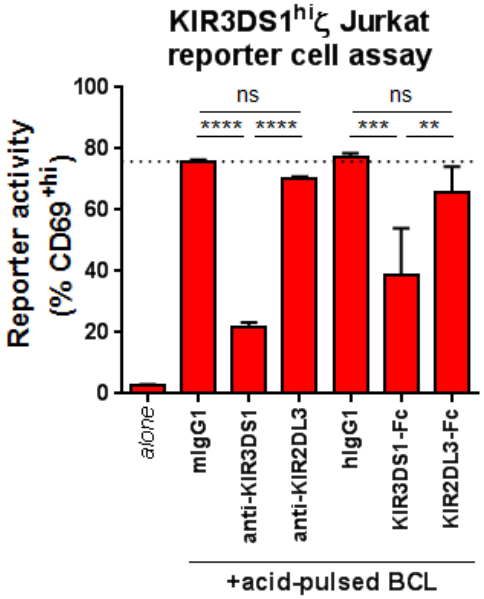

Figure 2.9: Anti-KIR antibody and KIR-Fc blockade of KIR3DS1^{hi}ζ Jurkat reporter cell triggering by HLA-F OC-expressing BCLs. KIR3DS1^{hi}ζ Jurkat reporter cells (*red bars*) were co-incubated for 2 h with acid-pulsed BCLs (reporter-to-target cell ratio = 1:10) in the presence of the indicated anti-KIR antibodies or KIR-Fc constructs and their respective isotype controls (each at 50 µg/mL) and reporter activity was measured. ***Labels:*** mIgG1, mouse IgG1 isotype control; anti-KIR3DS1, anti-KIR3DS1/L1 (clone: Z27) antibody; anti-KIR2DL3, anti-KIR2DL2/L3 (clone: DX27) antibody; hIgG1, human IgG1 isotype control; KIR3DS1-Fc, KIR3DS1-Fc fusion construct with Fc region of hIgG1; KIR2DL3-Fc, KIR2DL3-Fc fusion construct with Fc region of hIgG1. Data represents *n* = 3 technical replicates and is representative of *n* = 2 independent experiments.

2.4 MATERIALS AND METHODS

Cell lines and antibodies

721.221 and Jurkat (clone E6.1; ATCC) cell lines (including transductants) were grown in RPMI-1640 supplemented with 10% fetal bovine serum (Sigma-Aldrich), 2 mM L-glutamine (Gibco), 100 U/mL penicillin (Gibco), and 100 U/mL streptomycin (Gibco) at 37°C/5% CO_2. EBV-transformed B-cell lines (BCLs) were generated from peripheral blood mononuclear cells from donors bearing specific HLA genotypes; BCLs were also grown in the same media and conditions as 721.221 and Jurkat cells. The following purified antibodies were used for cell line-based staining and/or blocking assays: anti-KIR3DS1/L1 (clone: Z27.3.7, Beckman Coulter), anti-KIR3DL1 (clone: DX9, BioLegend), anti-KIR3DL1/L2/S1+2DS2/S4/S5/L2 (clone: 5.133, Miltenyi), anti-KIR2DL2/L3/S2 (clone: DX27, Miltenyi), anti-pan-HLA-I complex (i.e. anti-HLA-A,B,C,E,F,G +β_2m) (clone: W6/32, BioLegend), anti-HLA-B,C open conformers (clone: HC10; tebu-bio), and anti-HLA-A,G open conformers (clone: HCA2, tebu-bio), anti-CD3 (clone: HIT3a, BioLegend), anti-CD4 (clone: RPA-T4, BioLegend), and anti-CD69 (clone: FN50, BioLegend).

KIR-Fc binding to HLA-I-coated beads

Classical HLA-I-coated beads used were LABScreen single HLA-I beads (One Lambda). Acid pulsing of HLA-I-coated beads was performed by resuspending beads in 50 µL of 300 mM glycine (pH 2.4), incubating at room temperature for exactly 2 min, and washing three times with 1 mL of HBSS. Untreated and acid-pulsed beads were stained according to the manufacturer's instructions with KIR-Fc constructs (R&D

Systems) diluted to the indicated concentrations in PBS. Binding to beads was measured on a Bio-Plex 3D Suspension Array system using Luminex xMAP technology (Bio-Rad). To generate non-classical HLA-I-coated beads, biotinylated monomers of HLA-E/β_2m/VMAPRTLVL, HLA-F/β_2m, and HLA-G/β_2m/KGPPAALTL were purchased from Immune Monitoring Lab at Fred Hutchinson Cancer Research Center, Seattle, WA, and loaded onto streptavidin-coated beads (Life Technologies). Acid pulsing was performed as before. KIR-Fc staining was performed at the indicated concentrations for 45 min at 4°C while shaking. Beads were then washed and stained with goat anti-human IgG(Fc) F(ab')$_2$ PE-conjugated antibody (Life Technologies) diluted 1:50 for 30 min at 4°C while shaking. Beads were subsequently washed and fixed with 4% paraformaldehyde in PBS (Affymetrix) before flow cytometric analysis.

Lentiviral transduction/transfection

Jurkat cells stably expressing genes of interest were generated via lentiviral transduction. Gene constructs were designed accordingly and ordered from GeneArt (Life Technologies). Constructs were cloned into a lentiviral transfer vector containing an SFFV promoter and IRES-driven puromycin resistance. This backbone vector was generated by cloning the SFFV promoter from pAPM[59] into pLVX-EF1α-IRES-Puro (Clontech). HEK293T cells (ATCC) were transfected with a VSV-G envelope vector (pHEF-VSVG, obtained from NIH AIDS Reagent Program), HIV-1 gag-pol packaging vector (psPAX2, obtained from NIH AIDS Reagent Program), and the transfer vector of interest. Lentivirus-containing supernatants were harvested 3 d after transfection and used to transduce Jurkat cells, which were subsequently selected in 1 μg/mL puromycin

and sorted for gene expression by fluorescence-activated cell sorting (FACS). 721.221 HLA transductants were previously generated by retroviral transduction (by Christian Brander, Ragon Institute of MGH, MIT, and Harvard, Cambridge, MA) or generated via lentiviral transduction for this study, with the exception of HLA-G-expressing 721.221 cells, which were a kind gift from Jack Strominger (Department of Stem Cell and Regenerative Biology, Harvard University, Cambridge, MA). β_2m-knockout (β_2m-KO) Jurkat cells were generated KIRζ Jurkat reporter cell lines. For this, Jurkat cells were stably transduced with *S. pyogenes* Cas9 (lentiCas9-Blast was a gift from Feng Zhang[60]; Addgene plasmid # 52962) and selected in 5 μg/mL blasticidin S (Gibco). Jurkat-Cas9 cells were electroporated with a β_2m-targeting gRNA CRISPR vector (kindly provided by Leonardo Ferreira, Department of Stem Cell and Regenerative Biology and Department of Molecular and Cellular Biology, Harvard University, Cambridge, MA, and Thorsten Meissner, Department of Stem Cell and Regenerative Biology, Harvard University, Cambridge, MA; published in [61]) and sorted for loss of HLA expression. Jurkat-β_2m-KO cells were subsequently transduced with KIRζ chimeric constructs.

KIRζ Jurkat reporter cell assay

KIRζ-Jurkat reporter cells were incubated with target cells at a reporter:target cell ratio of 1:10 at 37°C/5% CO_2 for 2–2.5 h for acid-pulse experiments or for 8 h for experiments where acid pulsing was not a condition. For antibody blockade experiments, antibodies were pre-incubated with relevant cells (reporters or targets) for 30 min at 4°C before co-incubation of reporter and target cells; the antibodies remained

during the co-incubation. After the co-incubation, cells were stained with anti-CD3 and anti-CD69 antibodies and CD69 expression of reporter cells relative to negative and positive controls was assessed and used as a measure of reporter activity.

Surface Plasmon Resonance (SPR)

SPR measurements were conducted in HBS-EP buffer using a Biacore 3000 system (Biacore AB). To assess binding of various KIR-Fc constructs to HLA-F open conformers, biotinylated HLA-F monomers were immobilized onto a SA (streptavidin) sensor chip (GE Healthcare) to approximately 1000 response units (RU). A blank flow cell with no immobilized ligand was used as a reference flow cell. Injections of 60 µL of KIR-Fc constructs diluted in PBS to the indicated concentrations were performed at a flow rate of 20 µL/min, with a subsequent 10 min run of buffer to allow sufficient dissociation. Regeneration after each injection was done with two pulses of 100 µL of 10 mM glycine·HCl, pH 2.5, at a flow rate of 100 µL/min. Raw sensograms were corrected by double referencing (subtracting from the reference flow cell response and from PBS injection response). All experiments were done at standard temperature (25°C).

Data Acquisition and Analysis

Flow cytometry data were analyzed using FlowJo software version 7.6 (Tree Star) and statistical analyses were performed using GraphPad Prism 6 (GraphPad Software). KIR-Fc binding and CD69 reporter cell expression values are shown as mean values with error bars representing one standard deviation (SD). SPR data was

analyzed using BIAevaluation Software (GE Healthcare); given the dimeric nature of the KIR-Fc analyte, the bivalent analyte model was used to obtain proper fit of kinetic curves.

CHAPTER 3: The physiological impact and regulation of KIR3DS1:HLA-F interactions

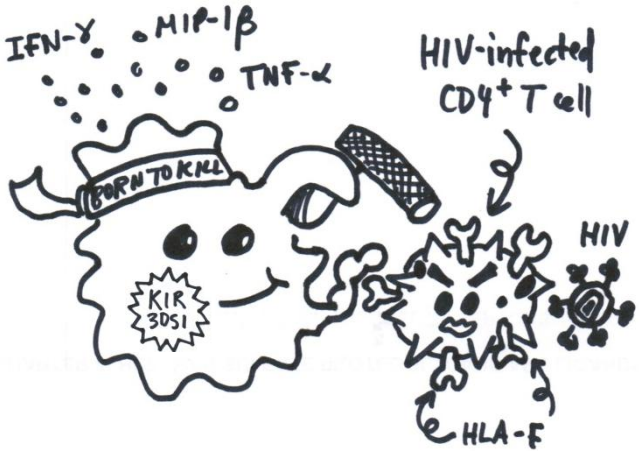

3.1 SUMMARY

The activating NK-cell receptor KIR3DS1 has been implicated in the outcome of various human diseases, including delayed HIV-1 disease progression, yet a ligand that accounts for its biological effects remained unknown. A previous screen revealed that KIR3DS1 binds HLA-F OCs, which was validated biochemically and functionally (see **Chapter 2**). In this study, we found that primary human KIR3DS1$^+$ NK cells degranulated and produced antiviral cytokines IFN-γ, MIP-1β, and TNF-α upon encountering HLA-F OCs. KIR3DS1$^+$ NK cells also exhibited a superior activity at suppressing HIV-1 replication *in vitro*, as has been previously reported. Exploring the cellular context of HLA-F expression, we found that CD4$^+$ T-cell activation triggered HLA-F transcription and expression and induced binding of soluble KIR3DS1-Fc. HIV-1 infection of activated CD4$^+$ T cells further increased HLA-F transcription, but partially decreased KIR3DS1 ligand expression, indicating an immune-evasion mechanism. In monocytic and T-cell lines transduced with FLAG-tagged HLA-F, we find that HLA-F is expressed intracellularly. However, mobilization of HLA-F to the cell surface could be achieved with cellular activation, IFN-γ treatment, and most potently by low-temperature incubation. Altogether, we established that KIR3DS1:HLA-F interactions are functionally relevant in primary human NK cells and demonstrate tight and complex regulation of HLA-F expression that may explain the widespread influence of KIR3DS1 in human diseases.

3.2 RESULTS

3.2.1 *HLA-F OCs potently trigger a polyfunctional response in primary KIR3DS1$^+$ NK cells*

To assess the functional impact of HLA-F OC binding to KIR3DS1 in primary human NK cells, KIR3DS1$^+$ and KIR3DS1$^-$ NK-cell clones (NKCLs) were generated via limiting dilution cloning from peripheral blood NK cells from a healthy KIR3DS1-homozygous donor. NKCLs were confirmed to be CD56$^+$KIR3DL1$^-$LILRB1$^-$ to ensure proper functionality, and had variable expression of KIR2Ds (**Supplementary Fig. S3.1**). These NKCLs were seeded into individual well plates coated with human IgG (for CD16 crosslinking), anti-KIR3DS1/L1 antibody (for KIR3DS1 crosslinking), or monomers of HLA-E, -F, or -G. To assess NKCL responses to plate-bound ligands, we measured cytotoxic granule exocytosis (i.e. degranulation), as determined by surface expression of CD107a, and production of antiviral cytokines IFN-γ, TNF-α, and MIP-1β by intracellular staining. Plate-bound HLA-F strongly and significantly triggered degranulation in KIR3DS1$^+$ NKCLs (**Fig. 3.1**) but not KIR3DS1$^-$ NKCLs (**Fig. 3.2**). The magnitude of this response was comparable to crosslinking of KIR3DS1 and CD16, and was able to be significantly reduced by addition of soluble anti-KIR3DS1/L1 antibody (**Fig. 3.2**). Plate-bound HLA-E and HLA-G produced a weak response in some but not all NKCLs, and this activation could not be blocked with soluble anti-KIR3DS1/L1 antibody. The observed effects were not due to intrinsic differences in response capacity, as all NKCLs (except for one that was CD16$^-$) were similarly triggered by CD16 crosslinking. In addition, HLA-F elicited production of antiviral cytokines IFN-γ, TNF-α, and MIP-1β in KIR3DS1$^+$ (but not KIR3DS1$^-$) NKCLs, and these responses

could be blocked with soluble anti-KIR3DS1/L1 antibody (**Fig. 3.1** and **Fig. 3.2**). Interestingly, KIR3DS1^{+} NKCLs had an intrinsic superior capacity to produce antiviral cytokines when compared to KIR3DS1^{-} NKCLs when encountering the same stimuli (**Supplementary Fig. S3.2**). Altogether, these data demonstrate that HLA-F triggers a potent activating signal via KIR3DS1 that results in polyfunctional responses by primary NK cells.

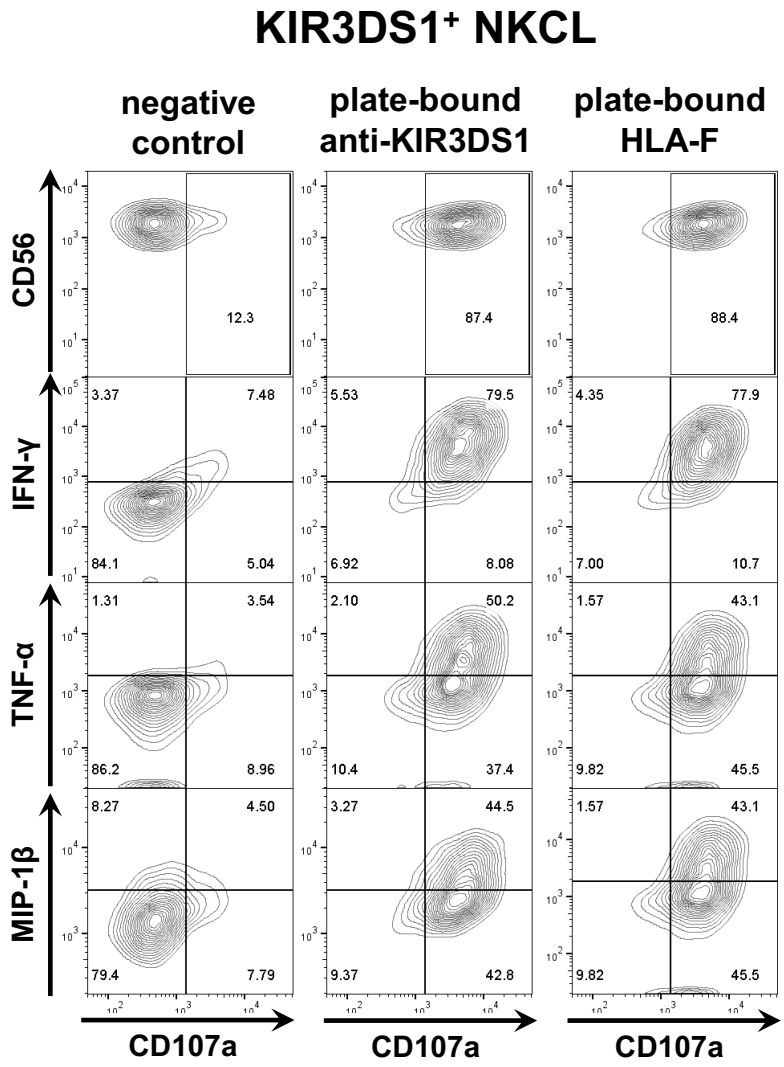

Figure 3.1: HLA-F OCs trigger a polyfunctonal response in KIR3DS1^{+} NK-cell clones. Flow plots of a KIR3DS1^{+} NKCL that was seeded onto well plates coated with irrelevant protein (negative control), anti-KIR3DS1/L1 antibody (plate-bound anti-KIR3DS1), or HLA-F monomers (plate-bound HLA-F), and incubated for 5 h in the presence of a fluorophore-conjugated anti-CD107a antibody and brefeldin A, followed by surface stain for NK-cell markers and intracellular cytokine stain for IFN-γ, TNF-α, and MIP-1β (for details, see **Materials and Methods**).

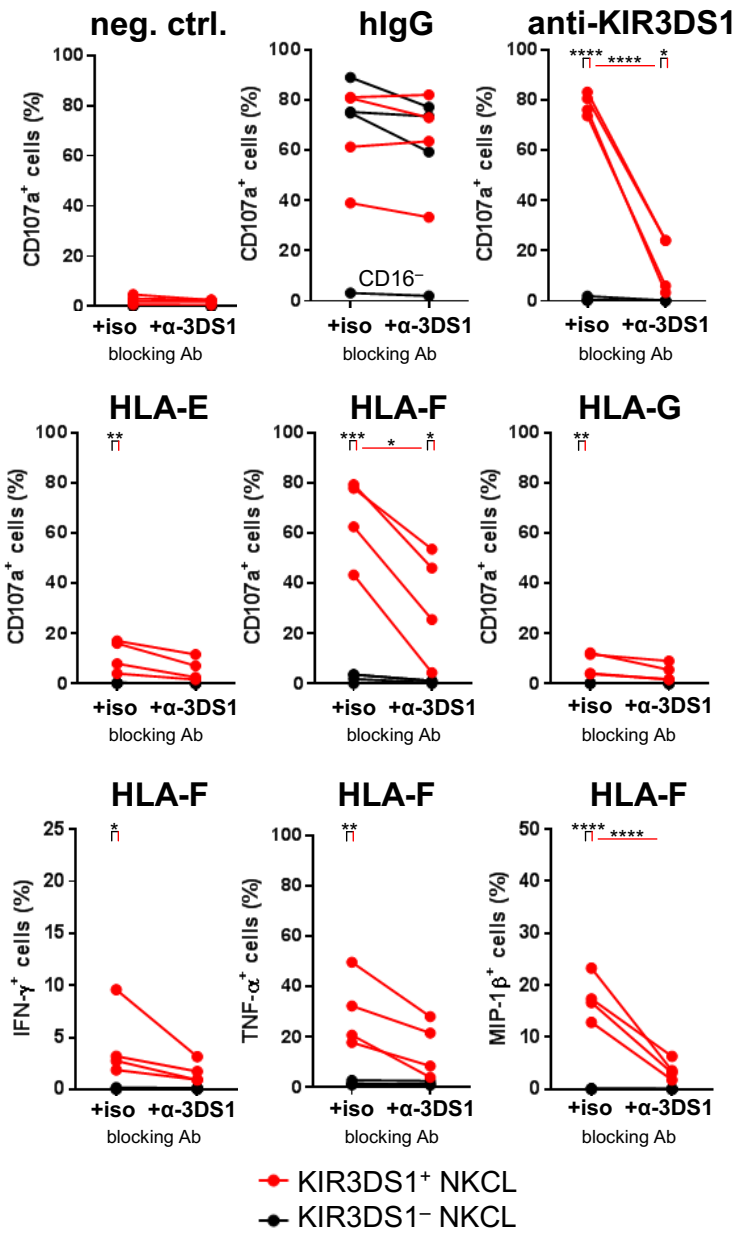

Figure 3.2: HLA-F OCs trigger degranulation and antiviral cytokine production in primary NK cells via KIR3DS1. KIR3DS1$^+$ (*red dots and lines*) and KIR3DS1$^-$ NKCLs (*black dots and lines*) were seeded onto well plates coated with irrelevant protein (fetal bovine serum; neg. ctrl.), human IgG (hIgG), anti-KIR3DS1/L1 antibody (clone: Z27; anti-KIR3DS1), or monomers of HLA-E, -F, or -G. For each plate-bound ligand condition, antibody-mediated blockade was performed by incubating NKCLs in the presence of mouse IgG1 isotype control antibody (+iso) or soluble anti-KIR3DS1/L1 antibody (+α-3DS1) (25 μg/mL each). NKCLs were incubated for 5 h with anti-CD107a fluorescent antibody and brefeldin A, followed by surface stain for NK-cell markers and intracellular cytokine stain for IFN-γ, TNF-α, and MIP-1β (for details, see **Materials and Methods**). The raw percentages of CD107a$^+$ NKCLs exposed to the indicated plate-bound ligands are presented in the upper six panels, and the raw percentages of IFN-γ$^+$, TNF-α$^+$, and MIP-1β$^+$ NKCLs exposed to plate-bound HLA-F are presented in the bottom three panels. One CD16$^-$ NKCL is indicated in hIgG. For each plate-bound ligand and marker, one-way ANOVA with Bonferroni multiple comparisons test comparing select columns was performed, and all statistically significant differences are presented (*, **, ***, and **** denote, p < 0.05, < 0.01, < 0.001, and < 0.0001, respectively).

3.2.2 *Activation of primary CD4$^+$ T cells induces KIR3DS1 ligand expression at the cell surface*

A previous study demonstrated that HLA-F can be expressed on the surface of activated lymphocytes[62]. To study KIR3DS1 ligand expression in a biologically relevant context, HLA-F expression and KIR3DS1-Fc binding to primary resting CD4$^+$ T cells and CD4$^+$ T cells stimulated with anti-CD3/28 beads and IL-2 was assessed. A Western blot-suitable anti-HLA-F antibody (validated in **Supplementary Fig. S3.3**) was used to assess protein levels, and resistance to endoglycosidase H (Endo H) digestion served as a measure of cell-surface expression. Endo H is a glycosidase that removes immature *N*-glycans from glycoproteins that have not undergone Golgi processing; thus, glycoproteins shuttled to the cell surface through the Golgi are rendered Endo H-resistant (i.e. there is no band shift on protein gel electrophoresis). Results showed that whereas unstimulated CD4$^+$ T cells do not have any detectable levels of HLA-F protein, stimulated CD4$^+$ T cells express HLA-F protein in a predominantly Endo H-resistant form, consistent with cell-surface expression (**Fig. 3.3a**); similar results were obtained with different stimulation conditions (48 h treatment with 12.5 ng/mL phorbol 12-myristate 13-acetate and 0.335 μM ionomycin; data not shown).

To determine if the up-regulation of HLA-F protein in activated CD4$^+$ T cells was transcriptionally induced, HLA-F mRNA levels were assessed via flow cytometry-based fluorescent *in situ* hybridization (FISH) (detailed in **Materials and Methods**). HLA-F mRNA-specific probes were used after testing their sensitivity and specificity in HLA-F$^+$ and HLA-F$^-$ cell lines (**Supplementary Fig. S3.4**). Activation of CD4$^+$ T cells increased the levels of HLA-F mRNA transcripts (**Fig. 3.3b**), indicating that HLA-F is

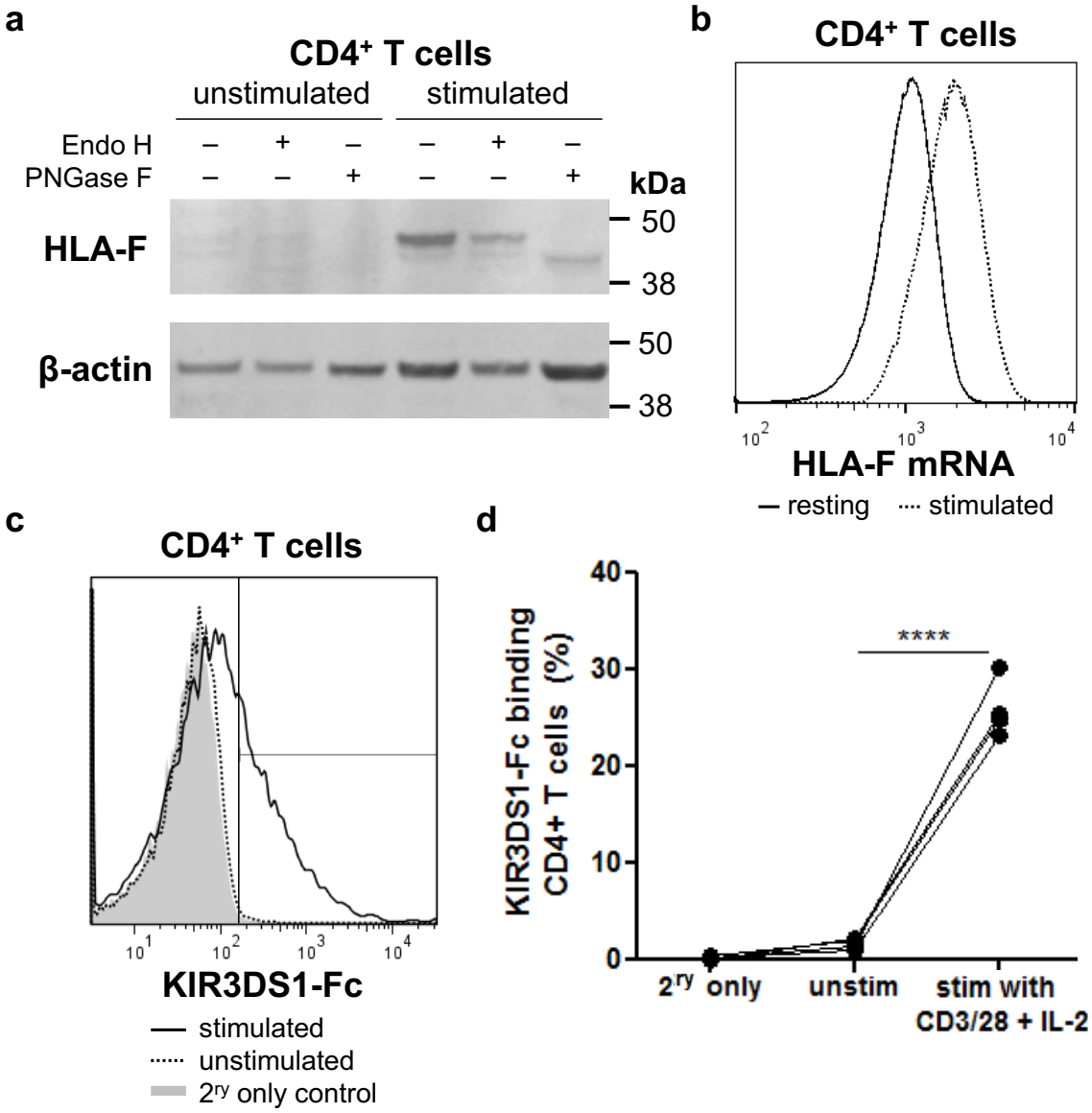

Figure 3.3: Activated CD4$^+$ T cells express HLA-F on the cell surface and bind KIR3DS1-Fc. (***a***) Purified CD4$^+$ T cells were unstimulated or stimulated with high-dose IL-2 (100 U/mL) and anti-CD3/28 beads for 14 days. Cell lysates underwent Endo H, PNGase F, or mock digestion, and reducing/denaturing SDS-PAGE was performed, followed by immunoblotting for HLA-F and β-actin (loading control). (***b***) CD4$^+$ T cells from a healthy donor were rested in culture medium or activated with PMA+ionomycin for 24 h before performing fluorescent *in situ* hybridization and flow cytometry to assess HLA-F mRNA levels; this data is representative of four independent donors. (***c***, ***d***) Purified CD4$^+$ T cells from four donors were activated with anti-CD3/28 beads and IL-2 (100 U/mL) for 6 d or left untreated and grown in modified media for 48 h prior to staining with KIR3DS1-Fc (25 µg/mL). The percentage of cells binding KIR3DS1-Fc was determined by setting gate based on sample stained only with secondary antibody (2ry only, i.e., no KIR-Fc) and these were plotted in ***d***; histograms from a representative donor are depicted in ***c***. Four donors were chosen based on HLA-B types, which were the following: B*08:01/B*18:01, B*08:01/B*14:02, B*44:02/B*44:02, and B*27:05/B*57:01. Paired *t* test was performed for unstimulated versus stimulated CD4$^+$ T cells (**** denotes $p < 0.0001$).

transcriptionally induced in $CD4^+$ T cells upon activation. Furthermore, KIR3DS1-Fc bound significantly to stimulated $CD4^+$ T cells, but not to unstimulated $CD4^+$ T cells (**Fig. 3.3c** and **Fig. 3.3d**, $p < 0.0001$). These results were consistent across donors with and without HLA-Bw4 allotypes, demonstrating that KIR3DS1 ligands are expressed on activated $CD4^+$ T cells regardless of their HLA-I genotype, and strongly suggesting KIR3DS1 binding to HLA-F expressed on activated $CD4^+$ T cells.

3.2.3 *HIV-1 infection of activated $CD4^+$ T cells increases HLA-F transcription but partially decreases KIR3DS1 ligand expression, and is suppressed by $KIR3DS1^+$ NK cells*

To assess the influence of HIV-1 infection on expression of KIR3DS1 ligands in $CD4^+$ T cells, HLA-F mRNA levels and KIR3DS1-Fc binding were assessed using activated $CD4^+$ T cells that were uninfected or infected with HIV-1 NL4-3. HLA-F mRNA levels were up-regulated in HIV-1–infected activated $CD4^+$ T cells when compared to uninfected activated $CD4^+$ T cells (**Fig. 3.4c**), indicating that HIV-1 infection further stimulated HLA-F mRNA transcription. In contrast, KIR3DS1-Fc binding was significantly decreased upon HIV-1 infection (**Fig. 3.4a** and **Fig. 3.4b**). The decrease in KIR3DS1-Fc binding was already observed in 'early' infected cells (defined as $p24^{dim}CD4^+HLA\text{-}I^+tetherin^+$), but was more pronounced in 'late' infected cells (defined as $p24^{hi}CD4^{dim}HLA\text{-}I^{dim}tetherin^{dim}$), indicating an as-yet-unknown mechanism by which HIV-1 might reduce KIR3DS1 ligand expression. This may be due to direct downregulation of HLA-F protein by HIV-1; however, due to the absence of an available flow cytometry-

suitable antibody against HLA-F, it was not possible to directly quantify HLA-F surface expression levels on HIV-1–infected cells.

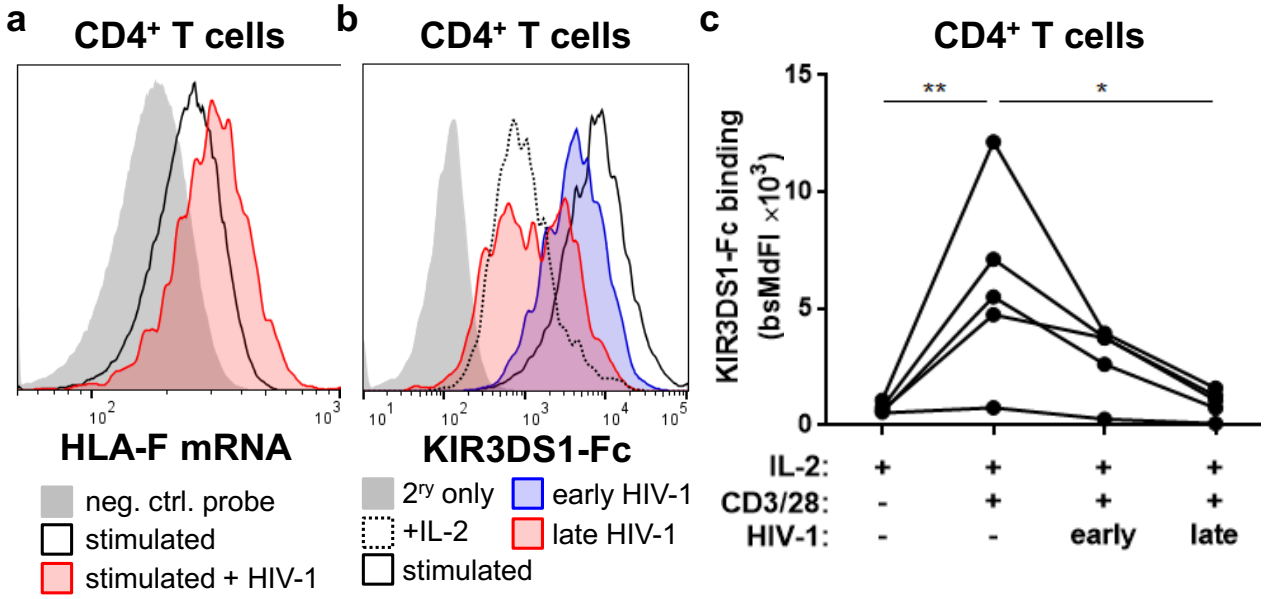

Figure 3.4: Effect of HIV-1 infection on HLA-F expression and KIR3DS1-Fc binding. (***a***) CD4$^+$ T cells from healthy donors were stimulated with IL-2 (100 U/mL) and anti-CD3/28 beads for 3 d, and were then cultured or infected with HIV-1 NL4-3. At 3 d post-infection (infection rate ~50%), fluorescent *in situ* hybridization and flow cytometry was performed to assess HLA-F mRNA levels. This data is representative of two independent experiments on two different donors. (***b***, ***c***) Purified CD4$^+$ T cells from five healthy donors were cultured in IL-2 (100 U/mL) and were either unstimulated or stimulated by plate-bound anti-CD3/28 stimulation for 7 d. Stimulated cells were then either continually cultured or infected with HIV-1 NL4-3. At 3 d post-infection (infection rate among five donors was ~100%), cells were stained for KIR3DS1-Fc (25 µg/mL) as well as intracellular HIV-1 p24 and additional markers to assess HIV-1 infection stage. Flow histogram in ***b*** depicts KIR3DS1-Fc binding to IL-2-cultured CD4$^+$ T cells, stimulated CD4$^+$ T cells, and stimulated CD4$^+$ T cells that are 'early' HIV-1–infected (p24^{dim}CD4$^+$HLA-I$^+$tetherin$^+$) or 'late' HIV-1–infected (p24^{hi}CD4^{dim}HLA-I^{dim}tetherin^{dim}). In ***c***, aggregate data for five healthy donors with background-subtracted median fluorescence intensities (bsMdFI) are shown with black lines connecting data points from each individual donor.

To evaluate the antiviral capacity of KIR3DS1$^+$ NK cells, HIV-1–infected autologous CD4$^+$ T cells were co-cultured for seven days with KIR3DS1$^+$ and KIR3DS1$^-$ NK-cell clones derived from a KIR3DS1 homozygous donor (for NK-cell receptor phenotypes, see **Supplementary Fig. S3.5**). Intracellular staining for HIV-1 p24 was performed to quantify the percentage of infected cells. Only KIR3DS1$^+$ NK-cell clones were effective at suppressing HIV-1 replication in autologous CD4$^+$ T cells, as seen by significantly less HIV-1 p24$^+$ CD4$^+$ T cells in the presence of KIR3DS1$^+$ NK cells (5.48 %

± 1.60 %), relative to KIR3DS1⁻ NK-cell clones (16.9 % ± 2.32 %; $p < 0.01$) or no NK cells added (mean 16.0 % ± 2.62 %, $p < 0.01$) (**Fig. 3.5a** and **Fig. 3.5b**). Thus, KIR3DS1⁺ NK cells have superior antiviral capacity towards HIV-1–infected autologous CD4⁺ T cells, as previously shown[13], and HIV-1–mediated downregulation of KIR3DS1 ligands on infected cells is not sufficient to enable complete immune evasion.

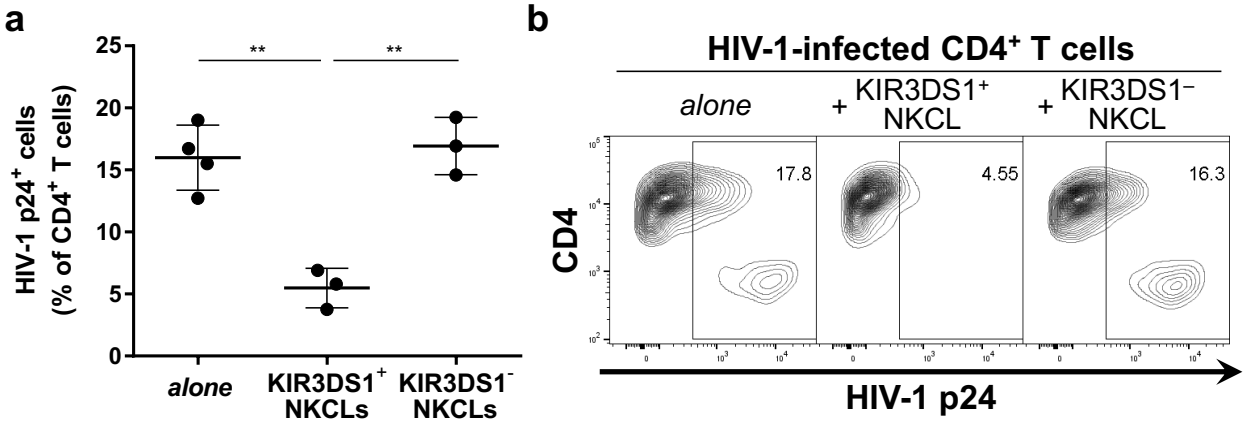

Figure 3.5: KIR3DS1⁺ NK cells efficiently suppress HIV-1 replication in autologous CD4⁺ T cell *in vitro*. (***a***, ***b***) KIR3DS1⁺ and KIR3DS1⁻ NKCLs were co-incubated with autologous HIV-1–infected CD4⁺ T cells for 7 d, after which intracellular staining for HIV-1 p24 and flow cytometry was performed to quantify amount of remaining HIV-1–infected CD4⁺ T cells. Aggregate results are presented ***a*** and representative flow cytometry plots are presented in ***b***. For ***a***, one-way ANOVA was performed with Tukey multiple comparisons test comparing all columns (** denotes $p < 0.01$).

3.2.4 *HLA-F is expressed intracellularly when transduced into T-cell, monocytic, and myeloid cell lines.*

To explore how HLA-F expression is regulated, various cell lines (i.e. Jurkat, THP-1, and K562 cells) were transduced with N-terminally FLAG-tagged HLA-F (HLA-F^{FLAG}) to allow detection by anti-FLAG antibody staining. Consistent with previous studies[56], all cell lines did not express HLA-F^{FLAG} on the cell surface, but rather expressed it intracellularly (**Fig. 3.6** and **Fig. 3.7**). To assess whether cellular activation or inflammatory cytokine treatment would mobilize HLA-F to the cell surface, as has been previously document in human immune and non-immune cells[62,63], THP-1 cells

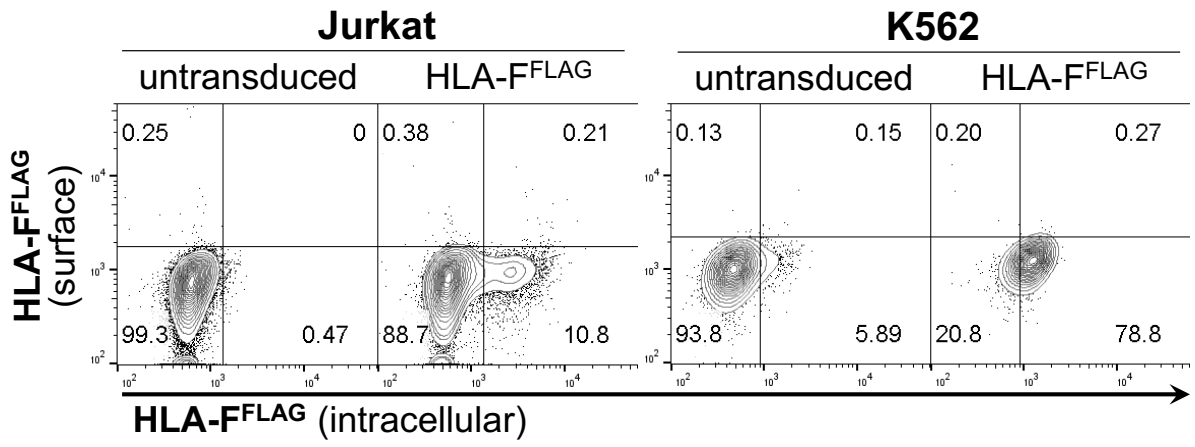

Figure 3.6: HLA-F is expressed intracellularly. Jurkat and K562 cells transduced with HLA-F^{FLAG} were stained with APC-conjugated anti-FLAG antibody to assess surface expression of HLA-F^{FLAG}, and then subsequently fix, permeabilized, and stained intracellularly with PE-conjugated anti-FLAG antibody to assess intracellular expression. ***Note*:** HLA-F^{FLAG} transduction efficiency differed by cell line.

were treated with PMA, IFN-γ, or both. PMA is a DAG analogue that activates protein kinase C and other cellular factors to induce potent cellular activation, and IFN-γ is a pro-inflammatory cytokine that upregulates MHC class I and II expression among many pleiotropic functions. Indeed, both PMA and IFN-γ induced cell-surface expression of HLA-F^{FLAG} in THP-1 cells, with IFN-γ being more potent than PMA, and both exhibiting synergy when combined (**Fig. 3.7**). Of note, IFN-γ treatment also induced expression of endogenous HLA-DR and HLA-G (data not shown), as has been previously reported for

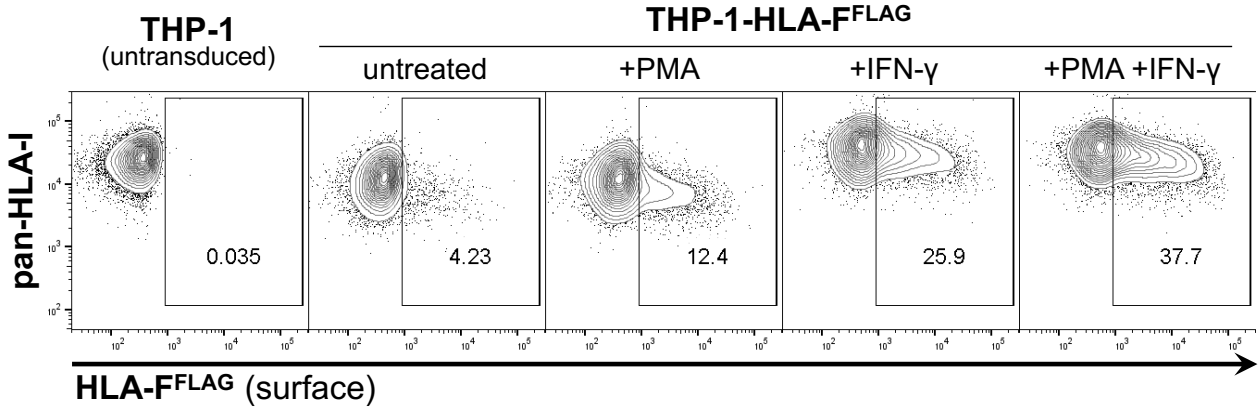

Figure 3.7: Cell-surface expression of HLA-F is induced by PMA and IFN-γ. THP-1 cells transduced with HLA-F^{FLAG} were either untreated or treated with 50 ng/mL PMA, 100 U/mL IFN-γ, or both for 48 h. Cells were subsequently stained with anti-FLAG antibody to assess cell-surface expression of HLA-F. Untransduced THP-1 cells were used as a negative control for staining.

THP-1 cells[64]. Of interest, we serendipitously discovered that incubation of THP-1-HLA-F^{FLAG} cells at a low temperature (26°C) potently mobilizes HLA-F^{FLAG} to the cell surface, resulting in very high surface expression (**Fig. 3.8**); this also occurred in Jurkat cells, although to a lesser extent (**Supplementary Fig. S3.6**). This finding, however, is not unprecedented given that lower temperatures increase the stability of HLA-I OCs and result in increased cell surface expression[65]; whether this increased stability is leading to increasing trafficking to the cell surface or decreasing endocytosis in the case of HLA-F remains to be determined. Altogether, our data shown that HLA-F is a predominantly intracellular HLA-I gene whose surface expression is tightly regulated and induced upon cellular activation or exposure to pro-inflammatory cytokines.

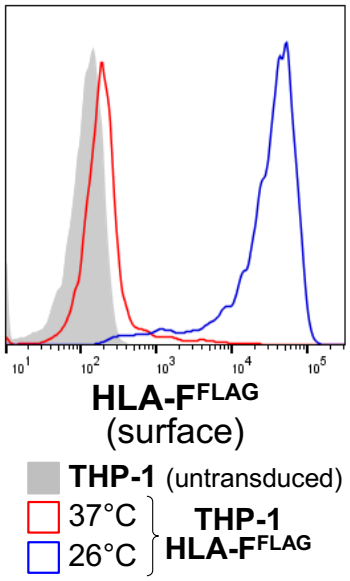

Figure 3.8: Low-temperature incubation potently mobilizes HLA-F to the cell surface. THP-1-HLA-F^{FLAG} cells were cultured under normal conditions (37°C and 5% CO_2) or incubated at 26°C (and 5% CO_2) for 18 h. Cells were subsequently stained with anti-FLAG antibody to assess cell-surface expression of HLA-F. Untransduced THP-1 cells were used as a negative control for staining.

3.3 MATERIALS AND METHODS

Cell lines

Jurkat (clone E6.1; ATCC), K562, and THP-1 cell lines (including transductants) were grown in RPMI-1640 supplemented with 10% fetal bovine serum (Sigma-Aldrich), 2 mM L-glutamine (Gibco), 100 U/mL penicillin (Gibco), and 100 U/mL streptomycin (Gibco) at 37°C/5% CO_2. The following purified antibodies were used for blocking or plate-bound ligand assays: anti-KIR3DS1/L1 (clone: Z27.3.7, Beckman Coulter), human.

Lentiviral transduction/transfection

Cell lines stably expressing genes of interest were generated via lentiviral transduction. Gene constructs were designed accordingly and ordered from GeneArt (Life Technologies). HLA-F sequence was obtained from NCBI (accession: P30511), and FLAG sequence was added after the signal peptide sequence. Constructs were cloned into a lentiviral transfer vector containing an SFFV promoter and IRES-driven puromycin resistance. This backbone vector was generated by cloning the SFFV promoter from pAPM[59] into pLVX-EF1α-IRES-Puro (Clontech). HEK293T cells (ATCC) were transfected with a VSV-G envelope vector (pHEF-VSVG, obtained from NIH AIDS Reagent Program), HIV-1 gag-pol packaging vector (psPAX2, obtained from NIH AIDS Reagent Program), and the transfer vector of interest. Lentivirus-containing supernatants were harvested 3 d after transfection and used to transduce cell lines, which were subsequently selected in 1 μg/mL puromycin and in some cases sorted for gene expression by fluorescence-activated cell sorting (FACS).

Primary human CD4$^+$ T-cell isolation, stimulation, infection, and staining with KIR-Fc and HLA-F mRNA probes

CD4$^+$ T cells were isolated from donor PBMCs by indirect magnetic labeling and negative selection, using the CD4$^+$ T cell isolation kit II (Miltenyi) according to the manufacturer's protocol. Stimulations were done differently depending on the experiment. Stimulations for Western Blots were done with anti-CD3/28 Dynabeads (Life Technologies) were done at a bead:cell ratio of 2:1 and culturing in supplemented RPMI with IL-2 (100 U/mL) for the indicated amounts of time. Stimulations for flow cytometry-based fluorescent *in situ* hybdridization were done with phorbol 12-myristate 13-acetate (12.5 ng/mL) and ionocymin (0.335 μM) (Cell Stimulation Cocktail used at 0.25X; eBioscience) for the indicated amounts of time. Stimulations for KIR-Fc staining and HIV-1 infection were done for the indicated amounts of time in supplemented RPMI with IL-2 (100 U/mL) on non-tissue culture-treated flat-bottom 48-well plates previously pre-coated with anti-CD3 (clone: OKT3, BioLegend) and anti-CD28 (clone: CD28.2, BioLegend) antibodies each at 10 μg/mL. HIV-1 infection was done by resuspending ~1 × 10^6 activated CD4$^+$ T cells in 1 mL of supplemented RPMI containing 100 U/mL of IL-2 and adding 1 × 10^5 $TCID_{50}$ of replication-competent HIV-1 NL4-3. Cell were immediately spinfected (centrifuging for 2 h at 1,500 × *g* at 37°C) and incubated at 37°C/5% CO_2 for 72 to allow for viral replication. For KIR-Fc staining of cells, cells were first stained with LIVE/DEAD® Fixable Blue Dead Cell Staining Kit (Life Technologies) following manufacturer's instructions, and then stained with 25 μg/mL of KIR3DS1-Fc for 45 min at 4°C while shaking, after which the cells were washed and stained with anti-CD3 (clone: UCHT1, BioLegend), anti-CD4 (clone: RPA-T4, BioLegend), anti-pan-

HLA-I complex (clone: W6/32, BioLegend), anti-tetherin (clone: RS38E), and goat anti-human IgG(Fc) $F(ab')_2$ PE-conjugated antibody (Life Technologies) for 30 min at 4°C while shaking. Cells were subsequently washed and subjected to fixation and permeabilization with the FIX & PERM ® Cell Fixation and Cell Permeabilization Kit (Life Technologies) to stain with anti-HIV-1 p24 (clone: KC57, BD Biosciences). Cells were subsequently washed and resuspended in PBS, except in assays where fixation and permeabilizationn was not done, in which case cells were fixed with 4% paraformaldehyde in PBS (Affymetrix) before flow cytometric analysis. Fluorescent *in situ* hybdridization was done with the PrimeFlow™ RNA Assay from Affymetrix with custom designed HLA-F mRNA specific probes following manufacturer's intructions. Flow cytometric analyses of samples were performed on a BD LSRFortessa.

Western Blot

2×10^6 Cells were lysed in 100 µL of lysis buffer (20 mM Tris·HCl, 100 mM NaCl, 1 mM EDTA, 0.5% Triton X-100, pH 8.0, all reagents from Sigma-Aldrich) containing 1X Halt™ protease and phosphatase inhibitor cocktail (Life Technologies). Nuclei were pelleted supernatants containing cytoplasmic and plasma membrane proteins were collected. Lysates were treated with Endo H_f (New England Biolabs), PNGase F (New England Biolabs), or mock treated according to manufacturer's instructions. Reaction products were denatured and reduced, and run on NuPAGE Novex 4-12% Bis-Tris protein gels (Life Technologies). Gel products were transferred over to a PVDF membrane, and dual immunoblotting was done with mouse anti-β-actin (clone: mAbcam 8224, Abcam) and rabbit anti-HLA-F (clone: EPR6803, Abcam) primary antibodies and

IRDye 800CW goat anti-human IgG(H+L) (LI-COR) and IRDye 680RD goat anti-rabbit IgG(H+L) (LI-COR) secondary antibodies. The blots were visualized using an Odyssey imaging system (LI-COR) and images were analyzed using Image Studio 3.1 software (LI-COR).

Generation of primary NK-cell clones

Primary human NK cells isolated from peripheral blood mononuclear cells (PBMCs) of healthy human donors were subcloned by limiting dilution in two manners. For the HIV-1 replication inhibition assay, NK cells were subcloned in the presence of feeders and maintained in NK-cell cloning medium consisting of supplement RPMI additionally supplemented with 5% human serum (Sigma-Aldrich), 1X MEM-NEAA (Gibco), 1X sodium pyruvate (Gibco), 100 µg/mL kanamycin, 450 U/mL IL-2 (AIDS Reagent Program, NIH) using a protocol adapted from a previously reported method[66]. Briefly, NK cells were isolated from peripheral blood mononuclear cells (PBMCs) from a *KIR3DS1*$^{+/+}$(homozygous) donor via magnetic negative selection (NK-cell isolation kit from Miltenyi), added to a mix of irradiated feeders consisting of freshly isolated allogeneic (PBMCs) combined with log-phase-growth RPMI 8866 cells (Sigma-Aldrich) at a 10:1 ratio in cloning medium containing 1 µg/mL phytohaemagglutinin (PHA; Fisher) and mixed thoroughly before plating at 100 µL/well (1 NK cell/well) in 96-well plates and incubated for 14 days at 37°C/5% CO_2. After 14 days, wells that had outgrowth of cells were transferred to 48-well plates and maintained in NK-cell medium with frequent media exchange (approximately every 3 days). For plate-bound ligand assays, NK cells were subcloned in the presence of irradiated K562 cells expressing

mbIL-15 and CD137L (kind gift from Dario Campana, published in [67]) and modified NK-cell cloning media consisting of RPMI supplemented with 15% fetal bovine serum (Sigma-Aldrich), 5% human serum (Sigma-Aldrich), 2 mM L-glutamine (Gibco), 1X MEM-NEAA (Gibco), 1X sodium pyruvate (Gibco), 100 µg/mL Primocin™ (Invivogen), 500 U/mL IL-2 (AIDS Reagent Program, NIH), with the addition of the following four cytokines to supplant the need for PBMC feeders: 5 ng/mL IL-15 (Peprotech), 10 ng/mL IL-12 (Peprotech), 40 ng/mL IL-18 (Peprotech), and 20 ng/mL IL-21 (Peprotech). NK-cell clones that grew out were continually cultured in modified NK-cell cloning media without additional cytokines. Cells were phenotyped by flow cytometry with the following antibodies: anti-CD56-BV421 (BioLegend), anti-CD16-BV785 (BioLegend), anti-NKG2A-APC (Beckman Coulter), anti-LILRB1-PE-Cy5 (BD Biosciences), anti-KIR3DL1/S1-PE (Beckman Coulter), anti-KIR2D1/S1-PerCP-Cy5.5 (clone: HP-MA4, BioLegend), and anti-KIR2DL2/L3 (clone: DX27, BioLegend). Only NK-cell clones that were $CD3^{-}CD56^{+}$ (rarely $CD16^{-}$) and $LILRB1^{-}$ were used for subsequent assays to ensure proper functionality.

NK-cell degranulation and intracellular cytokine staining assay

Non-tissue culture-treated flat-bottom 96-well plates were coated overnight at 4°C with 50 µL the following ligands diluted in PBS: 1 mg/mL human γ-globulins (Thermo Scientific), 1 µg/mL of both anti-CD335 (a.k.a. NKp46) (clone: 9E2, BioLegend) and anti-CD2 (clone: TS1/8, BioLegend) antibody, 1 µg/mL of anti-KIR3DS1/L1 (clone: Z27.3.7, Beckman Coulter), 10 µg/mL of HLA-E, -F, or -G monomer, or 0.5% bovine serum albumin (Miltenyi). ~1×10^4 NK cells in 100 µL of supplemented RPMI containing

3 µL of anti-CD107a-PE-Cy7 antibody (BioLegend) and 5 µg/mL brefeldin A (Biolegend) and in the presence of anti-KIR3DS1/L1 antibody or isotype control antibody (mouse IgG1, clone: MG1-45, BioLegend) were seeded onto ligand-coated plate wells. After a 5-h incubation at 37°C/5% CO_2, cells were first stained with LIVE/DEAD® Fixable Blue Dead Cell Staining Kit (Life Technologies) following manufacturer's instructions, and then stained with anti-CD56-BV421 (clone: HCD56, BioLegend) and anti-CD16-BV785 (clone: 3G8, BioLegend) antibodies for 15 min at 4°C. Cells were then fixed with BD Cytofix/Cytoperm solution (BD Biosciences) and permeabilized with BD Perm/Wash solution (BD Biosciences) following manufacturer's instructions, after which intracellular cytokine staining was carried out using the following antibodies: anti-IFN-γ-Alexa Fluor 647 (clone: 4S.B3, BioLegend), anti-TNF-α-BV650 (clone: Mab11, BioLegend), and anti-MIP-1β-PerCP-eFluor710 (clone: FL34Z3L, eBioscience). After washing, flow cytometric analysis was performed on a BD LSR Fortessa.

NK-cell co-incubation with HIV-1–infected autologous $CD4^+$ T cells

PBMCs from the same donor from which NK-cell clones were generated were thawed and $CD4^+$ T cells were enriched via magnetic negative selection with the EasySep™ Human $CD4^+$ T Cell Enrichment Kit (StemCell). $CD4^+$ T cells were cultured overnight in supplemented RPMI containing 50 U/mL of IL-2 and 1 µg/mL PHA. The next day, cells were washed and resuspended at 1×10^6 cells/mL in supplemented RPMI containing 50 U/mL of IL-2. HIV-1 JR-CSF was added to a final concentration of 1×10^4 $TCID_{50}$/mL, and cells were incubated for 4 h at 37°C/5% CO_2. Afterwards, infected $CD4^+$ T cells were washed, resuspended in NK cell medium, and plated in a round-

bottom 96-well plate at 5×10^4 cells/well. NK-cell clones from the same donor were added to individuals wells at 1.25×10^5 cells/well (NK cell:$CD4^+$ T cell ratio = 2.5:1). Cells were co-cultured for 7 days, after which surface staining for CD3 and CD4 and intracellular staining for HIV-1 p24 was performed for flow cytometry assessment.

Human Samples and Viruses

Frozen peripheral blood mononuclear cells (PBMCs) from healthy donors were used in this study in accordance to protocols approved by Partners Human Research Committee and Institutional Review Board of Massachusetts General Hospital. HLA/KIR genotypes of selected human samples were determined prior to this study by high-resolution HLA typing performed at the HLA-typing laboratory of the National Cancer Institute, National Institutes of Health, and Sanger Sequencing-based KIR genotyping performed by Mary Carrington's laboratory. HIV-1 NL4-3 and HIV-1 JR-CSF were purchased from the Virology Core of the Ragon Institute of MGH, MIT, and Harvard, and are quality controlled for infectivity and titered on stimulated human PBMCs by standard endpoint $TCID_{50}$ assay.

HLA-F^{FLAG}–transduced cell lines assays

For FLAG staining, PE- and APC-conjugated anti-FLAG antibodies (clone: L5, BioLegend) were used. In experiments that assessed cell-surface versus intracellular HLA-F^{FLAG} expression, cells were stained with APC-conjugated anti-FLAG antibody, and then fixed with BD Cytofix/Cytoperm solution (BD Biosciences) and permeabilized with BD Perm/Wash solution (BD Biosciences) following manufacturer's instructions, after

which intracellular staining with PE-conjugated anti-FLAG antibody was performed. Flow cytometric analysis followed.

Data Acquisition and Analysis

Flow cytometry data was acquired on BD LSR Fortessa and analyzed using FlowJo software version 7.6 (Tree Star) and statistical analyses were performed using GraphPad Prism 6 (GraphPad Software).

CHAPTER 4: Heparan sulfate proteoglycans are ligands of KIR3DS1 and other NK-cell receptors

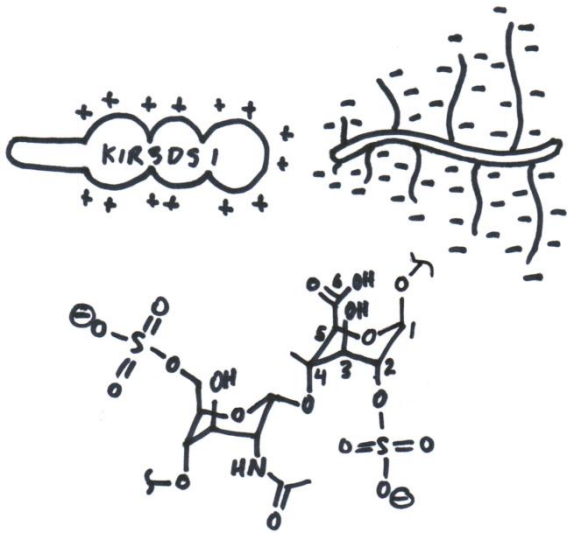

4.1 SUMMARY

While an overwhelming majority of NK-cell receptor:ligand interactions studied are protein:protein in nature, the role of protein:carbohydrate interactions in NK-cell function exists and could be more fully explored. In this study, we performed a genome-wide CRISPR/Cas9 knock-out screen for KIR3DS1 ligands and identified heparan sulfate (HS) as a KIR3DS1 ligand. This was validated biochemically by surface plasmon resonance and on cell lines, and was shown to be completely dependent on the presence of HS sulfate moieties. Further studies revealed that KIR3DL1, a highly homologous inhibitory allotype of KIR3DS1, also bound HS. As binding of other NK-cell receptors to HS has been described (for NKp30, NKp44, NKp46, and KIR2DL4), these data indicate that NK-cell receptor:HS interactions are widespread and could play important roles in NK-cell–receptor regulation and target-cell recognition that need to be further investigated.

4.2 BACKGROUND

Unlike T cells, which rely primarily on the T-cell receptor to recognize specific MHC complexes presenting peptides sampled from intracellular and/or extracellular compartments, NK-cell function is dictated by germline-encoded activating and inhibitory receptors that interact with a plethora of ligands expressed on target cells. Of all the receptor:ligand interactions studied, an overwhelming number are protein:protein in nature, leaving a major gap in our knowledge of the role of non-protein NK-cell–receptor ligands.

A major group of non-protein NK-cell–receptor ligands are carbohydrates expressed on target cells. Indeed, all cells in the body bear a glycocalyx, a term used to refer to the entire array of glycans coating the cell surface[68]. However, this term is highly misleading because it grossly underestimates the complexity and heterogeneity of these glycans. Cell surface glycans can be (*i*) non-covalently adsorbed to the cell surface, (*ii*) covalently linked to lipids, called glycolipids, or (*iii*) covalently linked to proteins in the form of glycoproteins or proteoglycans. Proteoglycans (PGs), in particular, consist of a core protein with one or more covalently linked glycosaminoglycans (GAGs), which usually dictate most or all of the PG's function. GAGs are long, unbranched polysaccharides whose disaccharide building blocks consist of an amino sugar and a uronic acid or galactose and can be modified extensively by acetyl and sulfate substitutions. These modifications are exquisitely intricate and diverse, and tightly regulated on individual cells.

There are five types of GAGs: hyaluronic acid (HA), keratan sulfate (KS), dermatan sulfate (DS), chondroitin sulfate (CS), and heparan sulfate (HS). The most

abundant GAGs found on most cell surfaces are HA and HS[69]. HA is a unique and relatively simple GAG that is unmodified (i.e. non-sulfated and non-acetylated) and does not exist as a PG. HS, on the other hand, is a GAG made as a PG by every cell in the body and plays a multitude of biological roles (reviewed in [70]) including: barrier function[71]; coagulation[72]; wound repair[73,74]; development[75,76]; endocytosis[77] and transcellular transport[78]; virus attachment and entry[79–84]; tumorigenesis[85]; cell adhesion and migration, including leukocyte homing[86]; signaling of growth factors[87,88], morphogens, cytokines[89], and chemokines[90]; and host defense[91]. HS biosynthesis begins in the endoplasmic reticulum (ER) with serial addition of specific glycosyl groups to generate a β-linked tetrasaccharide primer—Xyl(β1-4)Gal(β1-3)Gal(β1-3)Glc—on a serine residue of an HSPG protein core, a reaction catalyzed in series by XYLT1 and/or XYLT2, B4GALT7, B4GALT6, and B3GAT3. The possible HSPG protein cores are syndecans (1 through 4), glypicans (1 through 6), betaglycan, serglycin, and occasionally, neuropilin-1 and certain isoforms of CD44; all of these contain at least one Ser-Gly motif near a patch of acidic residues onto which HS is polymerized. Subsequent reactions by exostosin glycosyltransferases (EXT1 and EXT2) and exostosin-like glycosyltransferases (EXTL1, EXTL2, and EXTL3) add repeating β1-4-linked disaccharides of *N*-acetyl glucosamine and glucuronic acid. The extended polysaccharide can be subsequently modified in the Golgi by epimerization of glucuronic acid to iduronic acid catalyzed by GLCE, and by a complex array of sulfotransferase reactions. These sulfotransferase reactions are (*i*) *N*-deacetylation/*N*-sulfation of GlcNAc by any of four enzymes (NDST1–4); (*ii*) 6-*O*-sulfation by any of three enzymes (HS6ST1–3); (*iii*) 2-*O*-sulfation by a single enzyme (HS2ST1); and (*iv*)

more infrequently[92], 3-*O*-sulfation by any of several enzymes (HS3ST1–6). Fully formed HSPGs can be secreted or displayed on the cell surface, where they may be edited by sulfatases (SULF1 and SULF2). While the most well-known form of HS is heparin, a highly sulfated form that is made and secreted only by connective-tissue mast cells and used as an anti-coagulant, by far the most prevalent form is HSPGs found on cell surfaces. Much like DNA or RNA, HS does not have a single structure or sequence, but rather, the basic polysaccharide components that make HS vary depending on the cell type and cellular context under which they are made. Thus, HS has been referred to as "the most information-dense biopolymers found in nature"[93].

Among its biological functions, HS has been shown to interact with numerous immune receptors. The natural cytotoxicity receptors (NCRs) NKp30, NKp44, and NKp46, which are widely expressed activating NK-cell receptors[94], have been shown to bind to specific HS motifs. NKp30 and NKp46 bind to epitopes containing of 2-*O*-sulfated iduronic acid and 6-*O*- and *N*-sulfated glucosamine, whereas NKp44 binds to epitopes containing 2-*O*-sulfated iduronic acid and *N*-acetylated glucosamine[95]. In addition, a genome-wide siRNA screen discovered that another activating NK-cell receptor, KIR2DL4, bound to HS in a manner that depended on 3-*O*-sulfation[96] and that directly influenced KIR2DL4 signaling and NK-cell function.

In this study, while investigating possible non-HLA-I ligands for the activating NK-cell receptor KIR3DS1 through a genome-wide CRISPR/Cas9 knock-out screen, we found that KIR3DS1 binds HS. KIR3DS1 binding to HS was completely dependent on HS sulfation and upon further testing of other KIRs, we found that the functionally divergent inhibitory allotype KIR3DL1 also bound to HS, although to a lesser extent.

Similar to other described NK-cell receptor:HS interactions, which occur in *cis* and in *trans*, these findings uncover a novel KIR3DS1 ligand that may play influential roles in NK-cell tuning of receptor signaling and recognition of targets cells.

4.3 RESULTS

4.3.1 *KIR3DS1 ligands are expressed in several human cell lines of various tissue origins, but are variably expressed on primary cells.*

In order to screen cell lines for KIR3DS1 ligand expression, we used a KIR3DS1-Fc fusion chimera consisting of the extracellular domain of KIR3DS1 attached to the Fc region of human IgG1 (KIR3DS1-Fc), which confers increased avidity to KIR3DS1 ligands due to Fc dimerization. Surprisingly, KIR3DS1-Fc bound significantly to all human cell lines of T-cell origin (Jurkat), B-cell origin (721.221 and RAJI), monocytic origin (THP-1), and erythro-myeloid origin (K562) tested (**Fig. 4.1a**). To assess variability across human donors in transformed primary cells, we assessed KIR3DS1 ligand expression in various EBV-transformed B-cell lines (BCLs), all of which expressed KIR3DS1 ligands although at variable levels (**Fig. 4.1b**). In addition, upon staining peripheral blood lymphocytes isolated from healthy donors, we found that while B cells stained positively for KIR3DS1-Fc across donors, although variably, NK cells and $CD4^+$ and $CD8^+$ T cells did not (**Fig. 4.2a** and **Fig. 4.2b**).

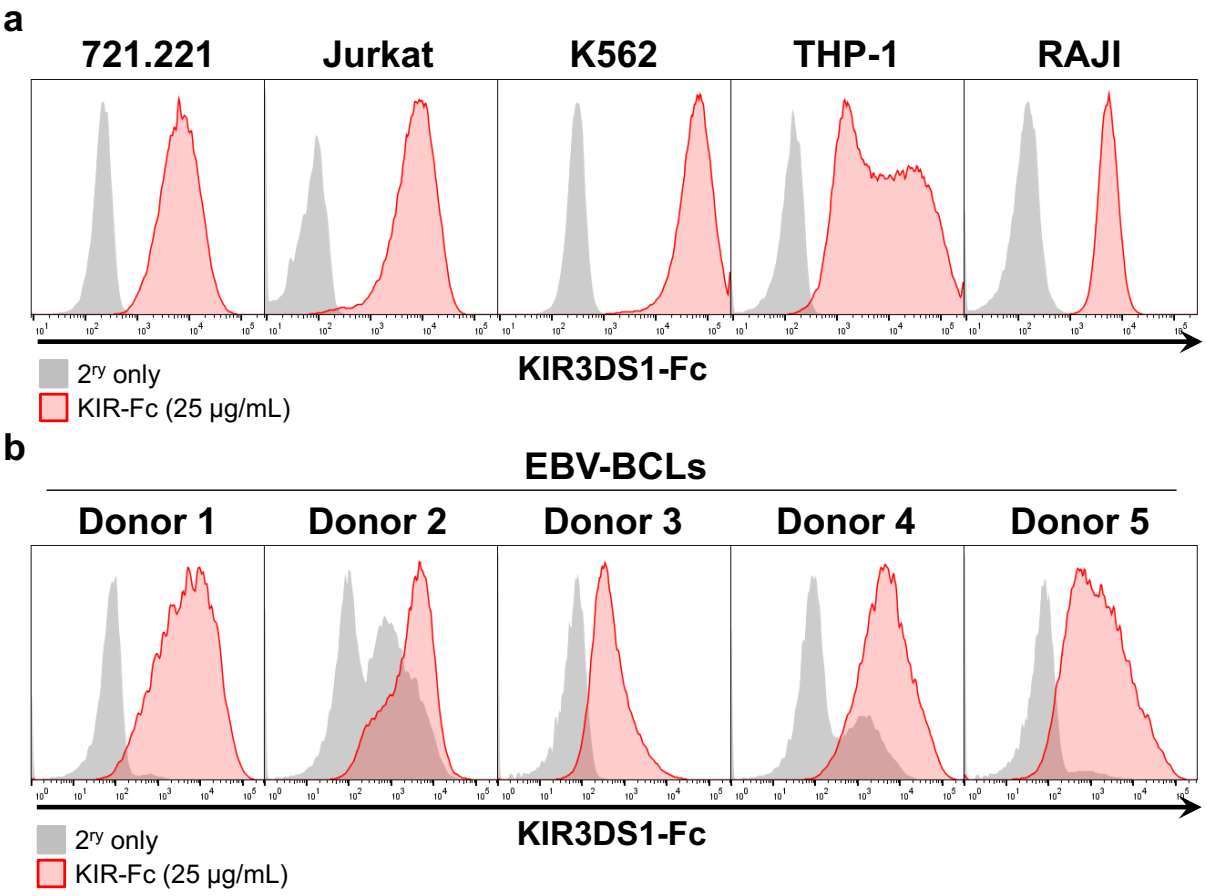

Figure 4.1: Human cell lines of various tissue origins express KIR3DS1 ligands. Human cell lines (in ***a***) and EBV-transformed B-cell lines (BCLs) from different donors (in ***b***) were stained with KIR3DS1-Fc to screen for KIR3DS1 ligands. (*Note:* Additional peaks in '2ry only' histograms in ***b*** are due to variable frequencies of IgG^+ BCL cells recognized by anti-hIgG(Fc)-PE secondary antibody)

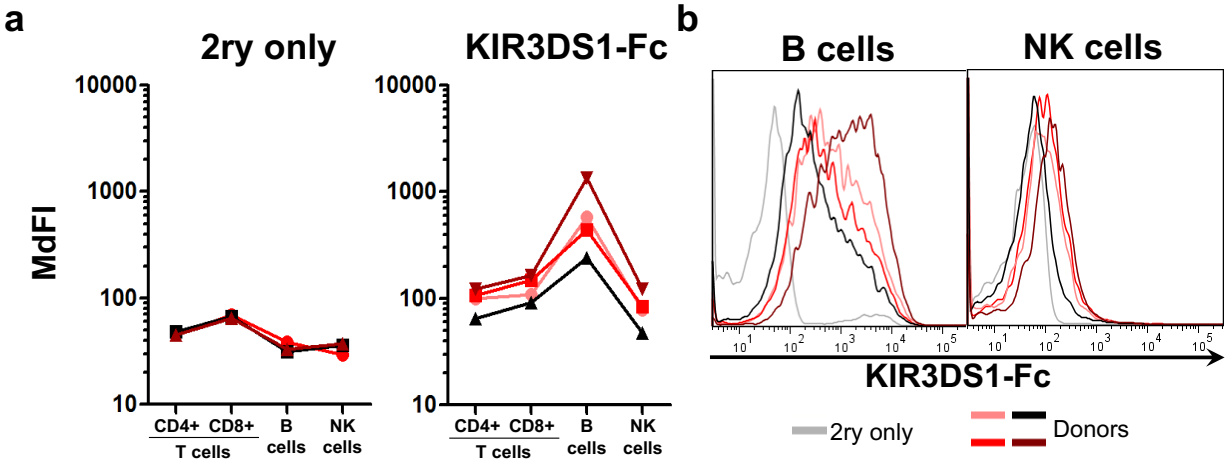

Figure 4.2: Peripheral blood lymphocytes show cell-type–dependent KIR3DS1 ligand expression. Peripheral blood mononuclear cells were isolated form four different donors, stained with KIR3DS1-Fc and lineage markers (anti-CD3, anti-CD4, anti-CD8, anti-CD19, anti-CD56, and anti-CD16 markers). Median fluorescence intensity (MdFI) of secondary only (i.e. anti-hIgG(Fc)-PE) staining and KIR3DS1-Fc staining is plotted in ***a***, and flow histograms for B cells and NK cells are ploted in ***b***.

4.3.2 *Genome-wide CRISPR/Cas9 knock-out screen reveals heparan sulfate biosynthesis enzymes are critical for KIR3DS1 ligand expression*

Given the widespread distribution of KIR3DS1 ligand expression across various human cell lines, we decided to perform a genome-wide CRISPR/Cas9 knock-out (GeCKO) screen in the highest expressing cell line—namely, K562 cells—as previously described[97] (**Fig. 4.3a**; see details in **Materials and Methods**). Briefly, ~1.8×10^8 K562 cells expressing Cas9 were transduced with a single-guide RNA library that individually targeted every human gene in individual cells, and were then cultured under selection to allow for gene knock-out to occur. 5×10^7 K562-GeCKO cells were then stained with KIR3DS1-Fc, followed by a secondary stain with a PE-conjugated anti-human IgG (Fc-specific) antibody, and a tertiary stain with a magnetic-bead–conjugated anti-PE antibody. The stained K562-GeCKO cells were then passed through a magnetic column to bind cells still bearing KIR3DS1 ligand, and flow-through cells were cultured, expanded, and then analyzed by flow cytometry. As **Fig. 4.3b** shows, while almost all pre-enriched library cells bound to KIR3DS1-Fc, magnetically depleted flow-through cultured cells had ~50% of cells staining very dimly for KIR3DS1-Fc binding.

In order to determine the genes knocked-out in K562 cells that resulted in loss of KIR3DS1-Fc binding, the enriched K562-GeCKO cells were deep sequenced to assess for enrichment of specific gRNA sequences (for details, see **Materials and Methods**). Remarkably, sequencing showed that the top nine enriched target genes were enzymes involved in HS biosynthesis (**Fig. 4.3c** and **Supplementary Table S4.1**). These enzymes were directly involved in either HS polysaccharide backbone polymerization (i.e. XYLT2, B4GALT7, B3GAT3, EXTL3, EXT1, EXT2), or in the synthesis of precursor

molecules needed for HS biosynthesis (i.e. UXS1, UGDH, and PAPSS1) (see **Illustration 4.1**). These results were highly suggestive of HS being necessary for KIR3DS1-Fc binding to K562 cells.

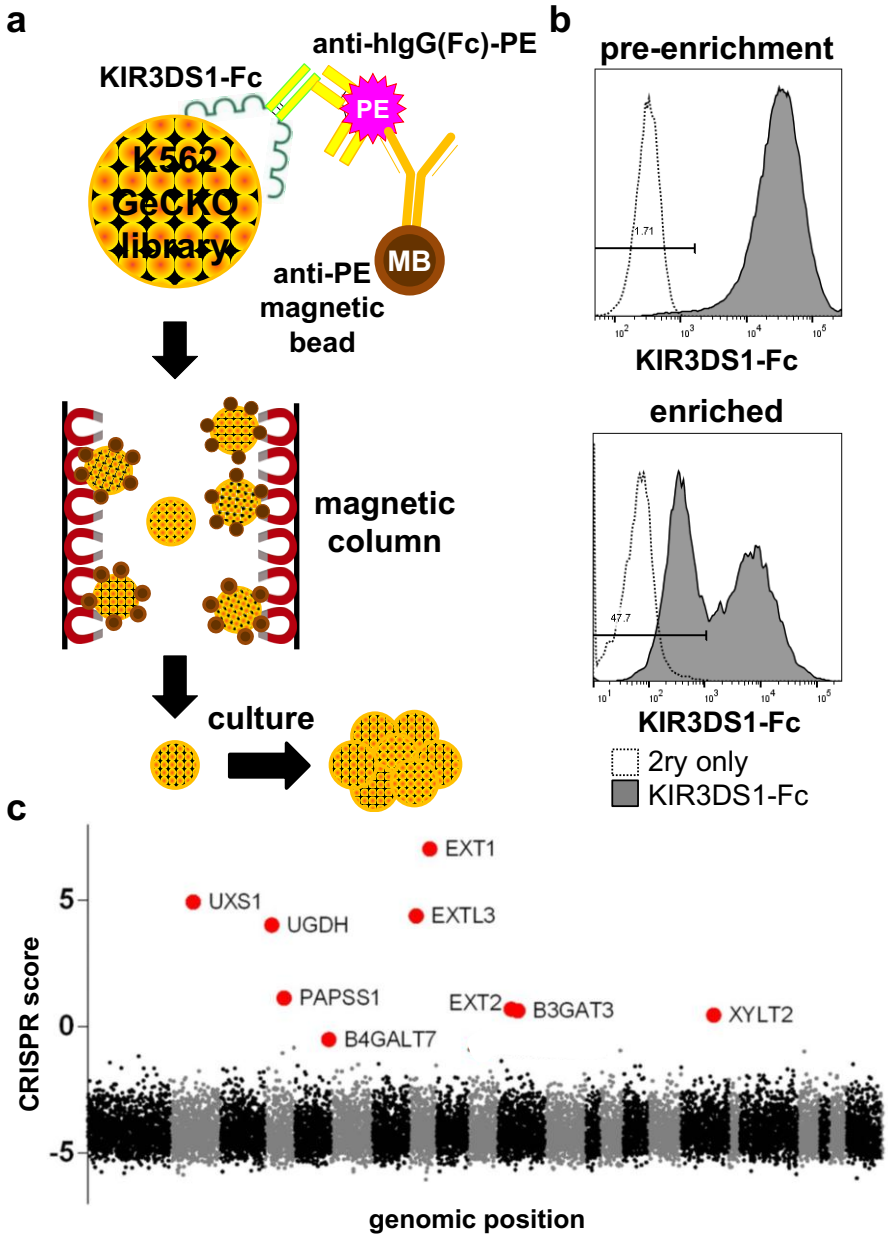

Figure 4.3: Genome-wide CRISPR/Cas9 knock-out screen for KIR3DS1 ligands identified heparan sulfate biosynthesis genes. (***a***) Strategy used to magnetically enrich for K562-GeCKO cells that lost KIR3DS1 ligand expression. (***b***) Flow cytometry histograms of K562-GeCKO cells before (*top*) and after (*bottom*) magnetic enrichment. (***c***) Graph depicting enrichment of gRNA-targeted genes calculated from sequencing analysis of enriched K562-GeCKO cells. CRISPR score calculation is described in **Material and Methods**. Each dot indicates a particular gene, and each alternating section of black and gray dots indicates individual chromosomes (chromosomes 1 – 22 and X+Y). Large red dots indicate top nine enriched genes (i.e. hits), all of which were involved in HS biosynthesis.

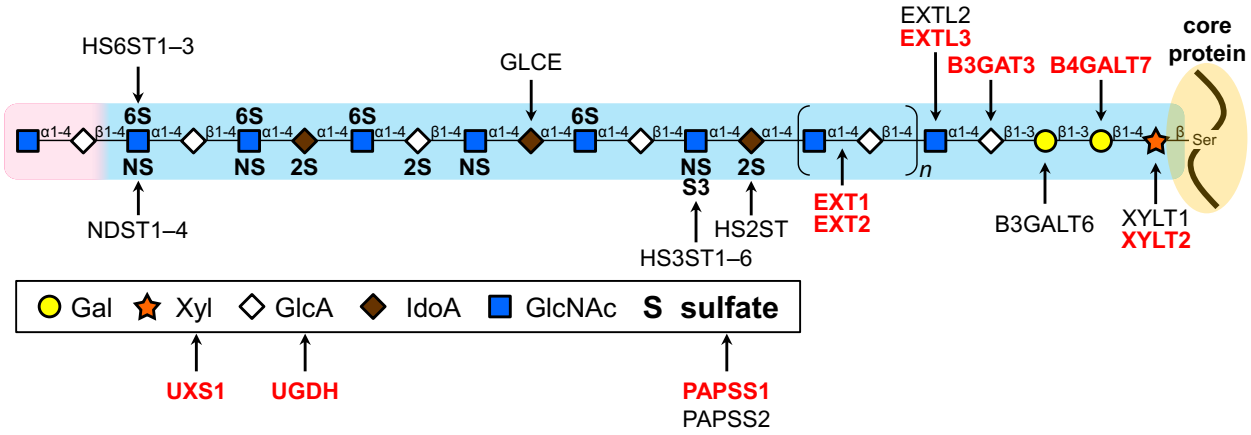

Illustration 4.1: Heparan sulfate biosynthesis. Diagram of HS structure and enzymes involved in its biosynthesis. GeCKO screening top nine hits are in red bolded text.

4.3.3 *Surface plasmon resonance confirms KIR3DS1 binding to heparan sulfate*

To confirm our findings, we performed surface plasmon resonance to comparatively assess the affinities of KIR3DS1 to different GAGs. Biotinylated hyaluronic acid (HA), chondroitin sulfate (CS), and heparan sulfate (HS) were immobilized onto individual flow cells of a streptavidin sensor chip at saturating concentrations, and KIR3DS1-Fc was flowed over. In concordance with our previous results, KIR3DS1-Fc bound significantly to HS, while exhibiting minimal to no binding to CS or HA (**Fig. 4.4a**), thus confirming the interaction between KIR3DS1 and HS.

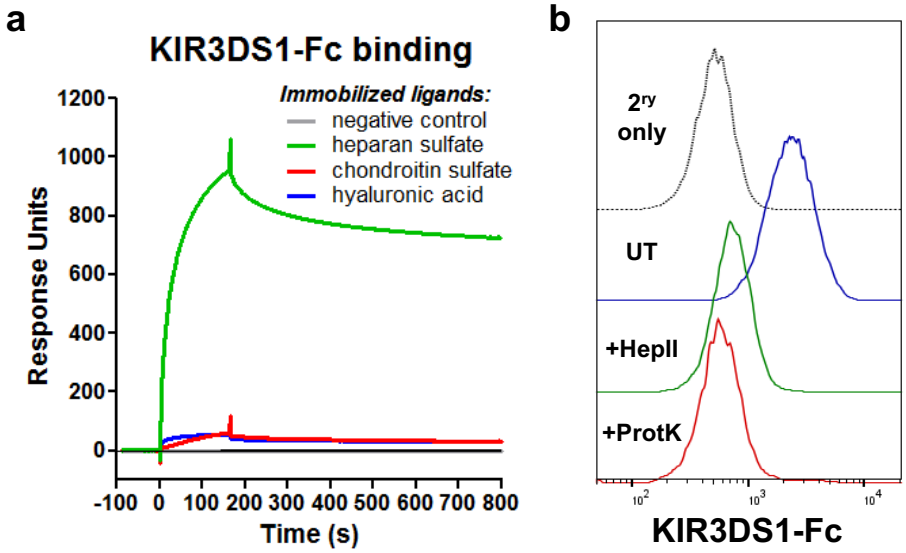

Figure 4.4: KIR3DS1 binds to heparan sulfate. (***a***) Surface plasmon resonance (SPR) sensogram of KIR3DS1-Fc (25 µg/mL) flowed over immobilized heparan sulfate, chondroitin sulfate, or hyaluronic acid for 3 min, and then allowed to dissociate by flowing over buffer for 10 min. (***b***) Flow histogram of 721.221 cells treated with heparinase II, proteinase K, or no enzyme and stained with KIR3DS1-Fc (25 µg/mL).

4.3.4 *Elimination of cell-surface heparan sulfate abrogates KIR3DS1-Fc binding*

Next, we investigated whether eliminating cell-surface HS reduced KIR3DS1-Fc binding to cell lines that exhibited high KIR3DS1-Fc binding. To accomplish this, 721.221 cells were enzymatically treated with heparinase II, proteinase K, or no enzyme. Heparinase II cleaves HS at glycosidic bonds between *N*-sulfated and glucuronic or iduronic acid residues, whereas proteinase K (a serine protease) will cleave cell-surface proteins including HS proteoglycan protein cores without affecting cell integrity. Indeed, enzymatic treatment with both heparinase II and proteinase K resulted in a dramatic decrease in KIR3DS1-Fc binding, proving that KIR3DS1-Fc is indeed binding to HSPGs (**Fig 4.4b**).

To determine whether KIR3DS1 binding to cell-surface HS was dependent on HS sulfate moieties, BCLs were cultured in sulfate-free media containing 50 mM sodium chlorate ($NaClO_3$). Chlorate (ClO_3^-) is an inhibitor of 3'-phosphoadenosine-5'-

phosphosulfate (PAPS) synthase, an enzyme required to generate PAPS, which is the universal sulfate donor for all cellular sulfotransferase reactions. In order to assess KIR3DS1-Fc binding and HS sulfation content after sulfation inhibition treatment, cells were stained at various time points with KIR3DS1-Fc and an anti-HS antibody (clone: 10E4) that recognizes *N*-sulfated GlcN residues[98]. Continuous culture in sulfate-free/$NaClO_3$-containing media resulted in loss of cell-surface HS sulfation and concomitant decrease in KIR3DS1-Fc binding (**Fig. 4.5a**). This demonstrated that KIR3DS1 binding to HS is dependent on the presence of sulfate moieties, which has been shown to be the case for other HS-binding proteins[93]. A separate experiment evaluating KIR3DS1 binding after culturing cells in sulfate-free media containing different concentrations of ClO_3^- for 48 h revealed that KIR3DS1-Fc binding was lost even at low concentrations of ClO_3^- (**Fig. 4.5b**). One report demonstrated that ClO_3^- concentrations of 5–20 mM resulted in selective loss of HS 6-*O*-sulfate moieties[92], which may implicate these specifically in KIR3DS1 binding to HS.

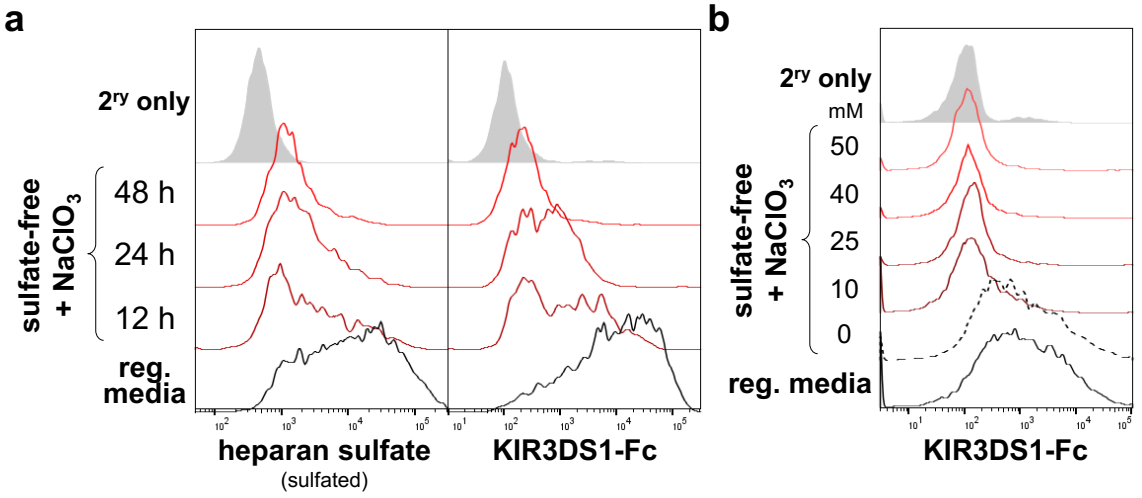

Figure 4.5: KIR3DS1 binding to heparan sulfate requires sulfation. (***a***) Human donor-derived BCL cells were cultured for the indicated amounts of time with sulfate-free media containing 50 mM $NaClO_3$ or regular media and separately stained with anti-HS antibody (clone: 10E4) and KIR3DS1-Fc (25 µg/mL). (***b***) BCL cells were cultures for 48 h in sulfate-free media containing the indicated concentrations (in mM) of $NaClO_3$, and then stained with KIR3DS1-Fc (25 µg/mL). For ***a*** and ***b***, flow histograms are presented, with gray filled histograms indicating isotype control or secondary only staining (iso).

4.3.5 *Other D0-domain containing KIRs exhibit HS binding*

Given that protein:HS binding is dominated by electrostatic interactions between positively-charged basic residues on proteins and negatively-charged sulfate residues on HS, we computationally determined the isoelectric point (pI) of various domains and regions of the extracellular portion of several KIRs to roughly assess their potential for interacting with HS. We found that the D0 domain of all known KIRs have an pI above physiological pH (**Fig. 4.6**), which signifies that they are net charge positive in the body and are more likely binding to HS. However, the D1 domain of all KIRs exhibited an pI below physiological pH and thus were net charge negative, with the exception of KIR3DS1, which was the only KIR with a D1-domain pI above physiological pH driven mainly by a L166R change (relative to KIR3DL1) that is critical to preventing binding to HLA-Bw4^{I80} proteins[24]. Indeed, a prior study showed that the D0 domain of KIR2DL4 (which along with KIR2DL5 is the only KIR2D that bears a D0-D2 domain structure) is responsible for binding of KIR2DL4 to HS. Thus, we proceeded to assess staining with other KIR-Fc constructs on B-cell lines there were or were not cultured in sulfate-free/$NaClO_3$-containing media. Sulfation inhibition did not affect KIR2DL3-Fc or KIR3DL2-Fc staining, but it did significantly decreased KIR3DL1-Fc staining (**Fig. 4.7**). This indicates that KIR3DL1—a highly homologous but functionally divergent allotype of KIR3DS1—also binds to HS, although to a lesser extent. Lack of KIR2DL3-Fc staining was expected, given the D1-D2 domain structure. However, the lack of KIR3DL2 binding to HS was surprising, but this may be due to (*i*) lack of optimal HS motifs/moieties necessary for KIR3DS1 binding on the tested B-cell lines, or

KIR	pre	D0	link	D1	link	D2	hinge
2DL1	7.03			6.02	4.31	8.05	6.27
2DL2	8.61			6.54	4.31	7.00	6.02
2DL3	7.03			7.14	4.31	8.05	4.87
2DS1	8.61			6.44	4.31	8.82	5.39
2DS4	6.93			6.54	4.31	8.06	6.02
2DL4	8.24	9.51	8.60			5.34	5.76
2DL5A	6.92	9.19	10.74			7.01	5.77
3DL1	10.84	8.82	11.72	7.01	4.75	9.69	6.27
3DS1	10.84	8.82	11.72	8.05	4.75	9.69	6.27
3DL2	10.84	9.30	11.72	5.79	4.31	8.82	8.08
3DL3	6.01	8.86	9.31	6.04	4.31	8.06	6.92

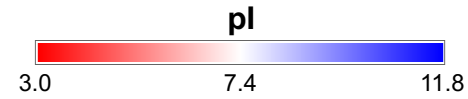

Figure 4.6: Calculated isoelectric point of KIR domains and regions. The isoelectric point (pI) of individual domains and regions of the indicated KIRs was calculated using the ExPASy Compute pI/Mw tool[99]. This was used as a rough estimate of the net charge status of each domain/region.

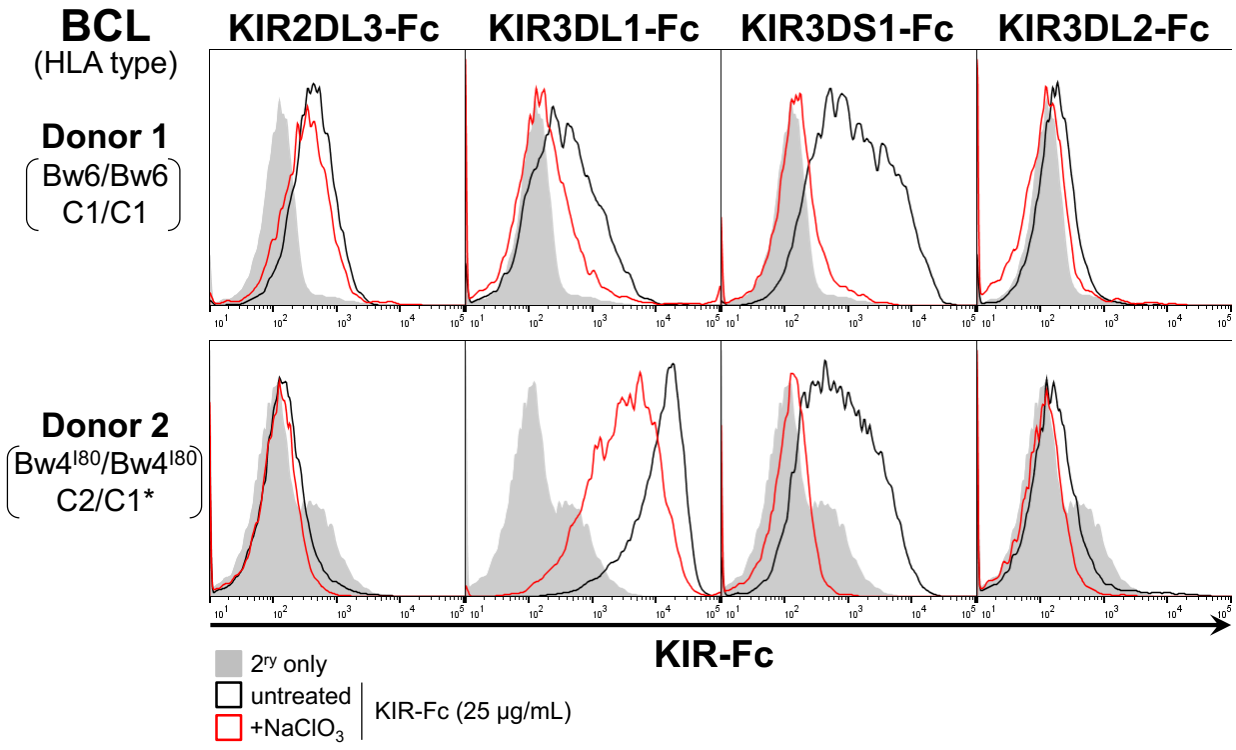

Figure 4.7: KIR-Fc staining of B-cell lines with and without sulfation inhibition. BCL cells from two donors (HLA-types indicated, C1* denotes non-KIR2DL3-binding C1 allotype) were cultured for 48 h in sulfate-free media containing 50 mM $NaClO_3$ (solid red line histograms) or regular media (solid black line histograms), and stained with the indicated KIR-Fc constructs (25 µg/mL each) and anti-hIgG(Fc)-PE secondary antibody. Controls were stained with anti-hIgG(Fc)-PE secondary antibody alone (2^{ry} only; gray filled histograms). (*Note:* Additional peaks in '2ry only' histograms are due to presence of IgG^+ BCL cells recognized by anti-hIgG(Fc)-PE).

(*ii*) repulsive electrostatic interactions between HS and the D1 domain of KIR3DL2, which has an unusually low pI and thus a high net negative charge.

Having discovered the binding that occurs between KIR3DL1 and HS, we saw the opportunity to do a test screen for known HLA-I protein ligands of KIR3DL1 in cell lines using KIR3DL1-Fc, which has been notoriously difficult due to what was previously called "high background." To this end, we cultured 721.221 cells and 721.221 cells stably transduced with HLA-B*08:01 (a non-ligand), HLA-B*57:01 (a potent KIR3DL1 ligand), or HLA-B*49:01 (a KIR3DL1 ligand) in regular or sulfate-free/$NaClO_3$-containing media and stained with KIR3DL1-Fc. As **Fig. 4.8** shows, KIR3DL1-Fc staining of cells cultured in regular media showed "high background" with only a small increase in staining to HLA-B*57:01 bearing cells, while cells cultured in sulfate-free/$NaClO_3$-containing media exhibited no staining in non–ligand-bearing cells but retained high staining of ligand-bearing cells. This massive increase in the signal-to-noise ratio in this proof-of-concept test screen of cell lines is one that may be applied to other "orphan" receptors that exhibit binding to HS that is physiologically relevant but obscures cell-based ligand-screening approaches.

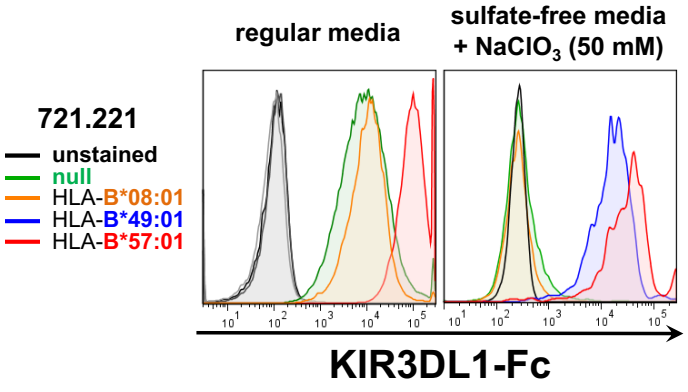

Figure 4.8: KIR3DL1-Fc staining of sulfation-inhibited cells results in significantly better detection of HLA-I ligands. 721.221 cells that were untransduced or transduced with HLA-B*08:01, HLA-B*57:01, or HLA-B*49:01 were cultured in regular media or in sulfate-free/$NaClO_3$-containing media and stained with KIR3DL1-Fc (25 μg/mL).

4.4 MATERIALS AND METHODS

Cell lines and antibodies

721.221 cell lines (including HLA transductants) were grown in RPMI-1640 supplemented with 10% fetal bovine serum (Sigma-Aldrich), 2 mM L-glutamine (Gibco), 100 U/mL penicillin (Gibco), and 100 U/mL streptomycin (Gibco) at 37°C/5% CO_2. EBV-transformed B-cell lines (BCLs) were generated from peripheral blood mononuclear cells from donors bearing specific HLA genotypes; BCLs were also grown in the same media and conditions as 721.221 cells. The following purified antibodies were used: anti-HS-FITC (clone: 10E4, US Biological; used at 1:10 dilution), anti-hIgG(Fc)-PE (Life Technologies), anti-CD3 (BioLegend), anti-CD4 (BioLegend), anti-CD8 (BioLegend), anti-CD19 (BioLegend), anti-CD56 (clone: HCD56, BioLegend), and anti-CD16 (clone: 3G8, BioLegend).

KIR-Fc staining

Cells were stained with KIR-Fc by washing extensively with PBS, incubating for 30–45 min with 25 μg/mL KIR3DS1-Fc (R&D) diluted in PBS at 4°C while shaking, followed by a secondary staining with anti-hIgG(Fc)-PE (Life Technologies) for 30 min at 4°C while shaking. After staining, cells were washed and fixed using 4% paraformaldehyde/PBS (Affymetrix) and flow cytometry analysis was performed on an BD LSR II or LSR Fortessa.

Genome-wide CRISPR/Cas9 knock-out (GeCKO) screen

Screen was performed as previously described in [97]. However, methods will be briefly described. *sgRNA Library Design.* The optimized sgRNA library was designed by first computationally filtering out potential off-target matches (except for sgRNAs that targeted multiple homologs), and also to have high cleavage activity (based on rules experimentally determined in another set of experiments). In total, we constructed a novel library, containing 178,896 sgRNAs targeting 18,166 protein-coding genes in the human consensus CDS (CCDS) and 1,004 non-targeting control sgRNAs. *Screen procedure.* K562 cells were lentivirally transduced with Cas9/eGFP vector. 2.40×10^8 Cas9-transduced cells were transduced with the viral pool containing the sgRNA library to achieve an average 1000-fold coverage of the library after selection with puromycin for 7 d. 5×10^7 K562-GeCKO cells were washed in PBS and stained in 1 mL of 25 μg/mL KIR3DS1-Fc (R&D) for 15 min at 4°C. Cells were then washed with PBS and stained with 1 mL of anti-hIgG(Fc)-PE (Life Technologies) diluted 1:50 in PBS. Fluorescently labeled cells were washed with PBS and stained with anti-PE Microbeads (Miltenyi) following manufacturer's instructions, except for using twice the recommended volumes. Magnetically labelled cells were then depleted in an LD column (Miltenyi) following manufacturer's instructions, and flow-through cells were collected and cultured. *Screen deconvolution.* sgRNA inserts were PCR amplified from 5 million genome equivalents of DNA from flow-through cells. The resultant PCR products were purified and sequenced on a HiSeq 2500 (Illumina); primer sequences are as follows:

sgRNA quantification primers:

F: AATGATACGGCGACCACCGAGATCTAGAATACTGCCATTTGTCTCAAG

R: CAAGCAGAAGACGGCATACGAGATCnnnnnnTTTCTTGGGTAGTTTGCAGT

TTT

(nnnnn denotes the sample barcode)

Illumina sequencing primer:

CGGTGCCACTTTTTCAAGTTGATAACGGACTAGCCTTATTTTAACTTGCTATTT

CTAGCTCTAAAAC

Illumina indexing primer:

TTTCAAGTTACGGTAAGCATATGATAGTCCATTTTAAAACATAATTTTAAAACT

GCAAACTACCCAAGAAA

Data analysis. Sequencing reads were aligned to the sgRNA library and the abundance of each sgRNA was calculated. Gene-based CRISPR scores (CS) were defined as the average log2 fold change of all sgRNAs targeting a given gene and calculated for the entire screen. To identify enriched genes, the CS distribution was mean-normalized to zero.

Sulfation inhibition treatment

Cells were grown for 48 h (or other time period if specified) in sulfate-free/$NaClO_3$-containing media, which consisted of custom-made Advanced RPMI-1640 (Life Technologies) deficient in magnesium sulfate, zinc sulfate, and copper (II) sulfate, supplemented with 10% dialyzed FBS (Gibco), 2 mM L-glutamine (Gibco), 100 U/mL penicillin (Gibco), 100 U/mL streptomycin (Gibco), 407 μM magnesium chloride (Sigma-Aldrich), 3.03 μM zinc chloride (Sigma-Aldrich), and 5 nM copper (II) chloride (Sigma-

Aldrich), and 50 mM sodium chlorate ($NaClO_3$; Sigma-Aldrich) (or other $NaClO_3$ concentration if specified).

Enzymatic treatment of cell lines

For surface enzymatic treatment of cells, 2.5×10^5 cells were washed three times with PBS, and then incubated in PBS containing 2 U/mL heparinase II (New England BioLabs), 1 U/mL proteinase K (New England BioLabs), or no enzyme for 1 h at 37°C/5% CO_2. Cells were then washed in ice-cold PBS and stained as indicated.

Computational analysis of pI

Isoelectric point analysis was determined by inputing Ig-domain sequences (from Cys to Cys) into ExPASy Compute pI/Mw tool, which calculates pI using pK_a values of amino acids[99]. The KIR sequences analyzed were obtained from Immuno Polymorphism Database (IPD)[100,101] and were the following: KIR2DL1*001, KIR2DL2*001, KIR2DL3*001, KIR2DL4*001, KIR2DL5A*001, KIR2DS1*002, KIR2DS4*001, KIR3DL1*001, KIR3DS1*013, KIR3DL2*001, and KIR3DL3*001.

Surface Plasmon Resonance (SPR)

SPR measurements were conducted in phosphate-buffered saline (PBS; Corning) containing 0.005% v/v surfactant P20 (GE Healthcare) using a Biacore 3000 system (Biacore AB). To assess binding of various KIR-Fc constructs to various GAGs, biotinylated hyaluronate (molecular weight = 29 kDa), biotinylated heparin (molecular weight = 18 kDa) and biotinylated chondroitin sulfate (molecular weight = 50 kDa) (all

from Creative PEGWorks), were immobilized onto individual flow cells of an SA (streptavidin) sensor chip (GE Healthcare) until saturation. A blank flow cell with no immobilized ligand was used as a reference flow cell. Injections of 60 µL of KIR-Fc constructs diluted in PBS to 25 µg/mL were performed at a flow rate of 20 µL/min, with a subsequent 10 min run of buffer to allow sufficient dissociation. Although not presented here, regeneration after each injection was achieved with two pulses of 100 µL of 0.2 M sodium hydroxide (NaOH) (GE Healthcare) at a flow rate of 100 µL/min. Raw sensograms were corrected by double referencing (subtracting from the reference flow cell response and from PBS injection response). All experiments were done at standard temperature (25°C).

Human Samples and Viruses

Frozen peripheral blood mononuclear cells (PBMCs) from healthy donors were used in this study in accordance to protocols approved by Partners Human Research Committee and Institutional Review Board of Massachusetts General Hospital.

Data Acquisition and Analysis

Flow cytometry data was acquired on BD LSR II or LSR Fortessa and analyzed using FlowJo software version 10.1 (FlowJo) and statistical analyses were performed using GraphPad Prism 6 (GraphPad Software).

CHAPTER 5: Influence of glycosylation inhibition on the binding of KIR3DL1 to HLA-B*57:01

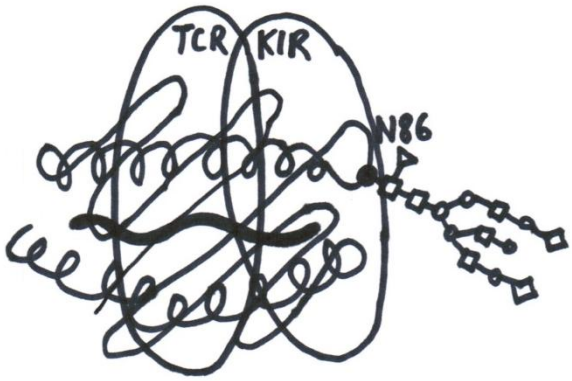

5.1 SUMMARY

Viral infections can affect the glycosylation pattern of glycoproteins involved in antiviral immunity. Given the importance of protein glycosylation in immune function, we investigated the effect that modulation of the highly conserved HLA class I (HLA-I) *N*-glycan has on KIR:HLA-I interactions and NK-cell function. We focused on the interaction between HLA-B*57:01 and KIR3DL1, which has been shown to play an influential role on the outcome of several human diseases, including HIV-1 infection. 721.221 cells stably expressing HLA-B*57:01 were treated with a panel of glycosylation enzyme inhibitors, and HLA-I expression and KIR3DL1 binding was quantified. In addition, the functional outcomes of HLA-B*57:01 *N*-glycan disruption/modulation on KIR3DL1ζ^+ Jurkat reporter cells and primary human KIR3DL1$^+$ NK cells was assessed. Different glycosylation enzyme inhibitors had varying effects on HLA-B*57:01 expression and KIR3DL1-Fc binding. The most remarkable effect was that of tunicamycin, an inhibitor of the first step of *N*-glycosylation, which resulted in significantly reduced KIR3DL1-Fc binding despite sustained expression of HLA-B*57:01 on 721.221 cells. This effect was paralleled by decreased activation of KIR3DL1ζ^+ Jurkat reporter cells, as well as increased degranulation of primary human KIR3DL1$^+$ NK cells when encountering tunicamycin-treated HLA-B*57:01-expressing 721.221 cells. Overall, these results demonstrate that *N*-glycosylation of HLA-I is important for KIR:HLA-I binding and has an impact on NK-cell function.

5.2 BACKGROUND

Natural killer (NK) cells are part of the innate immune system, and serve as a first line of defense against intracellular pathogens and malignantly transformed cells. NK cells can lyse target cells by secreting perforin and granzyme and by inducing FasL:Fas-mediated cell death, but can also activate and recruit other immune cells via secretion of pro-inflammatory cytokines and chemokines. The importance of NK-cell function is highlighted in the setting of human NK-cell deficiency syndromes, which cause increase risk of death in early life due to increased susceptibility to infections with commonly encountered viruses and intracellular bacteria (reviewed in [8,102]). NK-cell activity is regulated via a number of activating and inhibitory receptors (reviewed in [103]), including killer-cell immunoglobulin-like receptors (KIRs), which recognize human leukocyte antigen class I (HLA-I) ligands. Binding of KIRs to HLA-I is determined by the respective HLA-I and KIR allotypes, as well as the sequence of the HLA-I presented peptides[7,104]. Whereas binding of inhibitory KIRs to HLA-I molecules results in NK-cell inhibition, engagement of activating KIRs or loss of inhibitory KIR binding can lead to NK-cell activation[105,106]. The KIR-HLA interaction has been demonstrated to have an important impact on viral infections, including human immunodeficiency virus-1 (HIV-1). In HIV-1 positive individuals, KIR3DL1^{+} NK cells expanded preferentially in the presence of HLA-Bw4-80I, the ligand class for KIR3DL1 [14,27].

Protein glycosylation is a post-translational modification occurring in the endoplasmatic reticulum (ER) and Golgi apparatus. In multiple enzymatic steps, a complex oligosaccharide (i.e. glycan) is synthesized in the ER, transferred to a specific receptor sequence on its target protein, and subsequently cropped and remodeled in

the ER and Golgi[107]. In the case of asparagine *N*-glycosylation, the target amino acid sequence on the respective proteins is Asn-X-Ser/Thr, where the glycan is bound to the asparagine. It is estimated that over 7,000 distinct glycan structures can be generated in mammals[108], suggesting a wide range of functional properties, which can be modulated by differential glycosylation. The HLA-I glycan at position N86, which is located close to the Bw4 motif that is critical for KIR3DL1 binding, is highly conserved and present on all classical and non-classical HLA-I genes and allotypes[100,109,110]. Here we use a panel of glycosylation inhibitors to examine the effects of *N*-glycan modifications on KIR3DL1 binding to HLA-B*57:01 and their potential effect on NK-cell function, with a more in-depth characterization of the effect tunicamycin (TUN)—an antibiotic that can completely block *N*-glycosylation in eukaryotic cells by preventing the linkage of the glycan to the asparagine[111,112]—and castanospermine (CSP)—an α-glucosidase I and II inhibitor able to inhibit ER glycan trimming that is necessary for the assembly of a fully functional glycan[112,113].

5.3 RESULTS

5.3.1 *Effects of glycosylation enzyme inhibitors on HLA class I expression and KIR-Fc binding*

In order to examine the effect of different commercially available glycosylation inhibitors (see **Illustration 5.1**) on KIR:HLA interactions, we examined their effect on HLA-B*57:01 expression on HLA-B*57:01-transduced 721.221 cells (also referred to as 221 cells) and on KIR3DL1-Fc binding to those cells. As shown in **Fig. 5.1a** and **Fig. 5.1b**, inhibitors that targeted Golgi-resident α-mannosidase enzymes (KIF, SWA) increased HLA-B*57:01 surface expression, which resulted in increased KIR3DL1-Fc binding. The Golgi-resident sialyl transferase inhibitor (STI) tested, however, did not result in any appreciable changes in HLA-B*57:01 surface expression or KIR3DL1-Fc binding. Inhibitors that targeted ER-resident α-glucosidase II (CSP, DNM), which is an enzyme necessary for the last removal of glucose from *N*-glycans to allow anterograde transport to the Golgi, dramatically reduced HLA-B*57:01 surface expression and abrogated KIR3DL1-Fc binding. The ER-resident α-glucosidase I-specific inhibitor (AUS) minimally increased HLA-B*57:01 surface expression and KIR3DL1-Fc binding. However, in the case of TUN, we observed a major decrease in KIR3DL1-Fc binding while HLA-B*57:01 surface expression was only slightly increased. Thus, after preliminary testing of the effects that several different glycosylation inhibitors had on HLA-I surface expression and KIR binding, we decided to focus on TUN, the only inhibitor tested that did not decrease HLA-I surface expression but dramatically reduced KIR3DL1-Fc binding, and that had the unique function of completely inhibiting addition of *N*-glycans.

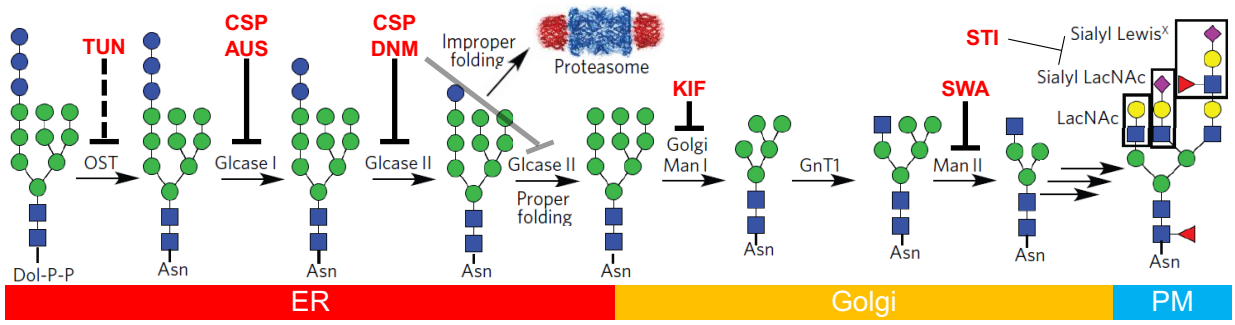

Illustration 5.1: *N*-glycan processing and glycosylation inhibitor. Diagram illustrating processing of *N*-glycans in endoplasmic reticulum (ER), Golgi, and their structure at the plasma membrane (PM) (based on [114]). Glycosylation inhibitors used in this study and the enzymes they target are indicated in red text and black blunt-head arrows (for full names of glycosylation inhibitors and target enzymes, see **Materials and Methods**).

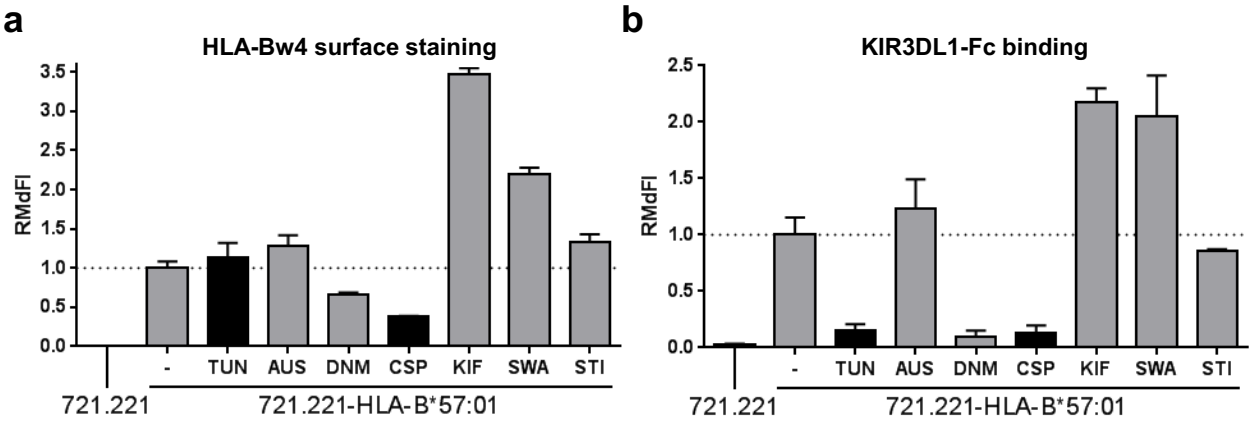

Figure 5.1: Glycosylation inhibitors screening. Relative median fluorescence intensities (RMdFI) of anti-HLA-Bw4 antibody staining (in ***a***) and KIR3DL1-Fc binding (in ***b***) of untransduced 721.221 cells and HLA-B*57:01–transduced 721.221 cells treated with a panel of glycosylation inhibitors (n = 2 for each) (for details, see **Materials and Methods**). Black bars indicate glycosylation inhibitors that were used in subsequent experiments.

We subsequently performed a titration assay in order to identify the minimal amount of glycosylation inhibitors required to observe a strong functional effect on the binding of KIR3DL1ζ$^+$ Jurkat cells to HLA-B*57:01-expressing target 721.221 cells (221-HLA-B*57:01 cells) while keeping target cell death to a minimum. We observed a dose-dependent effect of both TUN and CSP on KIR3DL1ζ Jurkat cell signaling, with the strongest measured effect (*i.e.* decreased activation of KIR3DL1ζ$^+$ Jurkat cells as measured by CD69 expression) corresponding to the highest treatment dose used in

previous studies: 0.5 μg/mL of TUN (**Supplementary Fig. S5.1a**) or 2 mM of CSP (**Supplementary Fig. S5.1b**). Higher doses of glycosylation inhibitors increased cell toxicity to a degree that interfered with our assay by causing cell death, while lower doses of inhibitors increased signaling of KIR3DL1ζ Jurkat cells after co-incubation, indicating a loss of glycosylation inhibition in target cells. Thus, we focused on the glycosylation inhibitor TUN at 0.5 μg/mL, the concentration used in previous studies to investigating the effects of TUN on HLA-I glycosylation[115,116].

5.3.2 *HLA class I N-glycan is necessary for KIR3DL1 binding to HLA-B*57:01*

We next sought to quantitatively assess the effects of TUN on HLA-B*57:01 surface expression and KIR3DL1-Fc binding. 221-HLA-B*57:01 cells (and wildtype 221 cells as control) were treated PBS, CSP or TUN for 24 h, and then stained with anti-Bw4 antibody, anti-pan-HLA-I antibodies, and KIR3DL1-Fc for flow cytometric assessment. TUN treatment of 221-HLA-B*57:01 cells significantly increased HLA-B*57:01 surface expression as measured by anti-HLA-Bw4 and anti-pan-HLA-I antibody staining (1.5-fold HLA-Bw4 MdFI increase, $p < 0.02$; 2.0-fold W6/32 MdFI increase, $p < 0.001$) (**Fig. 5.2** and **Fig. 5.3a**). In contrast, co-incubation with CSP significantly decreased HLA-I

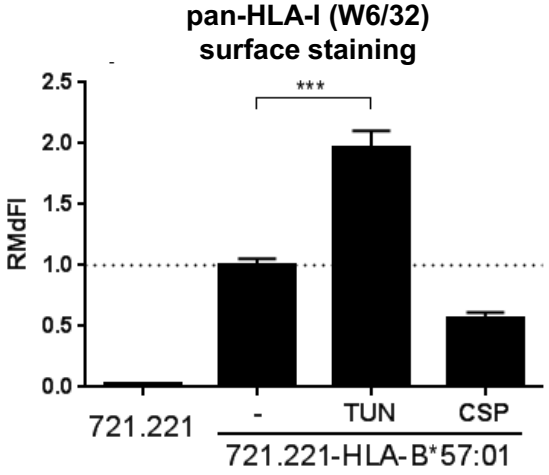

Figure 5.2: TUN treatment of 721.221-HLA-B*57:01 cells increases HLA-I surface expression. Relative median fluorescence intensity (RMdFI) of anti-pan-HLA-I (W6/32) staining was calculated for 721.221 cells and 721.221-HLA-B*57:01 cells treated with TUN, CSP, or untreated

expression (2.1-fold HLA-Bw4 MdFI decrease, $p < 0.02$; 1.7-fold W6/32 MdFI decrease, $p < 0.05$). Since glycosylation inhibition similarly affected staining with anti-HLA-Bw4 and anti-pan-HLA-I antibody, which only recognizes folded HLA-I complexes bound to β_2m, we believe that HLA- B*57:01 proteins expressed at the cell surface were folded complexes of HLA-B*57:01 and β_2-miroglobulin and not free heavy chains.

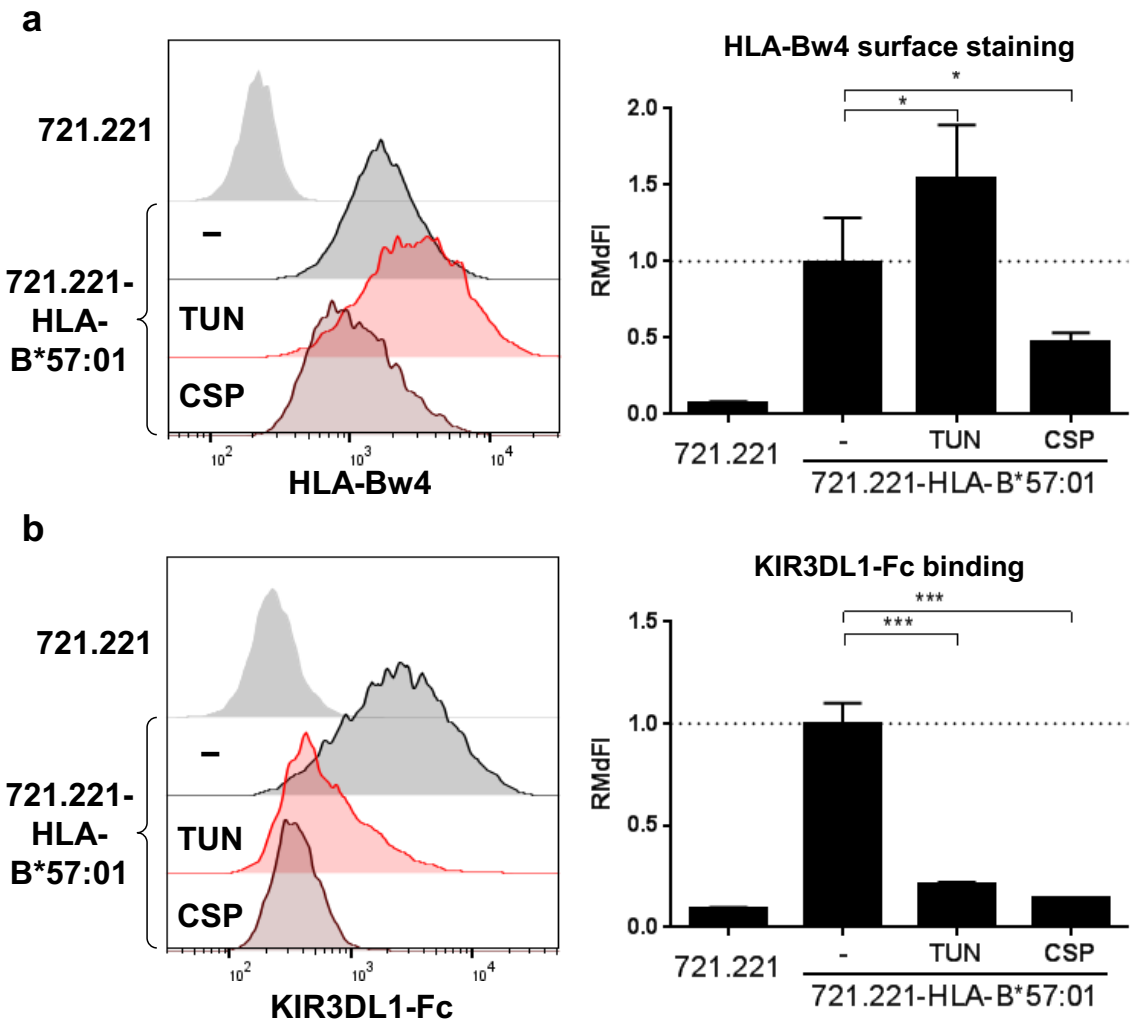

Figure 5.3: *N*-glycosylation inhibition increases HLA-B*57:01 surface expression while abrogating KIR3DL1-Fc binding. Anti-HLA-Bw4 antibody staining (in ***a***) and KIR3DL1-Fc staining (in ***b***) was performed on 721.221-HLA-B*57:01 cells treated with TUN, CSP, or untreated, and untransduced 721.221 cells. Representative histograms are on left panels and data representing $n = 5$ technical replicates are presented as bar graphs on right panels. One-way ANOVA with Dunnette multiple comparisons test was performed (*, $p < 0.05$; ***, $p < 0.001$).

Sustained expression of HLA-B*57:01 on 221-B*57:01 cells following TUN treatment enabled assessment of the consequences of HLA-I de-glycosylation on KIR3DL1 binding to HLA-B*57:01. Despite enhancement of overall HLA-B*57:01 expression, TUN treatment abrogated KIR3DL1-Fc binding. Cells treated with TUN bound KIR3DL1-Fc significantly less than untreated cells (4.7-fold KIR3DL1-Fc MdFI decrease, $p < 0.001$). 221-HLA-B*57:01 cells treated with CSP also exhibited reduced KIR3DL1-Fc binding (6.9-fold KIR3DL1-Fc MdFI decrease, $p < 0.001$) (**Fig. 5.3b**), which was expected given the reduced surface stating of HLA-B*57:01 on CSP-treated cells. Taken together, these data demonstrate that the presence of *N*-glycosylation is critical for KIR3DL1 binding to HLA-B*57:01.

5.3.3 *HLA class I N-glycan is necessary for functional signaling through KIR3DL1 in KIR3DL1ζ$^+$ Jurkat cells*

Jurkat reporter cells stably expressing a chimeric receptor of the extracellular and transmembrane domain of KIR3DL1 fused to the cytoplasmic tail of CD3ζ, referred to as 'KIR3DL1ζ', was employed to assess the functional consequences of glycosylation inhibition. KIR3DL1ζ engagement of its ligand HLA-B*57:01 results in an activating signal that triggers CD69 expression. Jurkat cells were gated by size, CD3 expression, and KIR3DL1ζ expression. Cells that were CD3$^+$KIR3DL1ζ$^-$ were, by definition, untransduced and thus were used as an internal negative control.

KIR3DL1ζ$^+$ Jurkat reporter cells were potently stimulated by 221-HLA-B*57:01 cells. However, stimulation of KIR3DL1ζ$^+$ Jurkat cells was abrogated by pre-treatment of 221-HLA-B*57:01 cells with TUN (4.4-fold CD69 MdFI decrease, $p < 0.001$) (**Fig. 5.4a**

and **Fig. 5.4c**). As expected, 221-HLA-B*08:01 cells and untransduced 221 cells did not stimulate KIR3DL1ζ^{+} Jurkat cells, and treatment with TUN had no effect (**Fig. 5.4a**). Untransduced Jurkat cells were not activated after co-incubation with any of the tested target cells regardless of TUN treatment (**Fig. 5.4b** and **Fig. 5.4c**). These results demonstrate that lack of *N*-glycosylation abrogates KIR3DL1:HLA-B*57:01 binding, and this has direct functional consequences on KIR3DL1ζ^{+} Jurkat cell function.

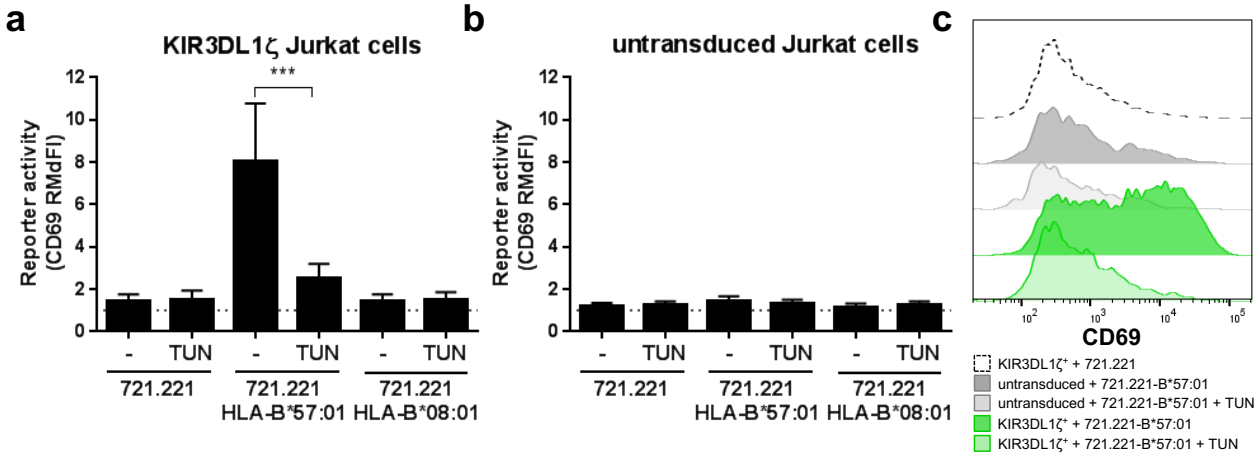

Figure 5.4: TUN treatment of 721.221-HLA-B*57:01 cells abrogates triggering of KIR3DL1ζ^{+} Jurkat reporter cells. Reporter activity of KIR3DL1ζ^{+} (in ***a***) and untransduced (in ***b***) Jurkat reporter cells was measured by calculating relative median fluorescence intensity (RMdFI) of CD69 relative to unstimulated Jurkat cells. Reporter assay was carried out for 2 h at a repoter-to-target cell ratio = 1:1. Bar graphs in ***a*** and ***b*** show the mean ± standard deviation of *n* = 10 replicates, whereas representative flow histograms are presented in ***c***.

5.3.4 *Primary human KIR3DL1^{+} NK cells are 'de-repressed' upon encountering tunicamycin-treated HLA-B*57:01^{+} target cells.*

We subsequently examined the effect of TUN on the interaction between primary human KIR3DL1^{+} NK cells and HLA-B*57:01^{+} target cells by assessing degranulation in KIR3DL1^{+} NK-cell clones co-incubated with TUN-treated or untreated 221-HLA-B*57:01 cells. NK cell clones were gated for FSC, SSC and expression of CD56, CD16, KIR3DL1 and CD107a (**Fig. 5.5a**). KIR3DL1^{+} NK cells exposed to 221 cells

degranulated extensively (74.47% ± 2.20% $CD107a^+$), but were significantly suppressed when exposed to 221-HLA-B*57:01 cells (27.20% ± 0.7% $CD107a^+$, 2.7-fold decrease compared to the 221 samples, $p < 0.0001$), which was still significantly higher than unstimulated NK cells (0.46% ± 0.11% $CD107a^+$) (**Fig. 5.5b**). However, TUN pre-treatment of 221-HLA-B*57:01 cells resulted in a significant increase in degranulation (38.53% ± 1.37% $CD107a^+$, 1.4-fold increase compared to 221-HLA-B*57:01, $p < 0.0001$) compared to untreated 221-HLA-B*57:01 cells. $KIR3DL1^-$ NK cells exposed to 221 cells (80.57% ± 1.87%) degranulated significantly more than when exposed to 221-B*57:01 cells (66.7% ± 1.05%, 1.2-fold decrease compared to 221, $p = 0.0007$) (**Fig. 5.5c**). Co-incubation of target cells with TUN had no significant effect on $KIR3DL1^-$ NK cells (221: $p = 0.6874$; 221-B57: $p = 0.1629$). Thus, TUN treatment of 221-HLA-B*57:01 cells 'de-repressed' $KIR3DL1^+$ NK cells that would normally have been suppressed by KIR3DL1 engagement of *N*-glycosylated HLA-B*57:01 proteins, suggesting a critical and functional role for HLA-I *N*-glycans in KIR binding and primary NK-cell function modulation.

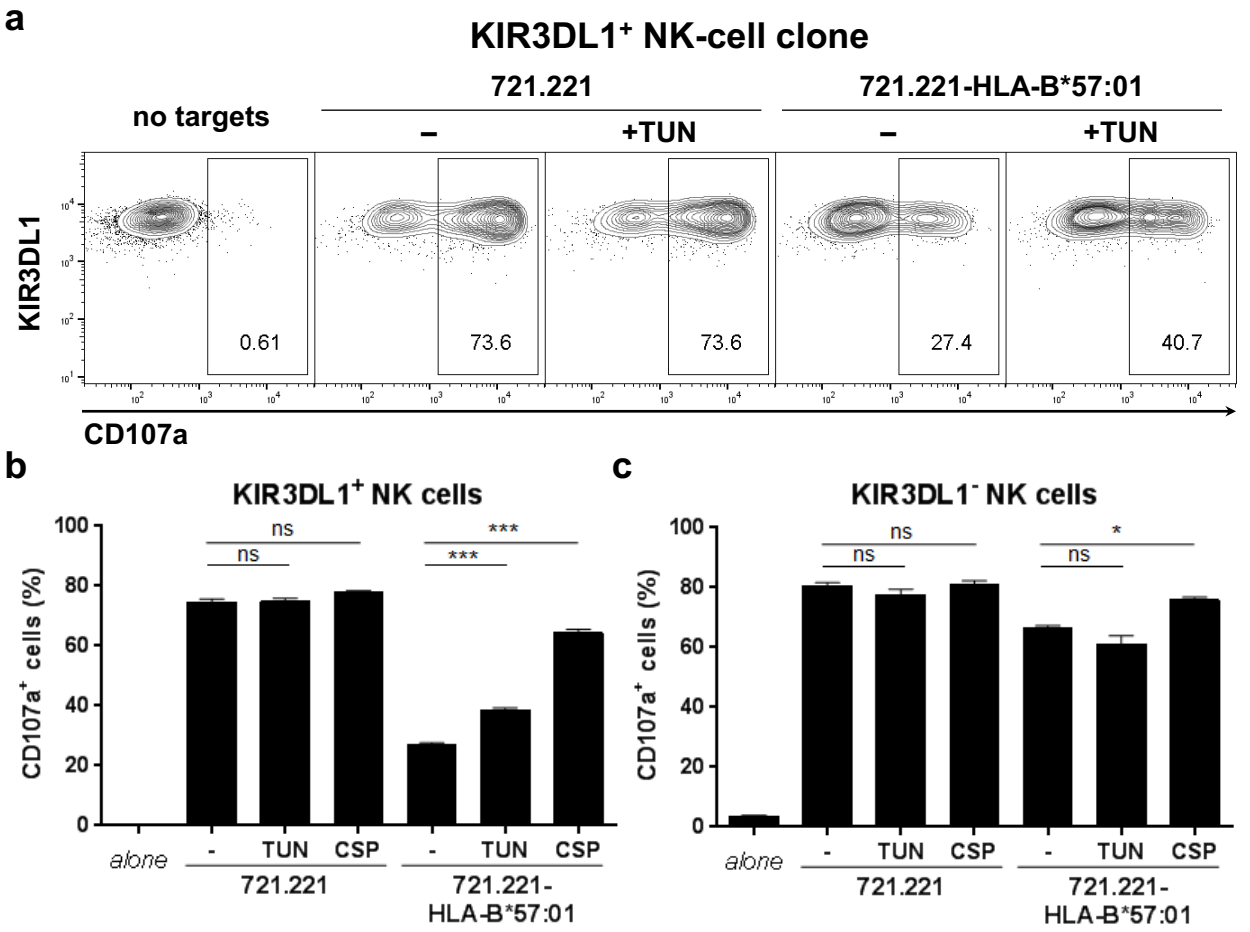

Figure 5.5: KIR3DL1$^+$ NK-cell clones are disinhibited by TUN treatment of 721.221-HLA-B*57:01 cells. (***a***) Representative flow plots of a KIR3DL1$^+$ NK-cell clone degranulating in response to TUN-pre-treated and untreated 721.221 and 721.221-HLA-B*57:01 cells. Degranulation was carried out for 2 h in the presence of fluorophore-conjugated anti-CD107a antibody before staining for surface NK-cell receptors. (***b***, ***c***) Bar graphs show frequency of degranulating KIR3DL1$^+$ (in ***b***) and KIR3DL1$^-$ (in ***c***) NK-cell clones co-incubated with the indicated target cells. Data represented mean ± standard deviation of *n* = 3 technical replicates. One-way ANOVE with Dunnett multiple comparisons test was performed (ns, non-significant; ***, $p < 0.001$; *, $p < 0.05$).

5.4 MATERIALS AND METHODS

Target Cells

HLA-I-deficient 721.221 cells (also referred to as '221 cells') stably expressing HLA-B*08:01 or HLA-B*57:01 were provided by Christian Brander (Ragon Institute of MGH, MIT and Harvard, Cambridge, MA). All cells were cultured at 37°C with 5% CO_2 in RPMI 1640 medium (Sigma-Aldrich) supplemented with 10% heat-inactivated fetal bovine serum (FBS) (Biochrom AG), 2500 U/mL penicillin and 2500 µg/mL streptomycin (Sigma-Aldrich) unless stated otherwise; this media was referred to as 'R10'.

Glycosylation inhibition screening and titration

Glycosylation inhibition was performed by incubating target cells for 24 h at 37°C/5%CO_2 in R10 supplemented with different glycosylation inhibitors: 5 mM of 1-deoxynojirimycin (DNM; Tocris Bioscience), an α-glucosidase II > I inhibitor; 500 µM of australine (AUS; Santa Cruz Biotechnology), an α-glucosidase I inhibitor; 2 mM of castanospermine (CSP; Tocris Bioscience), an α-glucosidase I and II inhibitor; 100 µM of kifunensine (KIF; Tocris Bioscience), an α-mannosidase I inhibitor; 500 µM of $3F_{ax}$-peracetyl-Neu5Ac (STI; EMD Millipore), a sialyltransferase inhibitor; 100 µM of swainsonine (SWA; Tocris Bioscience), an α-mannosidase II and lysosomal α-mannosidase inhibitor; 0.5 µg/mL of tunicamycin (TUN; Sigma-Aldrich), a GlcNAc phosphotransferase inhibitor; or phosphate buffered saline (PBS) as negative control. Optimal concentrations of glycosylation inhibitors were determined by using effective concentrations reported in the literature as well as lower and higher doses. Readouts measured were HLA expression, KIR3DL1-Fc binding, CD69 expression of KIR3DL1ζ^+

Jurkat cells, or degranulation of KIR3DL1^{+} NK cells after staining or co-incubating with glycosylation-inhibitor–pre-treated untransduced or HLA-transduced 721.221 target cells.

Quantification of HLA-I expression and KIR3DL1 binding

For HLA-I cell surface expression, target 221 cells (1.5×10^5 per well) were treated with TUN, CSP, or PBS for 24 h. After washing, cells were stained with either biotinylated anti-HLA-Bw4 antibody (One Lambda) followed by secondary staining with streptavidin-BV421 (BioLegend), or anti-pan-HLA-I-PE antibody (clone: W6/32) (BioLegend). For KIR-Fc binding assessment, target cells (1.5×10^5 per well) were grown for 48 h in modified media prior to KIR-Fc staining to reduce background staining. Modified media consisted of custom-made Advanced RPMI-1640 (Life Technologies) deficient in magnesium sulfate, zinc sulfate, and copper (II) sulfate supplemented with 10% dialyzed FBS (Gibco), 2 mM L-glutamine (Gibco), 100 U/mL penicillin (Gibco), 100 U/mL streptomycin (Gibco), 407 µM magnesium chloride (Sigma-Aldrich), 3.03 µM zinc chloride (Sigma-Aldrich), and 5 nM copper (II) chloride (Sigma-Aldrich), which was mixed with 150 mM sodium chlorate (Sigma-Aldrich) at a 5:1 volume ratio. During the last 24 h, TUN, CSP or PBS were added to the medium. After washing, cells were stained for 45 min with 25 µg/mL KIR3DL1-Fc (R&D) at 4°C while shaking, followed by a secondary staining with anti-hIgG(Fc)-PE (Life Technologies) for 30 min at 4°C while shaking. After staining, cells were fixed using 4% paraformaldehyde/PBS (Affymetrix) and flow cytometry analysis was performed on an LSR-II (BD).

Jurkat reporter cell assay

Jurkat cells (clone E6.1; ATCC) were cultivated in R10 medium. 24 h before performing experiments, 10% fetal bovine serum was added to the culture to reduce background activation. Jurkat cells stably expressing KIR3DL1ζ, a chimeric receptor composed of the extracellular and transmembrane domains of KIR3DL1 linked to the cytoplasmic tail of CD3ζ, which we denote as 'KIR3DL1ζ', were produced via lentiviral transduction/transfection. Briefly, gene constructs were designed and ordered via GeneArt (Life Technologies), and cloned into a lentiviral transfer vector containing an SFFV promotor and IRES-driven puromycin resistance. HEK293T cells (ATCC) were transfected with a VSV-G envelope vector (pHEF-VSVG, NIH AIDS Reagent Program), HIV-1 gag-pol packaging vector (psPAX2, NIH AIDS Reagent Program), and the transfer vector containing KIR3DL1ζ. Lentivirus-containing supernatants were harvested 72 h after transfection and used to transduce Jurkat cells, which were subsequently selected in R10 containing 1 µg/mL puromycin and sorted for gene expression by flow cytometry. In these KIR3DL1ζ$^+$ Jurkat cells, ligand engagement by KIR3DL1ζ results in an activating signal that triggers CD69 expression, making them a suitable reporter cell system. Prior to co-incubation with target cells, Jurkat cells were cultured for 24 h in R10 medium supplemented with an additional 10% fetal bovine serum. 221 cells expressing HLA-B*08:01, HLA-B*57:01, or no HLA-I underwent glycosylation inhibition and were washed twice. Target cells were washed to remove glycosylation inhibitors and then co-incubated with either KIR3DL1ζ$^+$ or untransduced Jurkat cells at a reporter-to-target cell ratio of 1:1 (1×10^5 each) for 2.5 h at 37°C/5%CO_2. Cells were then washed, stained with anti-CD3-PerCP-Cy5.5, anti-CD69-BV421, and anti-KIR3DL1-

APC (all from BD) for 30 min at 4°C, fixed with 4% paraformaldehyde/PBS, and analyzed on an LSR-Fortessa (BD). KIR3DL1ζ-transduced Jurkat cells were gated for KIR3DL1 expression, classifying them either as KIR3DL1ζ^{low}, KIR3DL1ζ^{dim} or KIR3DL1ζ^{bright}.

NK cell cloning and degranulation assay

Primary human NK cells isolated from peripheral blood mononuclear cells (PBMCs) of healthy donors were cloned by limiting dilution in the presence of feeders and maintained in NK cell cloning medium consisting of R10 supplemented with 5% human serum (Sigma-Aldrich), 1X MEM-NEAA (Gibco), 1X sodium pyruvate (Gibco), 100ug/mL Kanamycin, 200 U/mL IL-2 (AIDS Reagent Program, NIH) using a protocol adapted from a previously reported method (22). Briefly, NK cells were isolated from peripheral blood mononuclear cells (PBMCs) from a *KIR3DL1*$^{+}$ *HLA-Bw4*$^{+}$ donor via magnetic negative selection (NK cell isolation kit from Miltenyi), added to a mix of irradiated feeders consisting of freshly isolated allogeneic (PBMCs) combined with log-phase-growth RPMI 8866 cells (Sigma-Aldrich) at a 10:1 ratio in cloning medium containing 1 µg/mL phytohaemagglutinin (PHA; Fisher) and mixed thoroughly before plating at 100 µL/well (0.5 NK cell/well) in 96-well plates and incubated for 14 days at 37°C/5% CO_2. After 14 days, wells that had outgrowth of cells were transferred to 48-well plates and maintained in NK cell cloning medium with frequent media exchange (approximately every 3 days). Cells were phenotyped by flow cytometry to assess NK cell marker (e.g. CD56 and CD16) and KIR3DL1 expression. Degranulation assays were performed by co-incubating 5×10^4 NK cells with 2.5×10^5 target cells (effector-to-

target cell ratio of 1:5) in 200 µL of R10 containing 3 µL of anti-CD107a-PE-Cy7 antibody (BioLegend) for 2 h at 37°C/5% CO_2, and subsequently staining with anti-CD56-BV605 and anti-CD16-BV785 antibodies (both from BioLegend) for 30 min at 4°C, and then fixed with 4% paraformaldehyde/PBS. Flow cytometric analysis was performed on a BD LSRFortessa.

Ethics

PBMCs from healthy donors were obtained and frozen after obtaining written informed consent following procedures approved by the Partners Human Research Committee (ethics committee) and the Institutional Review Board of Massachusetts General Hospital. HLA-I types of selected human samples were determined prior to this study by high-resolution HLA-I typing performed at the HLA-typing laboratory of the National Cancer Institute, National Institutes of Health. KIR types were determined prior to this study by Sanger sequencing in the laboratory of Mary Carrington.

Statistics

Flow data was analyzed in FlowJo v10 (FlowJo LLC, Ashland, Oregon). Statistical analyses were performed using GraphPad Prism 6.0c (GraphPad Software Inc., La Jolla, California, USA). Normality tests (Kolmogorov-Smirnov test with Dallal-Wilkinson-Lilliefor P value) were performed on all data sets, statistical significance was calculated via one-way ANOVA, and multiple comparisons were corrected using Tukeys's test if not stated otherwise. All graphs show mean ± SD if not stated otherwise

in the figure legends. Significance levels were defined as the following: *, $p < 0.05$; **, $p < 0.01$; ***, $p < 0.001$; and ****, $p < 0.0001$.

CHAPTER 6: Discussion

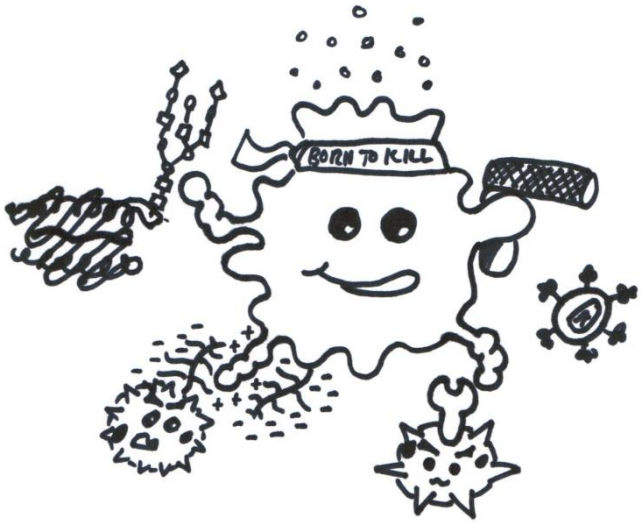

6.1 KIR3DS1 binds HLA-F

6.1.1 *KIR3DS1 binding to HLA-F is functionally and physiologically relevant*

The activating NK-cell receptor KIR3DS1 has been associated with the outcome of viral infections[31,42,49] including HIV-1[16,19], autoimmune disorders[41], transplantation[38–40], and cancer development/treatment[33,34,36,37]. However, the precise nature of a ligand that can account for such broad biological effects has remained—although extensively studied—unknown. Here, we identified HLA-F OCs as ligands for KIR3DS1, and showed that HLA-F OCs trigger polyfunctional responses in primary human NK cells through KIR3DS1. It was further demonstrated that KIR3DS1 ligands, in particular HLA-F, are expressed on the surface of activated $CD4^+$ T cells. However, upon HIV-1 infection of activated $CD4^+$ T cells, KIR3DS1 ligand surface expression was downregulated, yet this did not abrogate efficient suppression of viral replication by co-cultured $KIR3DS1^+$ NK cells *in vitro*. Our findings provide novel and significant insight into the protective effect of KIR3DS1 in HIV-1 infection, and provide an explanation for the widespread influence of KIR3DS1 in human disease.

6.1.2 *KIR3DS1 binding to HLA-F is not unique but is evolutionarily conserved*

Differential binding of KIR3DS1 and the other lineage II KIRs[3] to HLA-F is remarkable from a structural homology perspective, and is shared with other related receptors. The leukocyte immunoglobulin-like receptor (LILR) family is another group of HLA-I-binding receptors found near the KIR locus in the leukocyte receptor complex (LRC)[117]. The LILR family has inhibitory members (i.e. LILRBs) that bind HLA-I complexes and activating members (i.e. LILRAs) that bind HLA-I OCs[55,118], a property

that our data suggests is partially shared with KIRs; two members in particular, LILRB1 and LILRB2, exhibit robust binding to HLA-F[119]. From this present study, we find that all lineage II KIRs bind HLA-F OCs, with KIR3DS1 exhibiting the highest affinity binding to and the most potent functional signaling capacity upon engagement of HLA-F OCs on target cells. KIR3DL2, which has been previously shown to bind HLA-F OCs[120], shares ~86% extracellular domain sequence identity with KIR3DS1, which readily explains differences in binding affinity. However, it is remarkable that despite >97% extracellular domain sequence identity between KIR3DS1 and KIR3DL1, KIR3DS1 exhibits significantly higher-affinity binding to HLA-F OCs than KIR3DL1, whereas KIR3DL1 (but not KIR3DS1) bears high-affinity binding to HLA-Bw4 ligands. Structural studies indicate that the few amino acid differences between KIR3DS1 and KIR3DL1 occur at sites critical for HLA binding[24]. From an evolutionary standpoint, these different ligand-binding profiles of KIR3DL1 towards various HLA-Bw4 allotypes and KIR3DS1 towards HLA-F, which is also monomorphic with one predominant allele (*HLA-F*01:01* at >95% frequency)[121], provide an explanation for the high polymorphicity of KIR3DL1 and the relative monomorphicity of KIR3DS1.

6.1.3 *KIR3DS1:HLA-F axis may be a mode of detecting "stressed self" similar to NKG2D and its ligands*

This newly identified KIR3DS1:HLA-F axis has many similarities to the well-known stress-induced NKG2D:MIC-A/B axis, even in the context of HIV-1 infection. Although it is less well-studied, HLA-F bears unique and distinguishing characteristics that separates it from all other HLA-I genes. According to a study examining the genesis

and architectural evolution of the MHC locus, HLA-F acted as the ancestral progenitor to today's HLA-I and MIC-A/B genes[122]. HLA-F retains features that are similar to MIC-A/B genes, including being peptide-devoid and being able to refold *in vitro* with and without β_2m, indicating its unique ability to be stable as an OC[57], in line with data presented here. In agreement with previous studies[62,123], our data show that HLA-F OCs are expressed on the surface of activated $CD4^+$ T cells. Also, although only partially assessed in this study with B-cell lines, several studies have indicated that cancers of various tissue origins aberrantly express HLA-F[123,124]. Additionally, HIV-1 infection of $CD4^+$ T cells increased transcription of HLA-F but reduced KIR3DS1 ligand expression, particularly in late-infected cells, which might suggest the employment of an immune-evasion strategy, potentially through the downregulation of HLA-F by HIV-1 accessory proteins, similar to what has been described for HIV-1 Nef for HLA-A and HLA-B[125–127] and NKG2D ligands including MIC-A[128], but also HIV-1 Vpu for HLA-G[129] and HLA-C[130]. Our findings are therefore reminiscent of the up-regulation of the NKG2D ligands MIC-A and MIC-B on the surface of activated T cells, virally infected cells, and transformed cells, which are downregulated in the context of HIV-1 by the actions of the accessory protein Nef[128].

HLA-F expression is tightly regulated[131], with restricted tissue expression[119,123] and predominant localization to the endoplasmic reticulum. This indicates that HLA-F expression might serve as a marker for specific kinds of cell stress, such as endoplasmic reticulum stress. Similar to the phenomenon seen for MIC-A[132,133], HLA-F can be a target for humoral immune responses, as was shown in one study that reported the presence of anti-HLA-F antibodies in the sera of cancer patients but not

healthy controls[124]. Collectively, these studies underscore a critical role of HLA-F expression in human diseases, and our data demonstrating that KIR3DS1 recognizes HLA-F OCs uncovers a previously unknown mechanism of innate immune surveillance of stressed cells.

6.1.4 *Previous associations of KIR3DS1 to HLA-Bw4^{I80} are likely driven by KIR3DL1*

KIR3DS1 binding to HLA-F expounds its widespread influence on human diseases, but it does not fully explain the well-known association of KIR3DS1 to HIV-1 disease control described only for *HLA-Bw4*$^{+}$ patients. Several studies have confirmed, however, that in the context of HIV-1 infection, presence of KIR3DS1 and KIR3DL1 together associate with decreased viremia, delayed progression to AIDS, and better *in-vitro* viral inhibition by NK cells in patient bearing *HLA-Bw4*^{I80}[19,134]. This protective compound genotype can be explained by independent but functionally synergistic effects of KIR3DS1:HLA-F and KIR3DL1:HLA-Bw4 interactions, the latter of which has independently been linked to delayed HIV-1 disease progression[18]. Of note, a single recent study demonstrated KIR3DS1 binding to HLA-B*57:01 presenting two HIV-1 peptides that arose from an exhaustive screen of various viral peptide databases[25]. However, it is not clear whether this interaction has real functional consequences, or represents an exceptional case where a peptide can overcome KIR3DS1 mutations that normally abrogate HLA-Bw4 binding. Indeed, KIR3DS1 has been linked to many other human diseases without association to HLA-Bw4[31,34,36,40,42], suggesting that KIR3DS1 exerts disease modulatory effects independent of HLA-Bw4.

6.1.5 *KIR3DS1:HLA-F interactions may play roles in both elimination of pathologically altered cells and regulation of adaptive immunity*

KIR3DS1:HLA-F interactions between NK cells and pathologically altered target cells would incur the well-known innate function of NK cells to recognize and eliminate target cells expressing "stressed self" ligands. This is supported by our *in-vitro* co-culture assay, which showed that NK cells singly expressing KIR3DS1 are more effective at suppressing HIV-1 replication in autologous $CD4^+$ T cells as compared to $KIR3DS1^-$ NK cells. In addition, our data show that KIR3DS1:HLA-F interactions elicit NK-cell production of antiviral and pro-inflammatory cytokines such as IFN-γ, TNF-α, and MIP-1β, which would have pleiotropic effects on immune responses. Furthermore, KIR3DS1:HLA-F interactions between NK cells and activated $CD4^+$ T cells would also suggest a means of NK cell-mediated adaptive immune regulation. This notion is warranted by previous work in LCMV infection mouse models, which show that NK cells regulate adaptive immunity by killing activated $CD4^+$ T cells, resulting in decreased immunopathology[43]. Thus, KIR3DS1 recognition of HLA-F OCs expressed on activated immune cells and/or infected target cells provides a mechanistic link between KIR3DS1 and HIV-1 disease progression, and will also have relevance for the pathogenesis of other infectious diseases, autoimmune disorders, and tumor immune-surveillance.

In conclusion, the novel interaction between the activating NK-cell receptor KIR3DS1 and HLA-F OCs described here uncovers a previously unknown mechanism of target cell recognition by NK cells. Further studies will be required to determine how KIR3DS1:HLA-F interactions play a role in NK cell-mediated regulation of immunity

and/or elimination of pathologically altered target cells. Each of the clinical diseases KIR3DS1 has been implicated in, including autoimmune disorders[41], transplantation outcomes[38–40], cancer development/clearance[33,34,36,37], and viral infections[16,19,31,42,49], offers a variety of prospects to exploit KIR3DS1:HLA-F interactions therapeutically.

6.2 KIR3DS1 binds heparan sulfate

6.2.1 *KIR3DS1 binding to HS can be explained through electrostatic interactions and may be applicable to other KIRs.*

In this study, we found through a genome-wide CRISPR/Cas9 knock-out screen that HS is a ligand for KIR3DS1, which we confirmed biochemically and on primary cells and cell lines. KIR3DS1 domain analysis revealed that in contrast to other KIRs, each of its domains is predicted to be net charge positive at physiological pH. This is consistent with the interaction between KIR3DS1 and HS, which is usually electrostatically driven for other HS-binding proteins. The fact that KIR3DL1, a highly homologous inhibitory allotype with >97% extracellular domain protein sequence identity, also bound to HS although to a lesser extent is also unsurprising, as the critical L166R mutation that abrogates KIR3DS1 binding to HLA-Bw4^{I80} proteins[24] is also critical for conferring a net positive charge to its D1 domain. Indeed, whereas KIR2DL4 was previously shown to interact with HS via its net positively charged D0 domain[96], other potential HS-interacting receptors not tested here are the “orphan” inhibitory NK-cell receptors KIR2DL5 and KIR3DL3, both of which contain a net positively charged D0 domain. Interestingly, in the case of KIR2DL5, KIR2DL5-Fc fusion proteins have been described to exhibit “dull staining of, essentially, every human cell line…independent of the cells

HLA allotypes"[135]. To explain this, we believe it is very likely that KIR2DL5 also binds to HS, although this needs to be formally tested. Of particular practical interest was the finding that with sulfation inhibition treatment, the ability to detect binding of KIRs to HLA-I ligands was significantly increased due to the elimination of HS-interactions that obscure detection of binding (i.e. reduce signal-to-noise ratio). This may also prove to be a very useful adjunctive strategy for investigators seeking to perform cell-based screens for protein ligands of HS-interacting proteins.

6.2.2 *NK-cell "heparanosome" may regulate KIR3DS1 and other NK-cell receptors in* cis

Cis interactions between HS and NK-cell receptors like KIR2DL4 have been shown to cause clustering and block *trans* interactions, allowing for another level of tunable control over NK-cell–receptor signaling[96]. Interestingly, KIR3DS1-Fc did not bind to primary human NK cells from healthy donors, which may suggest that at baseline, *cis* interactions between KIR3DS1 and HS do not occur. However, it is conceivable that upon cellular activation, NK cells alter the composition of cell-surface HS—also referred to as the "heparanosome"—to alter receptor functionality. This is particularly interesting in light of the altered functionality in NK cells that express CD57, which is an epitope comprising a surface-expressed glucuronic acid 3-*O*-sulfate moiety produced by induction of B3GAT1. Expression of CD57 has been shown to correlate with a more "mature" NK-cell phenotype characterized by poor proliferative capacity, poor cytokine responsiveness, and increased sensitivity to CD16-mediated activation. The effect of induction or modulation of heparan sulfate biosynthetic enzymes on NK-

cell function, however, has not been appreciably studied, but in light of these data, may be highly influential on the signaling capacity of receptors such as KIR3DS1 and overall NK-cell function.

6.2.3 *KIR3DS1:HS interactions between NK and target cells may play a role in cancer immunesurveillance*

The binding of D0-domain–containing KIRs to HS can influence NK-cell function depending on whether these interactions occurs in *cis* and/or in *trans*. Interactions of KIRs and other NK-cell receptors in *trans* with target-cell–expressed HS would incur an understudied mode of target cell recognition mediated by protein-carbohydrate interactions. Indeed, specific cell types (and cellular contexts) exhibit precise heparanosome signatures that encode for a variety of motifs for HS-binding proteins to interact with. Cancer cells of various tissue origins significantly alter heparan sulfate biosynthesis genes to alter cell-surface HS, which has been shown to play a role in tumorigenesis. One mode of modulation that is widely found in cancer cells is methylation-associated silencing of HS sulfotransferase genes[136], which has been found to correlate with cancer progression and poor prognosis[137]. Although various biological processes that are hallmarks of cancer[138] (such as tissue invasion and altered growth factor signaling) are undoubtedly affected, it is conceivable that this may also contribute to immune evasion via decreased recognition by HS-binding NK-cell receptors.

The role of KIR3DS1:HS interactions in cancer immunosurveillance is of particular interest because it is an activating receptor associated to the outcome of various cancers[33–36]. Similar to NCR binding to specific HS motifs, it is possible that

KIR3DS1 and other KIRs have specific motifs or binding domains on HS they can dock onto, although a more careful analysis over-expressing and knocking-out specific sulfotransferase genes will be required for this kind of study. Understanding target-cell–expressed HS motifs recognized by NK-cell receptors, as well as their potential to be eliminated in cancer cells through the silencing of HS biosynthetic enzymes to evade NK cell recognition, is an area of study warranting further investigation. In the realm of autoimmunity, the use of HS mimetics that block these interactions may also be very useful, such as in the case of ankylosing spondylitis, which has been shown to be strongly associated to particular alleles of *KIR3DS1* and *KIR3DL1*.

Ultimately, it is clear that protein-carbohydrate interactions play a crucial role in NK-cell function, and studies that further explore the extent and specificity of these interactions will allow for the development of therapies that modulate these interactions, particularly in the context of cancer and autoimmunity.

6.3 KIR3DL1 binding to HLA-B*57:01 is *N*-glycosylation dependent

6.3.1 *Presence of N86 HLA-I* N-*glycan is necessary for KIR3DL1 to bind to and signal upon engagement of HLA-B*57:01*

N-glycosylation is a critical step in post-translational protein modification with functional importance that is not yet fully understood. In the case of all HLA-I allotypes, a single, highly conserved *N*-glycosylation site is located at position N86[100,109,110], in close proximity to the highly polymorphic motif spanning from amino acids 77 to 83, which constitutes the Bw4 motif in HLA-Bw4 allotypes and is critical for KIR3DL1 binding to these[24]. We therefore hypothesized that HLA-I *N*-glycosylation can modulate

binding between HLA-Bw4 proteins and KIR3DL1. To test this hypothesis, we employed a panel of glycosylation enzyme inhibitors to modify or eliminate *N*-glycan structures in HLA-B*57:01-expressing cells and assessed HLA-B*57:01 expression and binding to KIR3DL1. We demonstrate that presence of the *N*-glycan on HLA-B*57:01 is critical for binding to KIR3DL1, and that inhibition of *N*-glycosylation in target cells can have functional consequences on KIR3DL1$^+$ cell lines and primary KIR3DL1$^+$ NK cells.

Inhibition of different glycosylation enzymes led to different effects in terms of HLA-B*57:01 expression and KIR3DL1 binding. The most striking effect was observed for TUN-induced inhibition of *N*-glycosylation, which increased cell surface expression of HLA-B*57:01 while abrogating KIR3DL1 binding. This was in contrast to all other inhibitors, which either increased (for KIF, SWA), decreased (for CSP, DNM), or did not significantly alter (for AUS, STI) HLA-B*57:01 surface expression in a manner that correlated with increased, decreased, or unchanged KIR3DL1 binding, respectively. TUN-induced increase in HLA-B*57:01 surface expression was measured using two different antibodies—anti-HLA-Bw4 (clone: Bw4) and anti-pan-HLA-I (clone: W6/32)—demonstrating that the Bw4 motif, which is situated next to the *N*-glycosylation site, is still recognized, and that the HLA-I molecule is expressed as a complex bound to β_2-microglobulin. We further demonstrated that loss of KIR3DL1-Fc binding to TUN-treated HLA-B*57:01$^+$ target cells matched functional readouts using KIR3DL1ζ^+ Jurkat reporter cells and primary human KIR3DL1$^+$ NK cells. KIR3DL1ζ^+ Jurkat cells were stimulated by co-incubation with 221-HLA:B*57:01 cells, yet this stimulation was almost completely abrogated by treating target cells with TUN prior to co-incubation. In line with this, primary KIR3DL1$^+$ NK cells were potently inhibited by 221-HLA-B*57:01 cells, but were

'de-repressed' when 221-HLA-B*57:01 cells were pre-treated with TUN. These data indicates that *N*-glycosylation of HLA-B*57:01 plays a critical and functional role in KIR3DL1 binding and can modulate NK cell function, a finding that may extend to other KIR:HLA interactions that have not yet been studied in the context of *N*-glycolysation.

6.3.2 *This study uniquely describes* N-*glycan dependency in KIR:HLA interactions, and refutes prior studies*

Reports of the importance of *N*-glycosylation for KIR:HLA binding are scarce, save for one study suggesting that the HLA-I *N*-glycan does not influence KIR binding[139]. In contrast, several studies reported the consequences of HLA-I *N*-glycosylation modifications on T-cell receptor (TCR) binding[115,140–142]. Those reports all concluded that TCR binding to HLA-I (and MHC class I in mice) is independent of HLA-I glycosylation, given the relatively long distance between the TCR binding site and the HLA-I N86 glycan. KIR:HLA crystal structures, however, reveal a very close proximity between the KIR binding site on HLA-I and position N86, which in these structures is aglycosylated due to the production of these proteins in *E. coli* (**Illustration 6.1**). This suggests that the HLA-I N86 glycan may be contacting KIR and influencing binding avidity. Of note, the one study that concluded that HLA-I glycosylation was not necessary for KIR binding was based on a generally assumed interaction between HLA-B*08:01 and an undiscovered inhibitory KIR, which later was found to be the effects of the interaction between the inhibitory receptor NKG2A and HLA-E, which was not discovered at the time of the study[143]. Thus, to the best of our knowledge, our study is the first to implicate the HLA-I *N*-glycan as being critical for KIR:HLA binding, which may

serve as another means of modulating the interaction between NK cell receptors and target cell ligands.

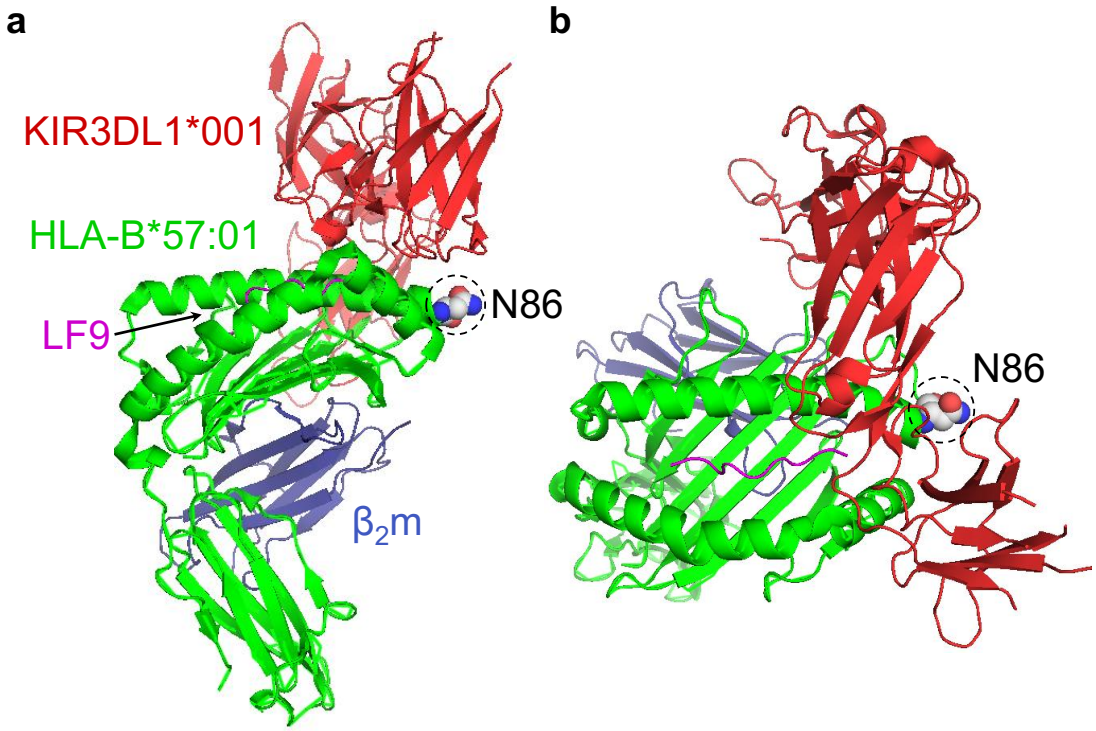

Illustration 6.1: N86 site on crystal structure of KIR3DL1 binding to HLA-B*57:01. KIR3DL1 (*red*) is shown binding to HLA-B*57 (*green*) complexed to β_2-microglobulin (β_2m; *blue-gray*) and presenting the LF9 peptide (*magenta*). Asparagine at position 86 (N86), the site of HLA-I *N*-glycosylation, is indicated from side view (***a***) and top view (***b***). Images were generated using PyMOL (DeLano Scientific LLC) based on the structure published in [24].

6.3.3 *HIV-1 may alter KIR:HLA interactions by modifying* N*-glycans as an immune evasion tactic*

It has been demonstrated that the glycosylation pattern of several immune receptor-ligand pairs can be influenced in the setting of infection. In HIV-1 infection, a global shift in the glycosylation pattern of IgG has been observed, with HIV-1-specific antibodies displaying the most distinct glycosylation patterns[144,145]. This shift in IgG glycosylation patterns can alter Fc receptor binding and is associated with improved antiviral activity and control of HIV-1, but has also been described for other viral and

bacterial infections[144,146]. Indeed, the *N*-glycan structure found on IgG is very similar to the HLA-I N86 glycan, and can be modified similarly by the addition of fucose, bisecting N-acetyl glucosamine, galactose, or sialic acid[110,147,148]. Furthermore, HIV-1 infection has been shown to alter glycosylation in host cells[149], with its envelope protein in particular incorporating an unusually large amount of high-mannose *N*-glycans[150]. Thus, it is conceivable that HIV-1 might affect HLA-I glycosylation, either as a host response mechanism or a direct immunevasive tactic depending on whether HLA-I binding to NK cell receptors is enhanced or diminished by the altered glycosylation pattern. It has been suggested that other viruses have taken advantage of this level of regulation, as in the case of hepatitis C virus, which downregulates HLA-I expression by inhibiting *N*-glycosylation in order to escape immune recognition[151].

While much about the role of modified glycosylation patterns remains to be elucidated, our data demonstrates the importance of glycosylation in KIR:HLA binding and that removal of the glycan has a functional effect on the activation of NK cells. The extent to which pathogens and the immune system can exploit this mechanism to their advantage or whether this mechanism can be harnessed for therapeutic purposes remains to be determined.

APPENDIX: Supplementary Data

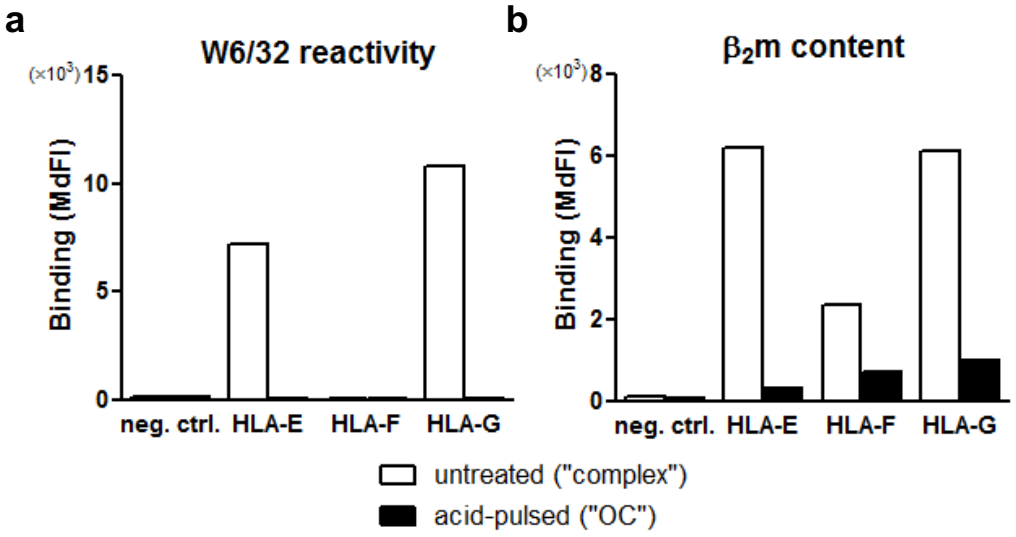

Supplementary Figure S2.1: Complex conformation and β_2m content assessment of non-classical HLA-I-coated beads. Non-classical HLA-I-coated beads (generated in this study) were untreated or acid-pulsed and stained with (***a***) anti-pan-HLA-I complex antibody (clone: W6/32) to assess for complex conformation on beads and (***b***) anti-β_2m antibody to quantify β_2m content.

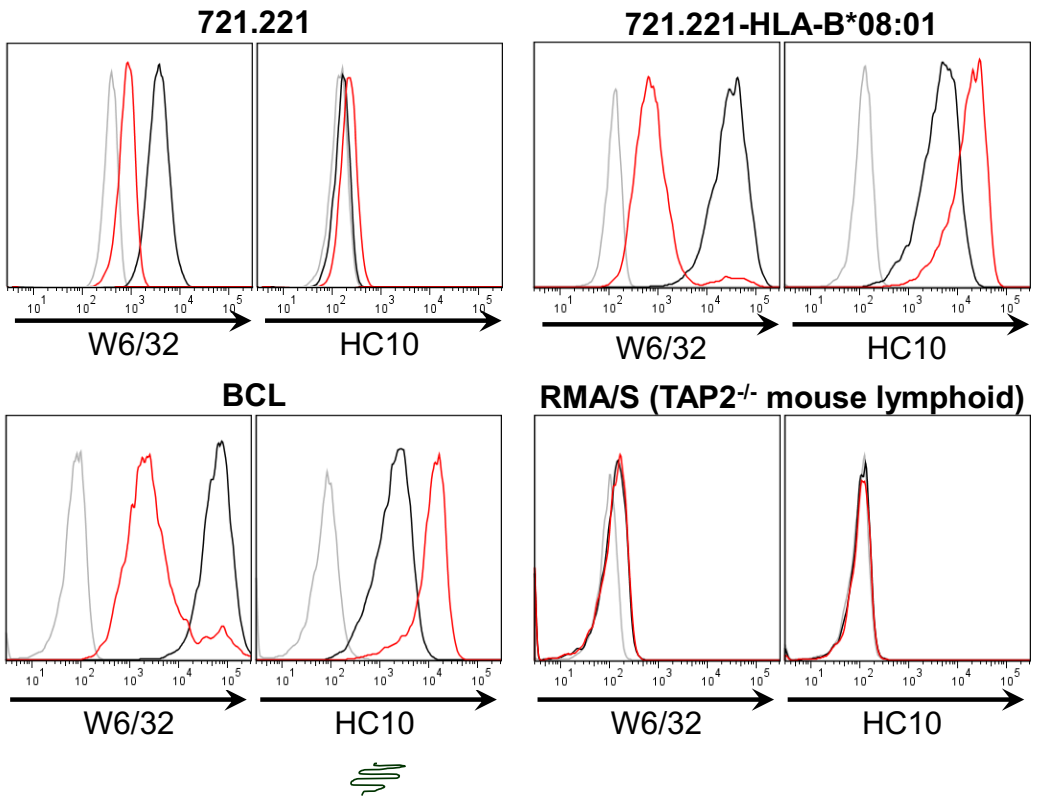

Supplementary Figure S2.2: HLA-I OC generation after acid pulsing. Indicated cell lines were stained with anti-HLA-I complex (W6/32) antibody and anti-HLA-B,C OC (HC10) antibody to confirm OC generation after acid pulsing protocol.

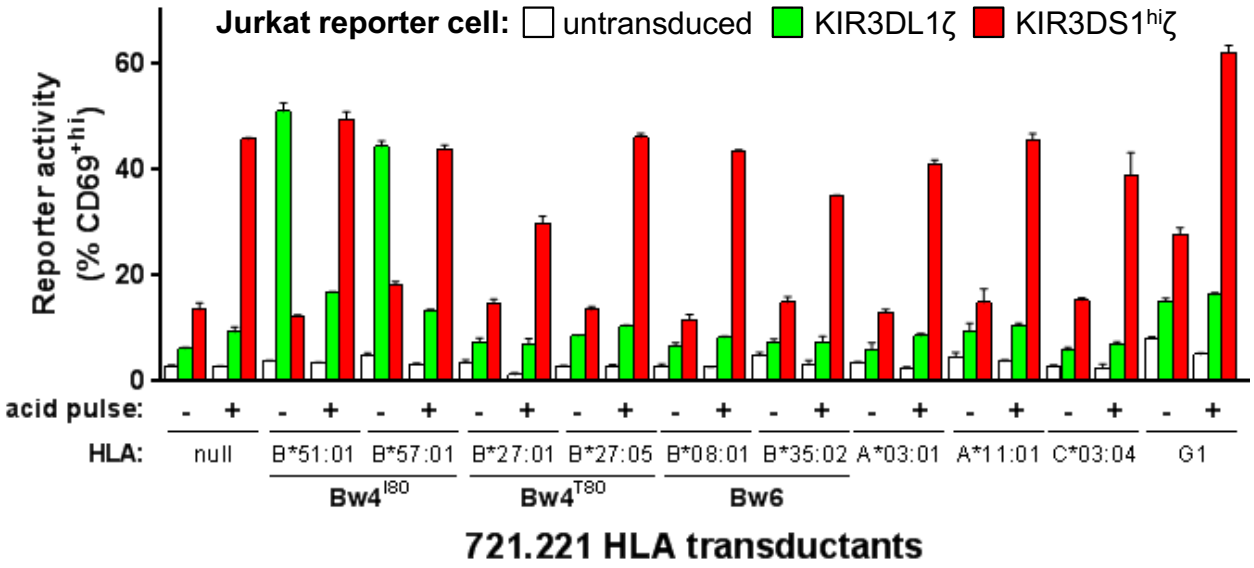

Supplementary Figure S2.3: 721.221 HLA transductants triggering of KIRζ Jurkat reporter cells. KIR3DL1ζ (*green bars*), KIR3DS1^{hi}ζ (*red bars*), and untransduced (*white bars*) Jurkat reporter cells were co-incubated with untreated (-) or acid pulsed (+) 721.221 cells expressing the indicated HLA-I proteins (2.5-h incubation and reporter:target cell ratio of 1:10); reporter activity was measured as the percentage of CD69^{+hi} Jurkat reporter cells. Data represent *n* = 3 technical replicates; independent experiments were performed for each 721.221 HLA transductant co-incubated with each Jurkat reporter cell line (*n* = 2 – 5; data not shown).

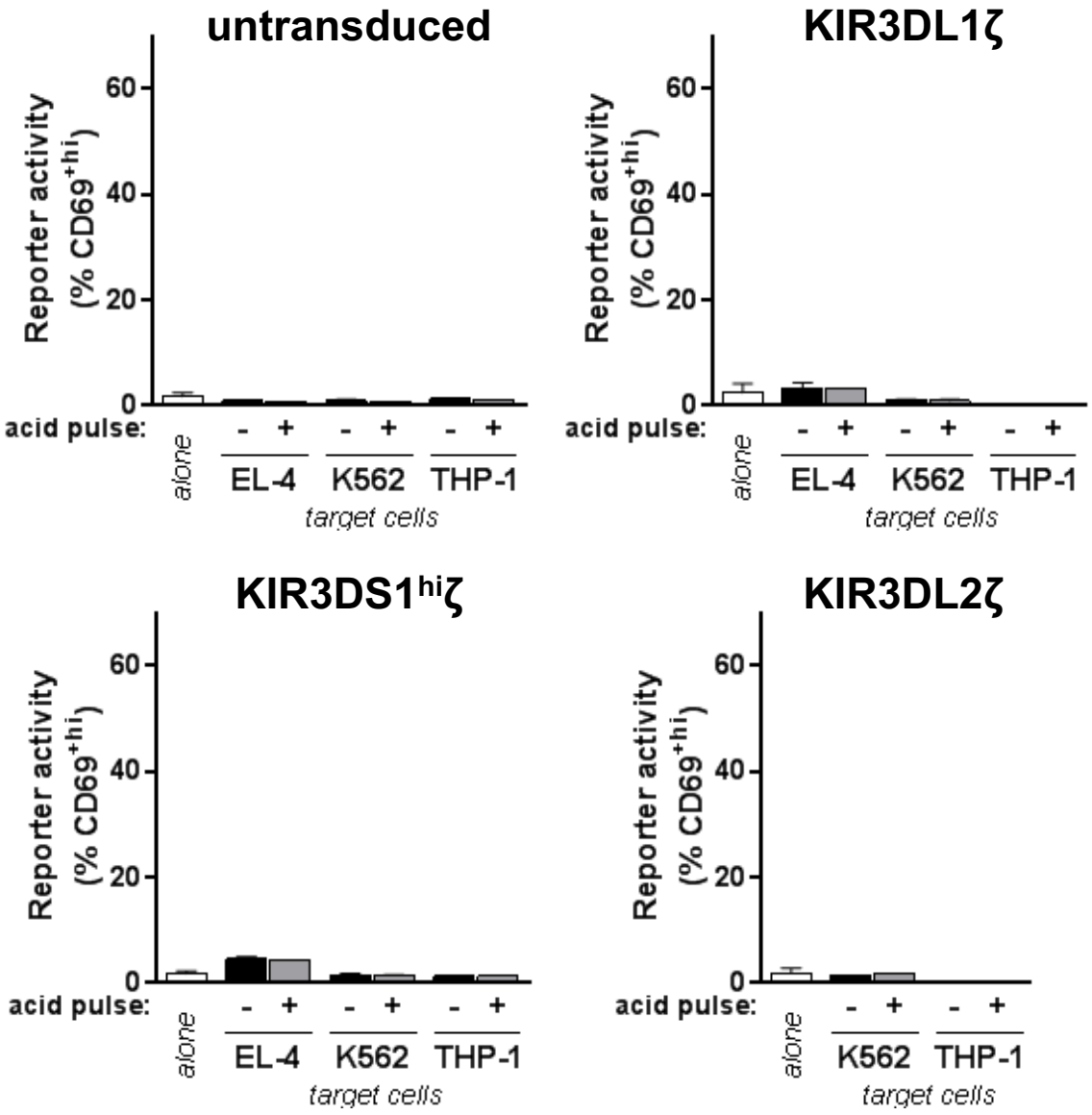

Supplementary Figure S2.4: HLA-F-deficient cell lines do not trigger KIR3DS1^{hi}ζ Jurkat reporter cells. KIR3DL1ζ (*top right panel*), KIR3DS1^{hi}ζ (*bottom left panel*), KIR3DL2ζ (*bottom right panel*), and untransduced (*top left panel*) Jurkat reporter cells were co-incubated with untreated (–; *black bars*) or acid-pulsed (+, *gray bars*) cell lines (2.5-h incubation and reporter:target cell ratio of 1:10); reporter activity was measured as the percentage of CD69^{+hi} Jurkat reporter cells. Cell lines used were EL-4 cells (mouse T-lymphoblastoid cell line), K562 cells (human chronic myelogenous leukemia line), and THP-1 cells (human acute monocytic leukemia line), all of which do not express HLA-F.

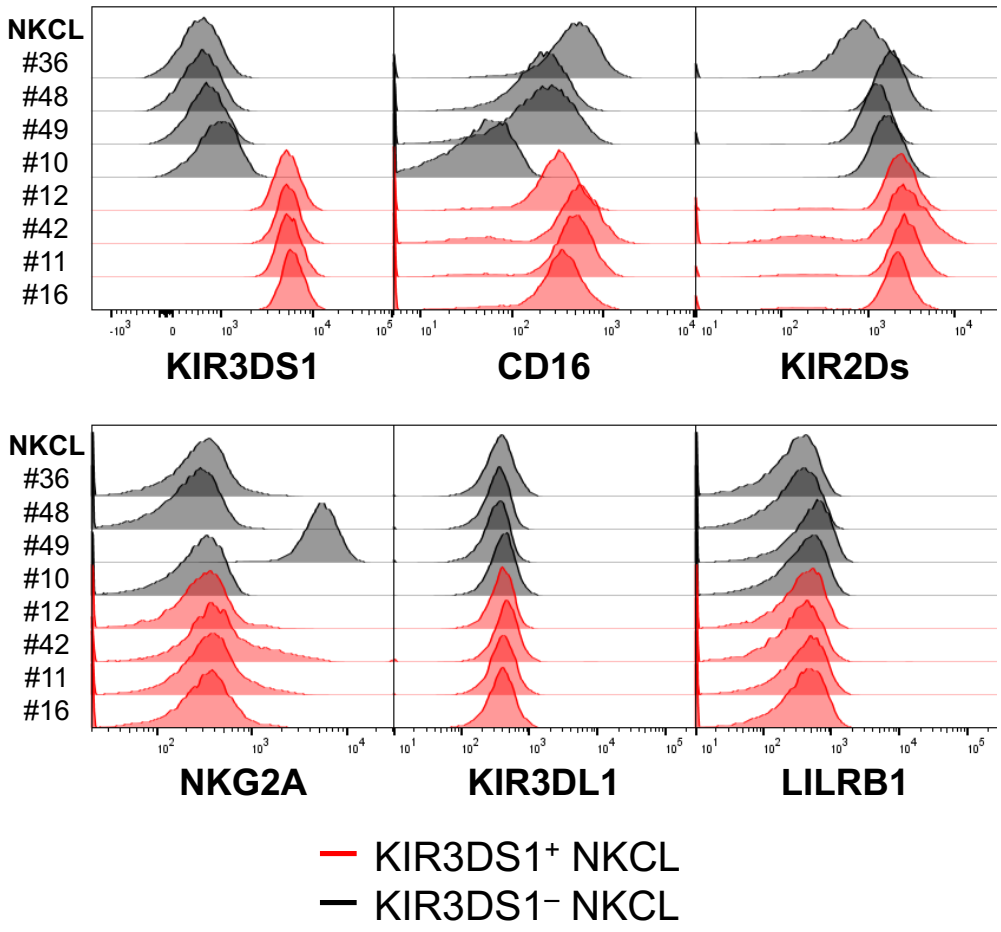

Supplementary Figure S3.1: NK-cell clone phenotypes for plate-bound ligand assay. NK-cell clones used for plate-bound ligand assays were stained for various NK-cell receptors, as indicated; KIR2Ds was measured by staining with anti-KIR2DL2/L3 (clone: DX27) and anti-KIR2DL1/S1 (clone: HP-MA4) having the same fluorophore.

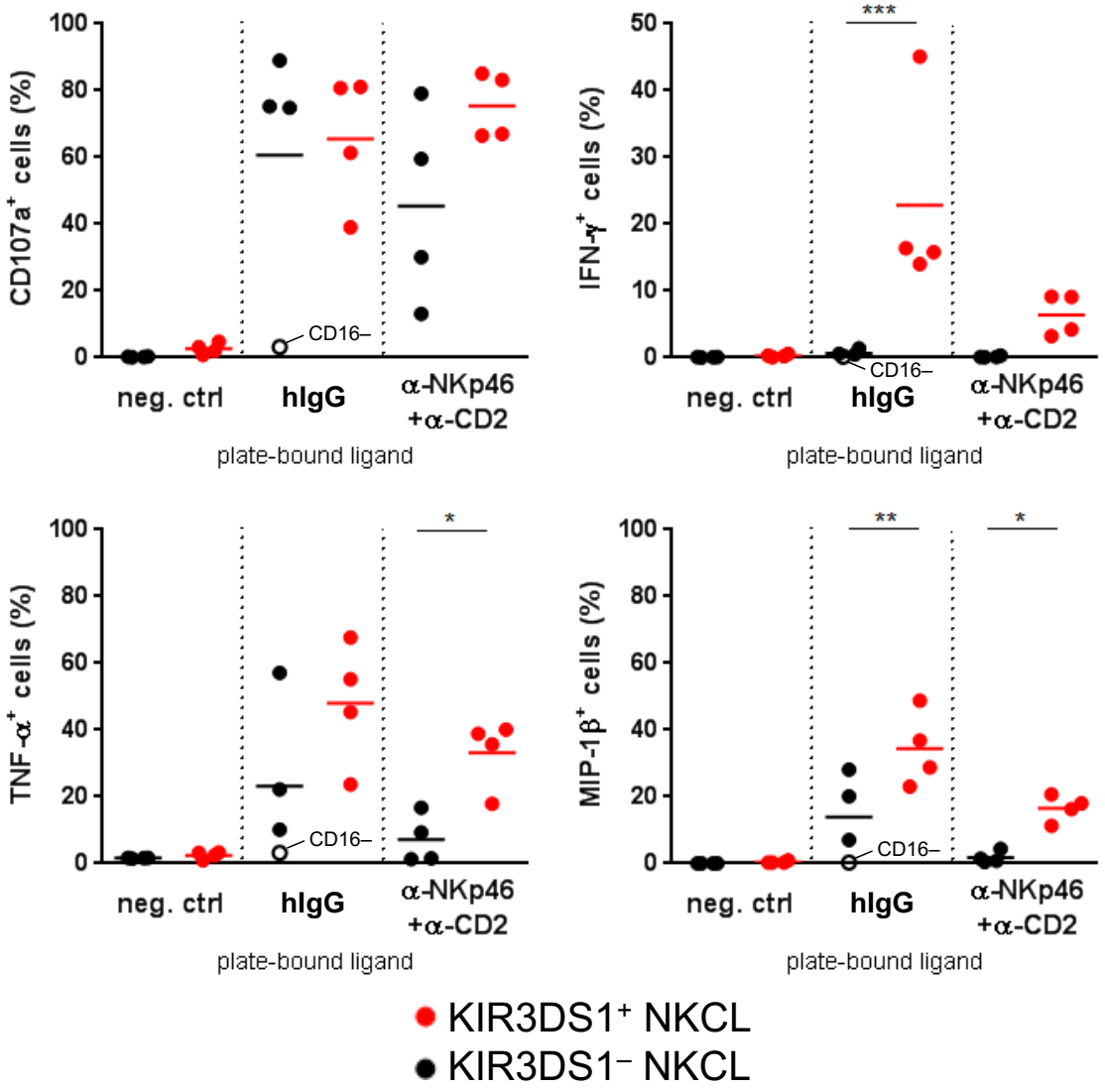

Supplementary Figure S3.2: KIR3DS1$^+$ NKCLs have superior intrinsic antiviral cytokine production capacity. KIR3DS1$^+$ (*red dots*) and KIR3DS1$^-$ NKCLs (*black dots*) were seeded onto well plates coated with irrelevant protein (neg. ctrl), human IgG (hIgG), or anti-NKp46 + anti-CD2 antibodies (α-NKp46+α-CD2). NKCLs were incubated for 5 h with anti-CD107a fluorescent antibody and brefeldin A, followed by surface stain for NK-cell markers and intracellular cytokine stain for IFN-γ, TNF-α, and MIP-1β (for details, see **Materials and Methods**). The raw percentages of CD107a$^+$ (*top left panel*), IFN-γ$^+$ (*top right panel*), TNF-α$^+$ (*bottom left panel*), and MIP-1β$^+$ (*bottom right panel*) NKCLs are presented. One-way ANOVA with Sidak multiple comparisons test comparing select columns was performed, and all statistically significant differences are presented (*, **, and *** denotes, $p < 0.05$, < 0.01, and < 0.001, respectively).

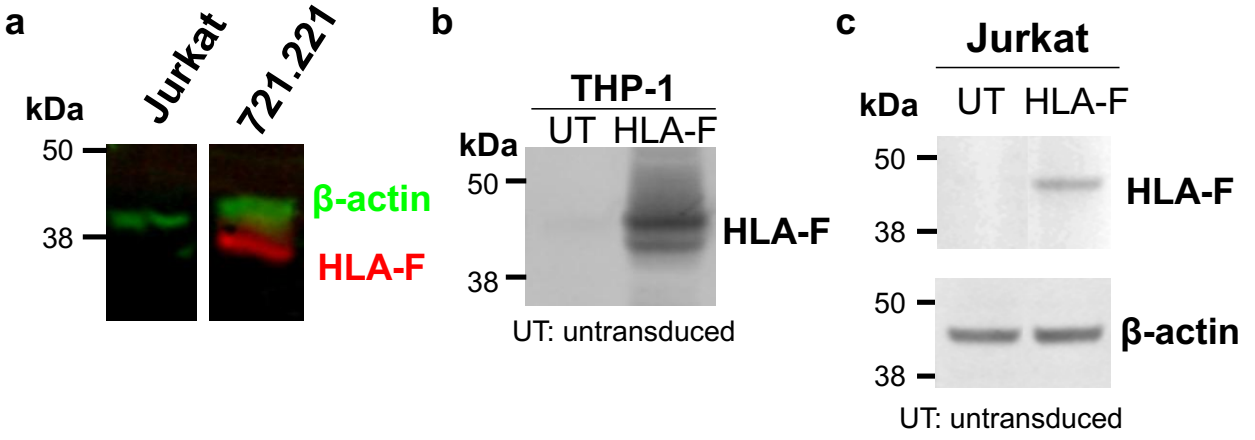

Supplementary Figure S3.3: Anti-HLA-F antibody (clone: mAbcam 8224) Western blot specificity testing. Cell lysates (non-nuclear) from cell lines were run on reducing/denaturing SDS-PAGE, followed by immunoblotting for HLA-F and β-actin (loading control) (for further details on immunoblotting, see **Materials and Methods**). In ***a***, Jurkat cells (HLA-F^{-}) and 721.221 cells (HLA-F^{+}) were compared. In ***b***, untransduced (UT) THP-1 cells (HLA-F-deficient) and THP-1 cells transduced with N-terminally FLAG-tagged HLA-F were compared. In ***c***, untransduced (UT) Jurkat cells and Jurkat cells transduced with N-terminally FLAG-tagged HLA-F were compared.

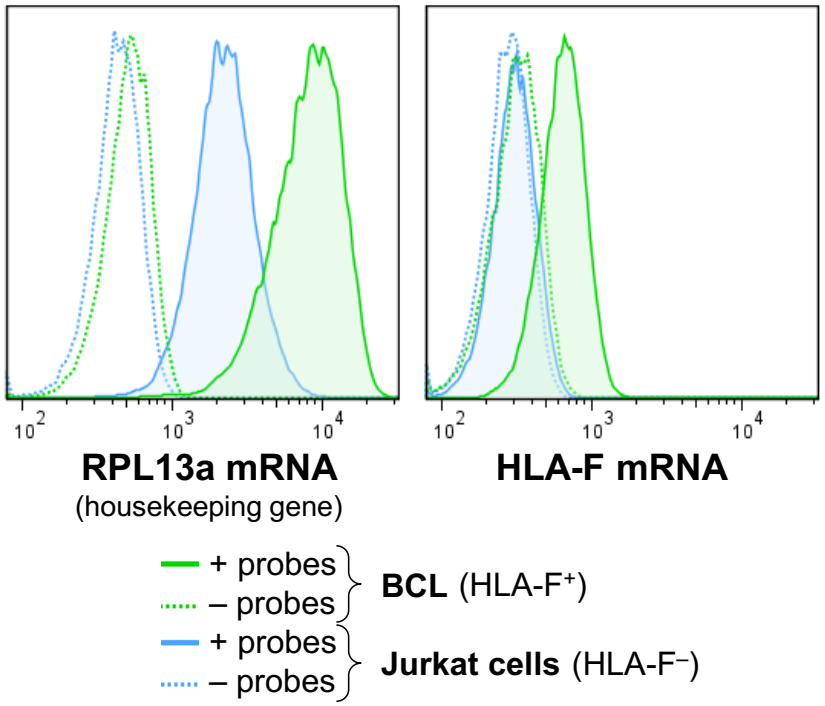

Supplementary Figure S3.4: Quality control testing of HLA-F mRNA probes in HLA-F$^+$ and HLA-F$^-$ cell lines. Fluorescent *in situ* hybridization and flow cytometry was done on an HLA-F$^+$ cell line (BCL) and an HLA-F$^-$ cell line (Jurkat cells) with probes for HLA-F mRNA and also RPL13a mRNA (a housekeeping gene). Dotted histograms indicate staining without probes ('– probe'; negative control) and solid-line, filled histograms are staining with probe ('+ probe').

NKCL		#33	#23	#36	#40	#27	#0
KIR	3DS1	+	+	+	-	-	-
	3DL2	-	-	-	+	-	-
	2DL2/L3	-	+	-	-	-	+/-
	2DL1/S1	+	-	-	+	-	+/-
NKG2A		+	+	+	+	+	+
LILRB1		-	-	-	-	-	-

Supplementary Figure S3.5: NK-cell clone phenotypes for co-culture assay. NK-cell clones used for HIV-1 replication inhibition assays were stained for various NK-cell receptors. '+' denotes >90% expression of the indicated receptor, '–' denotes a frequency of <5%, and '+/–' denotes a frequency >5% (in both cases for #0, ~10%).

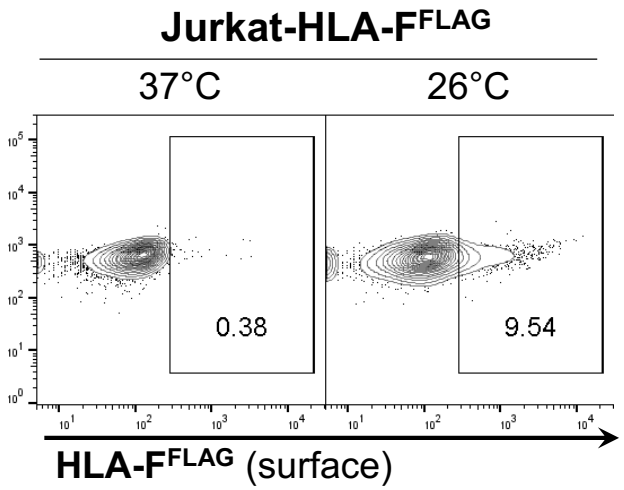

Supplementary Figure S3.6: Low-temperature incubation potently mobilizes HLA-F to the cell surface. Jurkat-HLA-F^{FLAG} cells (transduction efficiency ~10%) were cultured under normal conditions (37°C and 5% CO_2) or incubated at 26°C (and 5% CO_2) for 18 h. Cells were subsequently stained with anti-FLAG antibody to assess cell-surface expression of HLA-F.

Gene Symbol	Description	CRISPR Score
EXT1	exostosin glycosyltransferase 1	7.047
UXS1	UDP-glucuronate decarboxylase 1 (a.k.a. UDP-xylose synthase 1)	4.9493
EXTL3	exostosin-like glycosyltransferase 3	4.394
UGDH	UDP-glucose 6-dehydrogenase	4.0326
PAPSS1	3'-phosphoadenosine 5'-phosphosulfate synthase	1.1497
EXT2	exostosin glycosyltransferase 2	0.7124
B3GAT3	beta-1,3-glucuronyltransferase 3	0.6418
XYLT2	xylosyltransferase 2	0.4728
B4GALT7	xylosylprotein beta 1,4-galactosyltransferase 7	-0.4949

Supplementary Table S4.1: Genome-wide CRISPR/Cas9 knock-out screen top hits. Top nine enriched genes (symbol and description) are presented with their determined CRISPR score.

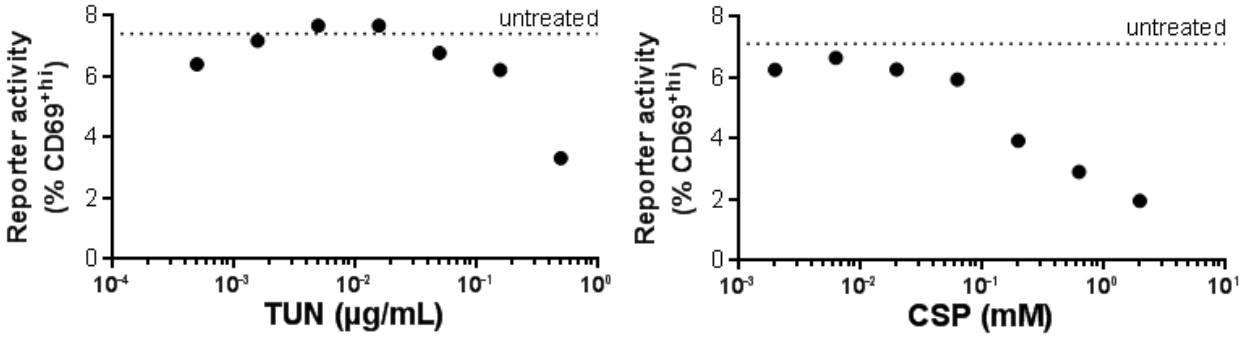

Supplemental Figure S5.1: Titration of glycosylation inhibitors. The effect of co-incubating 721.221-HLA-B*57:01 cells with different concentrations of TUN (in ***a***) and CSP (in ***b***) on the expression of CD69 in KIR3DL1ζ^{+} Jurkat cells (*n* = 1 for each). Reporter assay was carried out for 2 h at a reporter-to-target cell ratio = 10:1.

REFERENCES

1. Horowitz, A., Stegmann, K. A. & Riley, E. M. Activation of natural killer cells during microbial infections. *Front. Immunol.* **2,** 1–13 (2012).

2. Vivier, E. & Ugolini, S. Natural killer cells: From basic research to treatments. *Front. Immunol.* **2,** 2–5 (2011).

3. Parham, P., Norman, P. J., Abi-Rached, L. & Guethlein, L. A. Variable NK cell receptors exemplified by human KIR3DL1/S1. *J. Immunol.* **187,** 11–19 (2011).

4. Guethlein, L. A., Older Aguilar, A. M., Abi-Rached, L. & Parham, P. Evolution of killer cell Ig-like receptor (KIR) genes: definition of an orangutan KIR haplotype reveals expansion of lineage III KIR associated with the emergence of MHC-C. *J. Immunol.* **179,** 491–504 (2007).

5. Carr, W. H. *et al.* Cutting Edge: KIR3DS1, a gene implicated in resistance to progression to AIDS, encodes a DAP12-associated receptor expressed on NK cells that triggers NK cell activation. *J. Immunol.* **178,** 647–651 (2007).

6. Fadda, L. *et al.* Peptide antagonism as a mechanism for NK cell activation. *Proc. Natl. Acad. Sci.* **107,** 10160–10165 (2010).

7. Fadda, L. *et al.* Common HIV-1 peptide variants mediate differential binding of KIR3DL1 to HLA-Bw4 molecules. *J. Virol.* **85,** 5970–5974 (2011).

8. Orange, J. S. Natural killer cell deficiency. *J. Allergy Clin. Immunol.* **132,** 515–525 (2013).

9. Hillis, D. M. AIDS: Origins of HIV. *Science* **288,** 1757–1759 (2000).

10. UNAIDS. Fact Sheet 2015. *UNAIDS Rep.* 1–8 (2015).

11. Walker, B. D. & Yu, X. G. Unravelling the mechanisms of durable control of HIV-1. *Nat. Rev. Immunol.* **13,** 487–98 (2013).

12. Keele, B. F. *et al.* Identification and characterization of transmitted and early founder virus envelopes in primary HIV-1 infection. *Proc. Natl. Acad. Sci.* **105,** 7552–7557 (2008).

13. Alter, G. *et al.* Differential natural killer cell-mediated inhibition of HIV-1 replication based on distinct KIR/HLA subtypes. *J. Exp. Med.* **204,** 3027–3036 (2007).

14. Alter, G. *et al.* HIV-1 adaptation to NK-cell-mediated immune pressure. *Nature* **476,** 96–100 (2011).

15. Hölzemer, A. *et al.* Selection of an HLA-C*03:04-restricted HIV-1 p24 Gag sequence variant is associated with viral escape from KIR2DL3+ natural killer

cells: data from an observational cohort in South Africa. *PLoS Med.* **12,** 1–27 (2015).

16. Martin, M. P. *et al.* Epistatic interaction between KIR3DS1 and HLA-B delays the progression to AIDS. *Nat. Genet.* **31,** 429–434 (2002).

17. Cella, M., Longo, a, Ferrara, G. B., Strominger, J. L. & Colonna, M. NK3-specific natural killer cells are selectively inhibited by Bw4-positive HLA alleles with isoleucine 80. *J. Exp. Med.* **180,** 1235–1242 (1994).

18. Martin, M. P. *et al.* Innate partnership of HLA-B and KIR3DL1 subtypes against HIV-1. *Nat. Genet.* **39,** 733–740 (2007).

19. Jiang, Y. *et al.* KIR3DS1/L1 and HLA-Bw4-80I are associated with HIV disease progression among HIV typical progressors and long-term nonprogressors. *BMC Infect. Dis.* **13,** 405 (2013).

20. Guerini, F. R. *et al.* Under representation of the inhibitory KIR3DL1 molecule and the KIR3DL1+/BW4+ complex in HIV exposed seronegative individuals. *J. Infect. Dis.* **203,** 1235–1239 (2011).

21. Boulet, S. *et al.* Increased proportion of KIR3DS1 homozygotes in HIV-exposed uninfected individuals. *AIDS* **22,** 595–599 (2008).

22. Jennes, W. *et al.* Inhibitory KIR/HLA incompatibility between sexual partners confers protection against HIV-1 transmission. *Blood* **121,** 1157–1164 (2013).

23. Kim, S. *et al.* HLA alleles determine differences in human natural killer cell responsiveness and potency. *Proc. Natl. Acad. Sci.* **105,** 3053–3058 (2008).

24. Vivian, J. P. *et al.* Killer cell immunoglobulin-like receptor 3DL1-mediated recognition of human leukocyte antigen B. *Nature* **479,** 401–405 (2011).

25. O'Connor, G. M. *et al.* Peptide-dependent recognition of HLA-B*57:01 by KIR3DS1. *J. Virol.* **89,** 5213–5221 (2015).

26. Morvan, M. *et al.* Phenotypic and functional analyses of KIR3DL1+ and KIR3DS1+ NK cell subsets demonstrate differential regulation by Bw4 molecules and induced KIR3DS1 expression on stimulated NK cells. *J. Immunol.* **182,** 6727–6735 (2009).

27. Alter, G. *et al.* HLA class I subtype-dependent expansion of KIR3DS1+ and KIR3DL1+ NK cells during acute human immunodeficiency virus type 1 infection. *J. Virol.* **83,** 6798–6805 (2009).

28. Song, R. *et al.* HIV Protective KIR3DL1/S1-HLA-B Genotypes Influence NK Cell-Mediated Inhibition of HIV Replication in Autologous CD4 Targets. *PLoS Pathog.* **10,** 1–12 (2014).

29. Long, B. R. *et al.* Conferral of enhanced natural killer cell function by KIR3DS1 in early human immunodeficiency virus type 1 infection. *J. Virol.* **82,** 4785–4792 (2008).

30. Barbour, J. D. *et al.* Synergy or independence? Deciphering the interaction of HLA class I and NK cell KIR alleles in early HIV-1 disease progression. *PLoS Pathog.* **3,** 1540 (2007).

31. Zhi-ming, L. *et al.* Polymorphisms of killer cell immunoglobulin-like receptor gene: possible association with susceptibility to or clearance of hepatitis B virus infection in Chinese Han population. *Croat. Med. J.* **48,** 800–806 (2007).

32. Aranda-Romo, S. *et al.* Killer-cell immunoglobulin-like receptors (KIR) in severe A (H1N1) 2009 influenza infections. *Immunogenetics* **64,** 653–662 (2012).

33. López-Vázquez, A. *et al.* Protective effect of the HLA-Bw4I80 epitope and the killer cell immunoglobulin-like receptor 3DS1 gene against the development of hepatocellular carcinoma in patients with hepatitis C virus infection. *J. Infect. Dis.* **192,** 162–165 (2005).

34. Besson, C. *et al.* Association of killer cell immunoglobulin-like receptor genes with Hogkin's lymphoma in a familial study. *PLoS One* **2,** 1–10 (2007).

35. Cariani, E. *et al.* HLA and killer immunoglobulin-like receptor genes as outcome predictors of hepatitis C virus-related hepatocellular carcinoma. *Clin. Cancer Res.* **19,** 5465–5473 (2013).

36. Bonagura, V. R. *et al.* Activating killer cell immunoglobulin-like receptors 3DS1 and 2DS1 protect against developing the severe form of recurrent respiratory papillomatosis. *Hum. Immunol.* **71,** 212–219 (2010).

37. Carrington, M. *et al.* Hierarchy of resistance to cervical neoplasia mediated by combinations of killer immunoglobulin-like receptor and human leukocyte antigen loci. *J. Exp. Med.* **201,** 1069–1075 (2005).

38. Gabriel, I. H. *et al.* Interaction between KIR3DS1 and HLA-Bw4 predicts for progression-free survival after autologous stem cell transplantation in patients with multiple myeloma. *Blood* **116,** 2033–2039 (2010).

39. Gagne, K. *et al.* Donor KIR3DL1/3DS1 gene and recipient Bw4 KIR ligand as prognostic markers for outcome in unrelated hematopoietic stem cell transplantation. *Biol. Blood Marrow Transplant.* **15,** 1366–1375 (2009).

40. Venstrom, J. M. *et al.* Donor activating KIR3DS1 is associated with decreased acute GVHD in unrelated allogeneic hematopoietic stem cell transplantation. *Blood* **115,** 3162–3165 (2010).

41. Díaz-Peña, R. *et al.* Association of the KIR3DS1*013 and KIR3DL1*004 alleles

with susceptibility to ankylosing Spondylitis. *Arthritis Rheum.* **62,** 1000–1006 (2010).

42. Trydzenskaya, H. *et al.* The genetic predisposition of natural killer cell to BK virus-associated nephropathy in renal transplant patients. *Kidney Int.* **84,** 359–65 (2013).

43. Waggoner, S. N., Cornberg, M., Selin, L. K. & Welsh, R. M. Natural killer cells act as rheostats modulating antiviral T cells. *Nature* **481,** 394–398 (2011).

44. Alter, G. & Altfeld, M. Mutiny or scrutiny: NK cell modulation of DC function in HIV-1 infection. *Trends Immunol.* **32,** 219–224 (2011).

45. Paust, S. & von Andrian, U. H. Natural killer cell memory. *Nat. Immunol.* **12,** 500–508 (2011).

46. Benson, D. M. *et al.* Aphase 1 trial of the anti-KIR antibody IPH2101 in patients with relapsed/refractory multiple myeloma. *Blood* **120,** 4324–4333 (2012).

47. Rajalingam, R. Human diversity of killer cell immunoglobulin-like receptors and disease. *Korean J. Hematol.* **46,** 216 (2011).

48. Min-Oo, G., Kamimura, Y., Hendricks, D. W., Nabekura, T. & Lanier, L. L. Natural killer cells: Walking three paths down memory lane. *Trends Immunol.* **34,** 251–258 (2013).

49. Rivero-Juarez, A. *et al.* Natural killer KIR3DS1 is closely associated with HCV viral clearance and sustained virological response in HIV/HCV patients. *PLoS One* **8,** 8–13 (2013).

50. O'Connor, G. M. *et al.* Functional polymorphism of the KIR3DL1/S1 receptor on human NK cells. *J. Immunol.* **178,** 235–241 (2010).

51. Gillespie, G. M. a *et al.* Lack of KIR3DS1 binding to MHC class I Bw4 tetramers in complex with CD8+ T cell epitopes. *AIDS Res. Hum. Retroviruses* **23,** 451–455 (2007).

52. Gardiner, C. M. *et al.* Different NK cell surface phenotypes defined by the DX9 antibody are due to KIR3DL1 gene polymorphism. *J. Immunol.* **166,** 2992–3001 (2001).

53. Thananchai, H. *et al.* Cutting Edge: Allele-specific and peptide-dependent interactions between KIR3DL1 and HLA-A and HLA-B. *J. Immunol.* **178,** 33–37 (2007).

54. Sharma, D. *et al.* Dimorphic motifs in D0 and D1+D2 domains of killer cell Ig-like receptor 3DL1 combine to form receptors with high, moderate, and no avidity for the complex of a peptide derived from HIV and HLA-A*2402. *J. Immunol.* **183,**

4569–4582 (2009).

55. Arosa, F. A., Santos, S. G. & Powis, S. J. Open conformers: the hidden face of MHC-I molecules. *Trends Immunol.* **28,** 115–123 (2007).

56. Wainwright, S. D., Biro, P. a & Holmes, C. H. HLA-F is a predominantly empty, intracellular, TAP-associated MHC class Ib protein with a restricted expression pattern. *J. Immunol.* **164,** 319–328 (2000).

57. Goodridge, J. P., Burian, A., Lee, N. & Geraghty, D. E. HLA-F complex without peptide binds to MHC class I protein in the open conformer form. *J. Immunol.* **184,** 6199–6208 (2010).

58. Trundley, A., Frebel, H., Jones, D., Chang, C. & Trowsdale, J. Allelic expression patterns of KIR3DS1 and 3DL1 using the Z27 and DX9 antibodies. *Eur. J. Immunol.* **37,** 780–787 (2007).

59. Pertel, T. *et al.* TRIM5 is an innate immune sensor for the retrovirus capsid lattice. *Nature* **472,** 361–365 (2011).

60. Sanjana, N. E., Shalem, O. & Zhang, F. Improved vectors and genome-wide libraries for CRISPR screening. *Nat. Methods* **11,** 783–784 (2014).

61. Mandal, P. K. *et al.* Efficient Ablation of Genes in Human Hematopoietic Stem and Effector Cells using CRISPR/Cas9. *Cell Stem Cell* **15,** 643–652 (2014).

62. Lee, N., Ishitani, A. & Geraghty, D. E. HLA-F is a surface marker on activated lymphocytes. *Eur. J. Immunol.* **40,** 2308–2318 (2010).

63. Kumar, G., Date, O. S., Kim, K. S. & Manjunath, R. Infection of human amniotic and endothelial cells by Japanese encephalitis virus: Increased expression of HLA-F. *Virology* **471-473,** 29–37 (2014).

64. Yang, Y., Chu, W., Geraghty, D. E. & Hunt, J. S. Expression of HLA-G in human mononuclear phagocytes and selective induction by IFN-gamma. *J. Immunol.* **156,** 4224–4231 (1996).

65. Ljunggren, H.-G. *et al.* Empty MHC class I molecules come out in the cold. *Nature* **346,** 476–480 (1990).

66. Cella, M. & Colonna, M. in *Methods in Molecular Biology: Natural Killer Cell Protocols: Cellular and Molecular Methods* (eds. Campbell, K. S. & Colonna, M.) **121,** 1–4 (Humana Press, 1999).

67. Imai C., Iwamoto S., C. D. Genetic modification of primary natural killer cells overcomes inhibitory signals and induces specific killing of leukemic cells. *Leukemia* **106,** 376–383 (2005).

68. Tarbell, J. M. & Cancel, L. M. The glycocalyx and its significance in human medicine. *J. Intern. Med.* **280,** 97–113 (2016).

69. Esko, J. D., Kimata, K. & Lindahl, U. in *Essentials of Glycobiology* (2009). doi:10:0-87969-559-5

70. Sarrazin, S., Lamanna, W. C. & Esko, J. D. Heparan sulfate proteoglycans. *Cold Spring Harb. Perspect. Biol.* **3,** 1–33 (2011).

71. Bode, L. *et al.* Heparan sulfate and syndecan-1 are essential in maintaining murine and human intestinal epithelial barrier function. *J. Clin. Invest.* **118,** 229–238 (2008).

72. O'Brien, J. R. The effect of heparin on the early stages of blood coagulation. *J. Clin. Path.* **13,** 93–98 (1960).

73. Olczyk, P., Mencner, Ł. & Komosinska-Vassev, K. Diverse Roles of Heparan Sulfate and Heparin in Wound Repair. *BioMed Res. Int.* **2015,** 1–7 (2015).

74. Echtermeyer, F. *et al.* Delayed wound repair and impaired angiogenesis in mice lacking syndecan-4. *J. Clin. Invest.* **107,** R9–R14 (2001).

75. Inatani, M., Irie, F., Plump, A. S., Tessier-Lavigne, M. & Yamaguchi, Y. Mammalian brain morphogenesis and midline axon guidance require heparan sulfate. *Science* **302,** 1044–1046 (2003).

76. Crawford, B. E. *et al.* Loss of the heparan sulfate sulfotransferase, Ndst1, in mammary epithelial cells selectively blocks lobuloalveolar development in mice. *PLoS One* **5,** 1–10 (2010).

77. Zimmermann, P. *et al.* Syndecan recyling is controlled by syntenin-PIP2 interaction and Arf6. *Dev. Cell* **9,** 377–388 (2005).

78. Wang, L., Fuster, M., Sriramarao, P. & Esko, J. D. Endothelial heparan sulfate deficiency impairs L-selectin- and chemokine-mediated neutrophil trafficking during inflammatory responses. *Nat. Immunol.* **6,** 902–10 (2005).

79. Qiu, J., Handa, a, Kirby, M. & Brown, K. E. The interaction of heparin sulfate and adeno-associated virus 2. *Virology* **269,** 137–147 (2000).

80. Jones, K. S., Petrow-sadowski, C., Bertolette, D. C., Huang, Y. & Ruscetti, F. W. Heparan Sulfate Proteoglycans Mediate Attachment and Entry of Human T-Cell Leukemia Virus Type 1 Virions into. *J. Virol.* **79,** 12692–12702 (2005).

81. Kalia, M., Chandra, V., Rahman, S. A., Sehgal, D. & Jameel, S. Heparan sulfate proteoglycans are required for cellular binding of the hepatitis E virus ORF2 capsid protein and for viral infection. *J. Virol.* **83,** 12714–12724 (2009).

82. Xu, D. *et al.* Characterization of heparan sulphate 3-O-sulphotransferase isoform 6 and its role in assisting the entry of herpes simplex virus type 1. *Biochem. J.* **385,** 451–9 (2005).

83. Zhang, Z. *et al.* Heparin sulphate d-glucosaminyl 3-O-sulfotransferase 3B1 plays a role in HBV replication. *Virology* **406,** 280–285 (2010).

84. Shukla, D. & Spear, P. G. Herpesviruses and heparan sulfate: an intimate relationship in aid of viral entry. *J. Clin. Invest.* **108,** 503–510 (2001).

85. McDermott, S. P. *et al.* Juvenile syndecan-1 null mice are protected from carcinogen-induced tumor development. *Oncogene* **26,** 1407–1416 (2007).

86. Parish, C. R. Heparan sulfate and inflammation. *Nat. Immunol.* **6,** 861–862 (2005).

87. Jakobsson, L. *et al.* Heparan Sulfate in trans Potentiates VEGFR-Mediated Angiogenesis. *Dev. Cell* **10,** 625–634 (2006).

88. Yayon, A., Klagsbrun, M., Esko, J. D., Leder, P. & Ornitz, D. M. Cell-surface, heparin-like molecules are required for binding of basic fibroblast growth-factor to its high-affinity receptor. *Cell* **64,** 841–848 (1991).

89. Lortat-Jacob, H., Turnbull, J. E. & Grimaud, J. a. Molecular organization of the interferon gamma-binding domain in heparan sulphate. *Biochem. J.* **310 (Pt 2,** 497–505 (1995).

90. Lortat-Jacob, H., Grosdidier, A. & Imberty, A. Structural diversity of heparan sulfate binding domains in chemokines. *Proc. Natl. Acad. Sci.* **99,** 1229–1234 (2002).

91. Parish, C. R. The role of heparan sulphate in inflammation. *Nat. Rev. Immunol.* **6,** 633–643 (2006).

92. Safaiyan, F. *et al.* Selective effects of sodium chlorate treatment on the sulfation of heparan sulfate. *J. Biol. Chem.* **274,** 36267–36273 (1999).

93. Sasisekharan, R. & Venkataraman, G. Heparin and heparan sulfate: biosynthesis , structure and function. *Biopolymers* **4,** 626–631 (2000).

94. Hudspeth, K., Silva-Santos, B. & Mavilio, D. Natural Cytotoxicity Receptors: Broader Expression Patterns and Functions in Innate and Adaptive Immune Cells. *Front. Immunol.* **4,** 1–15 (2013).

95. Hecht, M. *et al.* Natural Cytotoxicity Receptors NKp30 , NKp44 and NKp46 Bind to Different Heparan Sulfate / Heparin Sequences Natural Cytotoxicity Receptors NKp30 , NKp44 and NKp46 Bind to Different Heparan Sulfate / Heparin Sequences. *J. Proteome Res.* 712–720 (2009). doi:10.1021/pr800747c

96. Brusilovsky, M. *et al.* Genome-wide siRNA screen reveals a new cellular partner of NK cell receptor KIR2DL4: heparan sulfate directly modulates KIR2DL4-mediated responses. *J. Immunol.* **191,** 5256–5267 (2013).

97. Wang, T. *et al.* Identification and characterization of essential genes in the human genome. *Science* **350,** 1096–1101 (2015).

98. van den Born, J. *et al.* Novel Heparan Sulfate Structures Revealed by Monoclonal Antibodies. *J. Biol. Chem.* **280,** 20516–20523 (2005).

99. Gasteiger, E. *et al.* in *The Proteomics Protocols Handbook* (ed. Walker, J. M.) 571–607 (Humana Press Inc., 2005). at <http://web.expasy.org/protparam>

100. Robinson, J. *et al.* The IPD and IMGT/HLA database: Allele variant databases. *Nucleic Acids Res.* **43,** D423–D431 (2015).

101. Robinson, J., Halliwell, J. A., McWilliam, H., Lopez, R. & Marsh, S. G. E. IPD - The Immuno Polymorphism Database. *Nucleic Acids Res.* **41,** 1234–1240 (2013).

102. Orange, J. S. Unraveling human natural killer cell deficiency. *J. Clin. Invest.* **122,** 798–801 (2012).

103. Long, E. O., Sik Kim, H., Liu, D., Peterson, M. E. & Rajagopalan, S. Controlling Natural Killer Cell Responses: Integration of Signals for Activation and Inhibition. *Annu. Rev. Immunol.* **31,** 227–258 (2013).

104. Fadda, L. *et al.* HLA-Cw*0102-restricted HIV-1 p24 epitope variants can modulate the binding of the inhibitory KIR2DL2 receptor and primary NK cell function. *PLoS Pathog.* **8,** 40 (2012).

105. Körner, C. & Altfeld, M. Role of KIR3DS1 in human diseases. *Front. Immunol.* **3,** 1–11 (2012).

106. Bashirova, A. a, Martin, M. P., McVicar, D. W. & Carrington, M. The killer immunoglobulin-like receptor gene cluster: tuning the genome for defense. *Annu. Rev. Genomics Hum. Genet.* **7,** 277–300 (2006).

107. Bieberich, E. Synthesis, processing, and function of N-glycans in N-glycoproteins. *Adv. Neurobiol.* **9,** 47–70 (2014).

108. Moremen, K. W., Tiemeyer, M. & Nairn, A. V. Vertebrate protein glycosylation: diversity, synthesis and function. *Nat. Rev. Mol. Cell Biol.* **13,** 4484–62 (2012).

109. Barbosa, J. a *et al.* Site-directed mutagenesis of class I HLA genes: role of glycosylation in surface expression and functional recognition. *J. Exp. Med.* **166,** 1329–1350 (1987).

110. Barber, L. D. *et al.* Unusual uniformity of the N-linked oligosaccharides of HLA-A,

-B, and -C glycoproteins. *J. Immunol.* **156,** 3275–3284 (1996).

111. Schönthal, A. H. Endoplasmic reticulum stress: its role in disease and novel prospects for therapy. *Scientifica (Cairo)* **2012,** 857516 (2012).

112. Esko, J. D. & Bertozzi, C. R. in *Essential of Glycobiology* (2009).

113. van Kemenade, F. J. *et al.* Glucosidase trimming inhibitors preferentially perturb T cell activation induced by CD2 mAb. *J. Leukoc. Biol.* **56,** 159–165 (1994).

114. Wolfert, M. a & Boons, G.-J. Adaptive immune activation: glycosylation does matter. *Nat. Chem. Biol.* **9,** 776–84 (2013).

115. Bagriacik, E. U., Kirkpatrick, A. & Miller, K. S. Glycosylation of native MHC class Ia molecules is required for recognition by allogeneic cytotoxic T lymphocytes. *Glycobiology* **6,** 413–421 (1996).

116. Ploegh, H. L., Orr, H. T. & Strominger, J. L. Biosynthesis and cell surface localization of nonglycosylated human histocompatibility antigens. *J. Immunol.* **126,** 270–275 (1981).

117. Allen, R. L., Raine, T., Haude, a, Trowsdale, J. & Wilson, M. J. Leukocyte receptor complex-encoded immunomodulatory receptors show differing specificity for alternative HLA-B27 structures. *J. Immunol.* **167,** 5543–5547 (2001).

118. Jones, D. C. *et al.* HLA class I allelic sequence and conformation regulate leukocyte Ig-like receptor binding. *J. Immunol.* **186,** 2990–2997 (2011).

119. Lepin, E. J. M. *et al.* Functional characterization of HLA-F and binding of HLA-F tetramers to ILT2 and ILT4 receptors. *Eur. J. Immunol.* **30,** 3552–3561 (2000).

120. Goodridge, J. P., Burian, A., Lee, N. & Geraghty, D. E. HLA-F and MHC class I open conformers are ligands for NK cell Ig-like receptors. *J. Immunol.* **191,** 3553–62 (2013).

121. Pan, F. H., Liu, X. X. & Tian, W. Characterization of HLA-F polymorphism in four distinct populations in Mainland China. *Int. J. Immunogenet.* **40,** 369–376 (2013).

122. Shiina, T. *et al.* Molecular dynamics of MHC genesis unraveled by sequence analysis of the 1,796,938-bp HLA class I region. *Proc. Natl. Acad. Sci.* **96,** 13282–13287 (1999).

123. Lee, N. & Geraghty, D. E. HLA-F surface expression on B cell and monocyte cell lines is partially independent from tapasin and completely independent from TAP. *J. Immunol.* **171,** 5264–5271 (2003).

124. Noguchi, K. *et al.* Detection of anti-HLA-F antibodies in sera from cancer patients. *Anticancer Res.* **42,** 3387–3392 (2004).

125. Le Gall, S. *et al.* Nef Interacts with the μ Subunit of Clathrin Adaptor Complexes and Reveals a Cryptic Sorting Signal in MHC I Molecules. *Immunity* **8,** 483–495 (1998).

126. Collins, K. L., Chen, B. K., Kalams, S. A., Walker, B. D. & Baltimore, D. HIV-1 Nef protein protects infected primary cells against killing by cytotoxic T lymphocytes. *Nature* **391,** 397–401 (1998).

127. Cohen, G. B. *et al.* The selective downregulation of class I major histocompatibility complex proteins by HIV-1 protects HIV-infected cells from NK cells. *Immunity* **10,** 661–671 (1999).

128. Cerboni, C. *et al.* Human immunodeficiency virus 1 Nef protein downmodulates the ligands of the activating receptor NKG2D and inhibits natural killer cell-mediated cytotoxicity. *J. Gen. Virol.* **88,** 242–50 (2007).

129. Derrien, M. *et al.* Human immunodeficiency virus 1 downregulates cell surface expression of the non-classical major histocompatibility class I molecule HLA-G1. *J. Gen. Virol.* **85,** 1945–1954 (2004).

130. Apps, R. *et al.* HIV-1 Vpu mediates HLA-C downregulation. *Cell Host Microbe* **19,** 686–695 (2016).

131. Boyle, L. H., Gillingham, A. K., Munro, S. & Trowsdale, J. Selective export of HLA-F by its cytoplasmic tail. *J. Immunol.* **176,** 6464–6472 (2006).

132. Jinushi, M., Hodi, F. S. & Dranoff, G. Therapy-induced antibodies to MHC class I chain-related protein A antagonize immune suppression and stimulate antitumor cytotoxicity. *Proc. Natl. Acad. Sci.* **103,** 9190–9195 (2006).

133. Jinushi, M. *et al.* MHC class I chain-related protein A antibodies and shedding are associated with the progression of multiple myeloma. *Proc. Natl. Acad. Sci.* **105,** 1285–1290 (2008).

134. Pelak, K. *et al.* Copy number variation of KIR genes influences HIV-1 control. *PLoS Biol.* **9,** (2011).

135. Cisneros, E., Moraru, M., Gómez-Lozano, N., López-Botet, M. & Vilches, C. KIR2DL5: An orphan inhibitory receptor displaying complex patterns of polymorphism and expression. *Front. Immunol.* **3,** 1–8 (2012).

136. Miyamoto, K. *et al.* Methylation-associated silencing of heparan sulfate D-glucosaminyl 3-O-sulfotransferase-2 (3-OST-2) in human breast, colon, lung and pancreatic cancers. *Oncogene* **22,** 274–280 (2003).

137. Bui, C. *et al.* Epigenetics: methylation-associated repression of heparan sulfate 3-O-sulfotransferase gene expression contributes to the invasive phenotype of H-EMC-SS chondrosarcoma cells. *FASEB J.* **24,** 436–450 (2010).

138. Hanahan, D. & Weinberg, R. A. Hallmarks of cancer: the next generation. *Cell* **144,** 646–674 (2011).

139. Storkus, W. J., Alexander, J., Payne, J. A., Cresswell, P. & Dawson, J. R. The alpha1/alpha2 domains of class I HLA molecules confer resistance to natural killing. *J. Immunol.* **143,** 3853–3857 (1989).

140. Goldstein, S. A. N. & Mescher, M. F. Carbohydrate moieties of major histocompatibility complex class I alloantigens are not required for their recognition by T lymphocytes. *J. Exp. Med.* **162,** 1381–1386 (1985).

141. Hart, G. W. The role of asparagine-linked oligosaccharides in cellular recognition by thymic lymphocytes. *J. Biol. Chem.* **257,** 151–158 (1982).

142. Miyazaki, J.-I., Appella, E., Zhao, H., Forman, J. & Ozato, K. Expression and function of a nonglycosylated major histocompatibility class I antigen. *J. Exp. Med.* **163,** 856–871 (1986).

143. Braud, V. M. *et al.* HLA-E binds to natural killer cell receptors CD94/NKG2A, B and C. *Nature* **391,** 795–799 (1998).

144. Ackerman, M. E. *et al.* Natural variation in Fc glycosylation of HIV-specific antibodies impacts antiviral activity. *J. Clin. Invest.* **123,** 2183–2192 (2013).

145. Chung, A. W. *et al.* Identification of antibody glycosylation structures that predict monoclonal antibody Fc-effector function. *AIDS* **28,** 2523–2530 (2014).

146. Vestrheim, A. C. *et al.* A pilot study showing differences in glycosylation patterns of IgG subclasses induced by pneumococcal, meningococcal, and two types of influenza vaccines. *Immunity, Inflamm. Dis.* **2,** 76–91 (2014).

147. Parham, P., Alpert, B. N., Orr, H. T. & Strominger, J. L. Carbohydrate moiety of HLA antigens: antigenic properties and amino acid sequences around the site of glycosylation. *J. Biol. Chem.* **252,** 7555–7567 (1977).

148. Nagae, M. & Yamaguchi, Y. Function and 3D structure of the N-glycans on glycoproteins. *Int. J. Mol. Sci.* **13,** 8398–8429 (2012).

149. Lantéri, M. *et al.* Altered T cell surface glycosylation in HIV-1 infection results in increased susceptibility to galectin-1-induced cell death. *Glycobiology* **13,** 909–918 (2003).

150. Raska, M. *et al.* Glycosylation patterns of HIV-1 gp120 depend on the type of expressing cells and affect antibody recognition. *J. Biol. Chem.* **285,** 20860–20869 (2010).

151. Tardif, K. D. & Siddiqui, A. Cell surface expression of major histocompatibility complex class I molecules is reduced in hepatitis C virus subgenomic replicon-

expressing cells. *J. Virol.* **77,** 11644–11650 (2003).